HARDING UNIVERSITY

Sky Vision: Final Design

Philip Varney
Cristina Belew
Julianne Pettey
Peng Yang

12/7/2010

Table of Contents

Requirements Specification…… 4

Overview…….. 5
Problem Statement……... 5
Requirements……6
Deliverables……..6
User Manual……..7
Test Plans ……7

System Design……...9

Background……10
System Overview……11
Organization and Management……...13
System Block Diagram……...15
Functional Descriptions of Subsystems ……16

Final Design……19

Stabilization System Design……..……20
Mechanical Imaging Design……...37
Electrical Imaging Design……..45
Platform Design……..48
Tethering Design……59
Power System Design……61
Communication System Design……70
User Interface Design……82

Budget ……83

Budget Overview……84
Subsystem Budgets……85

Project Management……...88

Fall 2010 Gantt Chart……89
Fall 2010 Work-Breakdown Schedule……90
Fall 2010 Network Diagram ……..91
Fall 2010 Schedule Analysis……..92
Spring 2011 Gantt Chart……93
Spring 2011 Work-Breakdown Schedule ……..94
Spring 2011 Network Diagram……...96

References……...97

Appendices ……..…99

Appendix A: FAA Regulations…….100
Appendix B: Propeller Justification MATLAB Code……..105
Appendix C: Maximum Wind Force MATLAB Code ……107
Appendix D: APC 10 x 4.7 Propeller Data Sheet……109
Appendix E: Hacker A20 - 20L Motor Data Sheet……...112
Appendix F: Wind Alignment MATLAB Code……...115
Appendix F – 1: Wind Response MATLAB Code ……..117
Appendix G: Elevation Rotation Motor Holding Torque MATLAB Code……..120
Appendix H: Hitec HS-81 Servomotor Data Sheet……..122
Appendix I: Transmissibility MATLAB Code……124
Appendix J: Sorbothane Vibration Isolation Material……..126
Appendix J – 1: Hitec HS-81 Attachment Kit……..129
Appendix K: Booster Vision GearCam……131
Appendix L: Balloon Data Sheet……..133
Appendix M: Microprocessor……...135
Appendix N: Microprocessor Power Demands……139
Appendix O: Schmart Board……141
Appendix P: Voltage Regulators……..143
Appendix Q: Auxiliary to USB Connector ……..146
Appendix R: Remote controller system……148
Appendix S: Transmitter……...151
Appendix T: Receiver……...153

Requirements Specification

Overview

The goal of *Sky Vision* is to design and construct a cost effective, mobile flight platform with the capability to remotely capture video and transmit the data to a user on the ground in real time. The need for aerial imaging spans a wide array of markets, such as search and rescue, law enforcement, construction, the media, fire fighting, and general recreation.

Aerial imaging greatly expands the capabilities of the aforementioned markets. It reduces the manpower (and thus costs and risks) needed for many dynamic situations, such as monitoring the scene of a crime or surveying the extent of a wildfire. In short, aerial imaging extends the sensing capabilities of a market from a two dimensional field into a third dimension: the sky.

Currently, this capability is far too often accomplished through the use of expensive rotary and fixed wing aircraft. The costs of the prior options often far eclipse the resources of many markets, thus necessitating a cost effective alternative. The goal of *Sky Vision* is therefore to create an aerial imaging product which meets both the high performance and low cost requirements of many under resourced markets.

Problem Statement

Obtaining aerial imaging of a dynamic situation can be both costly and complicated. There is a need spanning a wide range of markets for an aerial device with the capability of remotely capturing aerial images at a low cost. In order to fulfill the market requirements, the device should have the capability to be easily transported to the area of interest.

Requirements

- The power system should allow for a minimum of 1 hour flight time and also a minimum of 30 minutes of live video, not necessarily continuous, from the camera system.
- The motion of the device and/or camera should allow for both 360° of azimuth rotation and 90° of elevation rotation of the camera in order to provide a stabilized image (Stabilized: no more than 25% displacement within a 0.5 s interval of a screen centered, locked object).
- The 360 degrees of azimuth rotation should be accomplished in a 5 minute time interval.
- The camera system will be able to lock on (via either user control or automation) to some object on the ground and remain fixed on that object until the user acquires a new target object.
- The device will be able to rise to a maximum height of no less than 36.6 meters (120 ft) in order to ensure customer's needs for aerial imaging are met.
- The device should obey all pertinent FAA regulations (FAA regulation 101, subparts A and B; see Appendix A).
- The communication range of the device should be at least 50 meters.
- The device should be able to withstand maximum winds of no less than 5 m/s.
- The device should be no more than 0.43 m^3 (15 cu. ft) and the dimensions should not exceed 1.30 m x 1.04 m x 0.56 m. when deflated, in order to fit into the trunk of a standard mid-sized car (based on stats for 2011 Honda Accord).
- The device development costs should not exceed 1,000 USD.

Deliverables

- Parts manual and corresponding budget
- User manual
- Detailed schematic and final report on device capabilities
- System capability specifications

- Aerial surveillance device
- User interface
- Non-supplied parts:
  - Helium gas will be provided for testing purposes, but the customer will be responsible for obtaining helium gas for later flight.
  - A user provided laptop computer will be necessary to view the live video feed.

User Manual

1. Remove device from storage and ensure the tether system is correctly connected to the blimp.
2. Connect the power system to the tethering system and power on the device and user interface.
3. Add necessary helium gas to the blimp until fully inflated.
   - User must supply helium gas.
4. Slowly extend tethering line to allow blimp to rise to desired elevation.
5. Obtain desired imaging using camera and blimp positioning systems, done via the user interface.
6. Slowly reel in tethering line until blimp has reached ground level.
   - Maintenance: ensure blimp is intact with no leaks.
   - Maintenance: when reeling in tethering line, check visually for damaged areas.
7. Remove gas from blimp and disconnect tether system from power system.
8. Place system in storage.

Test Plans

- The power system will be connected to the imaging and stabilization systems and tested at a short vertical height for 1 hour to verify power needs (this includes 30 min. of video feed testing). The time duration will be tested using a commercial stopwatch device.
- To test image stability, 1 minute of continuous video will be recorded with the camera locked onto a single object for the entire 1 minute duration. The 1 minute video clip will then be broken into 0.5 second intervals and it will be verified that the locked object did not drift more than 25% of the screen size during each interval.
- To test 360° of azimuth rotation and 90° of elevation rotation, the device will be flown indoors and the 360° will be verified by the ability of the camera to capture a full panoramic picture (or protractor in case of camera failure), and the 90° elevation

rotation measured using a protractor. The 360° azimuth rotation will be timed using a commercial stopwatch device to verify the 5 minute rotation duration.

- The device will be flown outdoors to verify camera locking ability. An object on the ground will be preselected and the camera should keep the object in the video feed for a duration of 5 minutes.
- To verify the maximum flight height of no less than 36.6 meters, the device will be flown and the amount of tethering cable measured using a measuring tape and related appropriately (accounting for cable droop due to the weight of the cable) to the height of the device. This will cause the measured tether cable to be greater than the maximum flight height. The appropriate relation for cable droop will be provided following appropriate testing and analysis.
- The device will be flown in 5 m/s or greater winds to test flight stability. To verify flight stability, the positioning and camera systems should still be capable of locking onto an object on the ground and remaining locked onto that object for a duration of 5 minutes with 5 m/s wind present.
- To allow for wind variability, a 2 week testing period will be selected and the device tested at different states of wind speed. The extended testing time allows for adjustments to be made to the device, as well as to account for random wind speed variation.
- The communication system will be tested by flying the device at its maximum height of 36.6 meters and ensuring communication is not lost.
- The dimensions of the deflated device will be measured to ensure that both the volume and dimensions of the device do not exceed the specified dimension/volume requirements. The dimensions will be measured using a standard measuring tape.

System Design

Background

Sky Vision will meet the needs provided in the Requirements Specification by being far less expensive than the current methods used to obtain aerial images. *Sky Vision* aerial imaging will be an alternative to renting or purchasing expensive equipment outright. Using *Sky Vision* will be much more convenient for the customer, since the system can be easily transported to the required location. *Sky Vision* will use helium to fly a small video camera to the altitude necessary to obtain the desired live video feed. The camera will transmit the live video feed to a user interface on the ground. The system will be stabilized by a lightweight stabilization system. The stabilization system will be remote-controlled from the user interface on the ground.

System Overview

The goal of *Sky Vision* is to provide a cost effective method of aerial surveillance for dynamic situations. *Sky Vision* will consist of a lighter-than-air aerial platform with stable live video imaging and a stabilization system. Since most markets with a need for aerial surveillance also demand high adaptability, *Sky Vision* will measure no more than 1.30 m x 1.04 m x 0.56 m. To satisfy the needs of the customer, *Sky Vision* will be capable of providing both 360° of azimuth rotation and 90° of elevation rotation of the imaging system. Azimuth rotation is defined as a horizontal rotation in a fixed reference plane; in this case the fixed reference plane is the plane perpendicular to an axis fixed to the device which passes vertically through the center of gravity of the device when it is in a vertical orientation (see Figure 1). Ninety degrees of elevation rotation is defined as a rotation from the previously mentioned fixed plane to a position perpendicular to the plane, directed downward. The stabilization system will provide stabilization against wind force. The elevation rotation and azimuth rotation will be provided independent of the stabilization system.

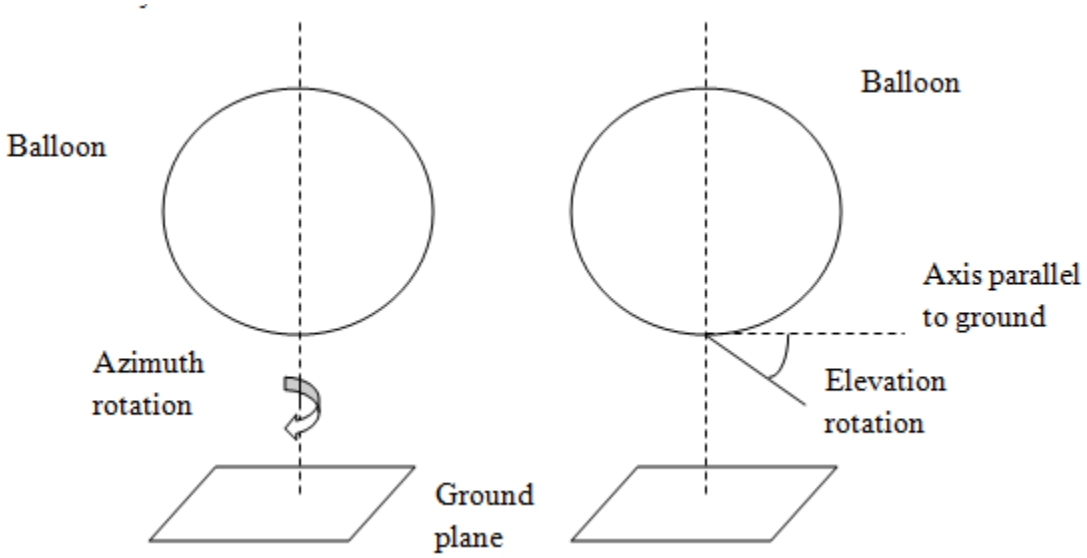

Figure 1: Azimuth and elevation rotation

Sky Vision will be operated by the customer using a portable user interface device. The user interface will provide three important functions: (1) control of the imaging system and simultaneous viewing of the live video feed, (2) control of the stabilization system, and (3) control of deflation of the balloon.

To use *Sky Vision*, the user will remove the system from storage and ensure the aerial platform is correctly secured to the tethering system (prior to inflation with helium gas). The

platform will then be connected to the power source and both the platform and user interface will be powered on. The user will then add the required volume of helium gas to inflate the platform (note that the customer will provide any required helium gas, except for that required by system development and testing). The tethering system will then be slowly released, allowing *Sky Vision* to slowly rise to the desired altitude. Once *Sky Vision* has reached the desired altitude, the user may then utilize the imaging and stabilization systems to obtain the desired field of view for the live video feed. Once imaging is complete, the user will slowly reel in the device, while visually inspecting the tether for damage. Once the platform has reached ground level, the user will inspect it to ensure the integrity of the platform has not been compromised. The valve system will then be used to remove the helium gas from the platform. Following helium gas removal, the system will be powered off and returned to storage.

Platform Selection

Three options were considered concerning the type of platform the aerial imaging system would be mounted on. The three choices were a fixed wing aircraft, a fully mobile and un-tethered blimp, or a tethered spherical balloon with limited propulsion/mobility. A downside of the fixed wing aircraft is that it would have been too difficult to design in the allotted time; also, it would not have provided the necessary level of imaging stability. One disadvantage of the spherical balloon is that it would not have given the freedom for the user to move to the desired location needed for imaging. The first choice considered was the blimp; this option would have provided an easier method for moving the blimp to the desired imaging location dictated by the user. However, the problem which arose when looking at blimp-shaped balloons was the price: most small blimp-shaped balloons were between $500 and $1000. The decision matrix utilized to decide on a platform is shown in Table 1.

Table 1: Decision matrix between balloon, airplane and blimp.

	Weight	Balloon	Airplane	Blimp
Stability	0.3	3	2	2
Cost	0.3	3	1	1
User Control	0.2	3	1	4
Complexity	0.2	4	1	2
Total	1.0	3.2	1.3	2.1

Organization and Management

Sky Vision's team consists of two electrical engineering students and two mechanical engineering students. The project tasks will be distributed between the project members as follows:

- **Philip Varney** (Mech. Eng.) - Phil is the project manager of *Sky Vision*, and primarily responsible for making sure the subsystem plans are completed, integrated, and tested on time. Phil is also responsible for finalizing all required reports and ensuring they are completed on time. Phil will also be responsible for the design and implementation of the stabilization system and the camera rotation system. Phil will work with Cristina to assist her with any difficulties that arise during the development of her responsibilities.

- **Julianne Pettey** (Elec. Eng.) - Julianne is responsible for project financing; specifically, ensuring the budget is under control. The purchasing of any system components will be done through her to ensure the budget outline is followed. Julianne will also be responsible for the design and implementation of the camera system and communication system. She will be responsible for integrating all of the electrical subsystems and ensuring they function properly with the mechanical systems. Julianne will work with Peng to ensure his tasks are done properly and efficiently.

- **Peng Yeng** (Elec. Eng.) - Peng is primarily responsible for designing and implementing the power system. He will also design the user interface system, including controls for both the imaging and stabilization systems. Peng will also work with Julianne to make sure her tasks are completed on schedule and also to

assist her in any difficulties which arise during the design and implementation of the camera and communication systems.

- **Cristina Belew** (Mech. Eng.) - Cristina is responsible for the design and implementation of the platform (balloon and mounting frame) and tethering systems. She is also responsible for examining any relevant FAA regulations and dictating to the entire team what is required to ensure FAA regulations are adhered to. Cristina will collaborate with Peng on the mechanical aspect of the user interface design. She will also assist Phil in any difficulties encountered during the design and implementation of the stabilization and mechanical imaging systems.

System Block Diagram

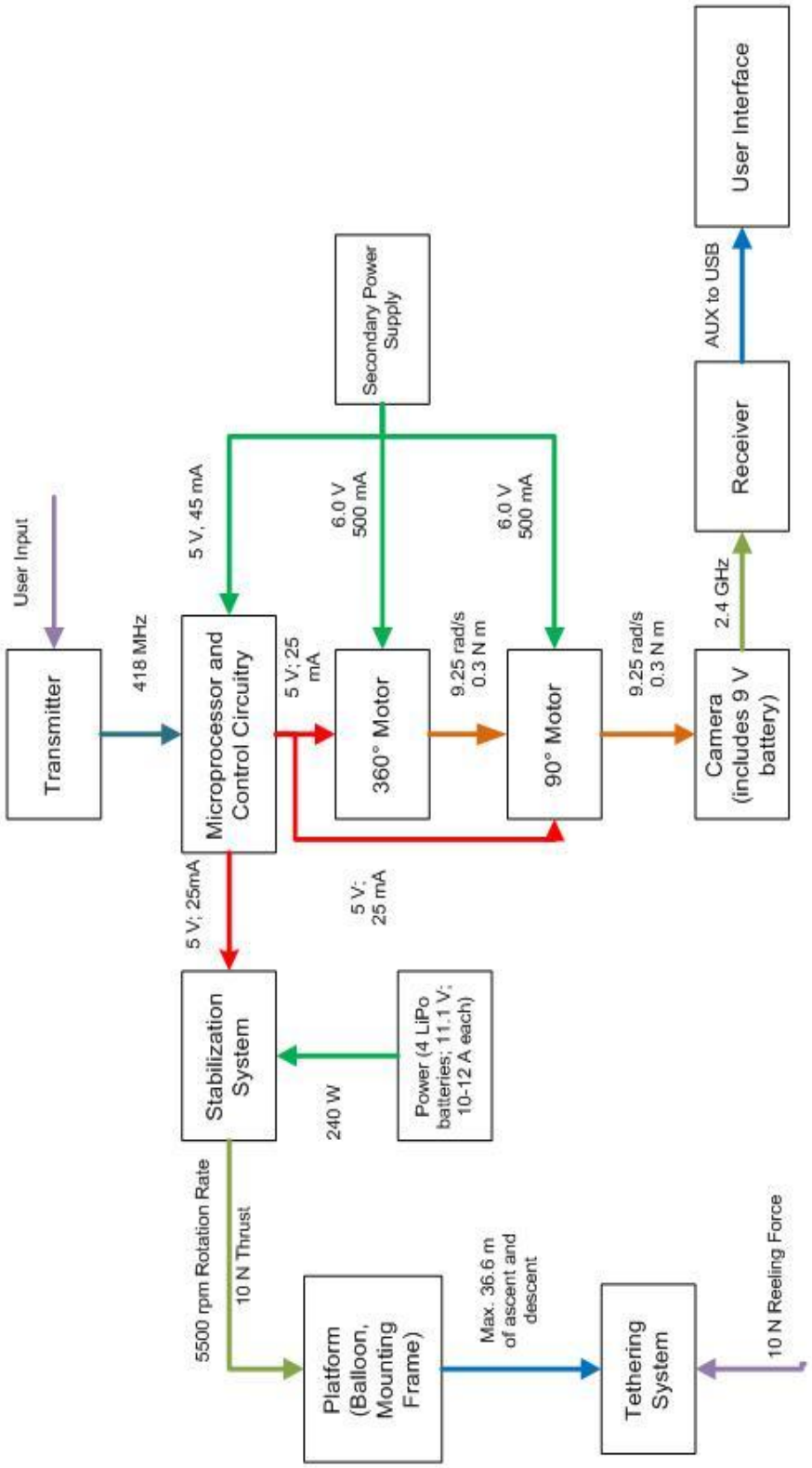

Functional Descriptions of Subsystems

Stabilization System:

The stabilization system will consist of two propellers mounted on a shaft. A wind alignment plate will align the propellers in a direction parallel to the wind velocity. The propellers will be capable of providing stability against wind-induced lateral translation of balloon.

Input: User control signal from user interface via motor control circuit (see 'User Interface' functional description for specifics on user input mechanism)

Output: Stabilization of balloon (maximum of 10 N thrust to stabilize against wind speed range specified in Requirements Specification) and alignment of propellers with wind direction.

Communication System:

The communication system will remotely control the stabilization system and imaging rotation motors. It will transmit a signal from the user interface via a DSPIC30F6015 microprocessor to a motor control circuit that determines stabilization thrust. The signal will be transmitted wirelessly and will be in compliance with all relevant FCC communication standards and regulations.

Input: Signal generated from remote-control device on user interface and transmitted at radio frequency at 2.4 GHz.

Output: Signal to a DSPIC30F6015 microprocessor, motor control circuit and camera control circuit; which sends power to the stabilization units and camera; 5 V and 25 mA control signal to stabilization system and imaging rotation motors

Power System:

The power system provides the necessary power for the stabilization system, user interface, and communication system (power for camera is described under Imaging System). The power system consists of a system of four lithium polymer batteries (2500 mAh, 11.1 V), two voltage regulators, and an 11.1 V 850 mAh secondary battery. The power system will provide power to the system for a minimum of one hour, including 30 minutes of power to the imaging system and a variable amount of power to the stabilization system as dictated by imaging position needs and wind speed.

Input: Power of batteries (11.1 V, 2500 mAh and 850 mAh).

Output: Power to systems (Maximum of 120 W to each Hacker A20-20L propeller motor, 5 V and 45 mA to microprocessor, receiver, and decoder, and 6.0 V and 0.5 A to imaging rotation servomotors).

Tethering System:

The tethering system includes both a reel device to allow for ascending and descending of the balloon and also a tethering cable which is capable of securing the balloon. The device should be deployable to and from its maximum height of 36.6 meters within 10 minutes. In order to ensure that the height of the device does not exceed 36.6 meters, the tethering system will only be capable of letting out 36.6 meters of cable. The tethering material will have a factor of safety against rupture of at least 2.0

Inputs: 10 N mechanical reeling force.

Outputs: Change in device elevation, from 0 meters to the maximum height of 36.6 meters.

Imaging System:

The imaging system will consist of a small camera mounted onto the balloon. The camera will be capable of 90° elevation rotation and 360° of azimuth rotation, accomplished via independently controlled motors. The live video feed will be transmitted to the ground and made viewable on the user interface. The camera will be adjusted to focus at a distance sufficient to accommodate the maximum flight height.

Inputs: Control signal from user interface. 9 volt power supply from battery to camera. 6.0 V and 500 mA to servomotors.

Outputs: Live video feed displayed on the user interface. 90° elevation rotation and 360° of azimuth rotation at 9.52 rad/s and 0.3 N m.

Platform:

The platform consists of both a helium filled balloon and the required mounting infrastructure. The helium filled balloon will provide enough lift to bring the system to the desired elevation, and the required mounting infrastructure will support the imaging and stabilization systems.

Input: 5 m^3 of helium gas required to lift system (helium gas can lift approximately 1.1 kg/m^3 at 20° C and 1 atm .

Output: Desired elevation of the system.

User Interface:

The user interface consists of the user provided laptop used to view the live video feed. The live video feed will be viewable on the user interface, which will be a user-supplied laptop computer.

Input: AUX signal from transmitter.

Output: Viewing of live video feed on laptop computer via USB

Final Design

Stabilization System Design

Overview

The goal of the stabilization system is to provide platform stabilization in varying wind conditions, as dictated by the Requirements Specification. The stabilization system consists of two propellers driven by high rpm electric brushless motors mounted on the same rigid shaft beneath the balloon. In order to effectively stabilize against wind, the propellers must provide a thrust force equal but opposite to the drag force on the balloon caused by the wind. To fully stabilize against the wind, the thrust force generated by the propellers must therefore be opposite in direction of the drag induced by the wind. In order to align the thrust force opposite to the drag force, the propeller assemblies must be capable of 360° horizontal rotation. To accomplish the necessary rotation, a light-weight alignment plate will be attached perpendicular to the shaft supporting the motors. The drag force on the alignment plate will cause a moment which will rotate the propellers to the position necessary to stabilize against the wind.

Stabilization System Components

The main components of the stabilization system are the following:

1. Propellers
2. Electric motors driving the propellers
3. Shaft/bracket connecting the propeller/motor assemblies to the same shaft
4. High frequency passive (not powered) vibration damping/isolation bolts/brackets
5. Wind alignment plate

Stabilization System Justification

In order to justify the use of a dedicated stabilization system, a simulation was created and performed which analyzed the dynamics of the system both with the stabilization system and without it. The simulation used a free-body analysis of the balloon to calculate the tension in the tethering cable and the angular deflection of the balloon about an axis parallel to the ground.

The first step in the simulation was to develop a dynamic model of the system. The model developed is provided below in Figure 2.

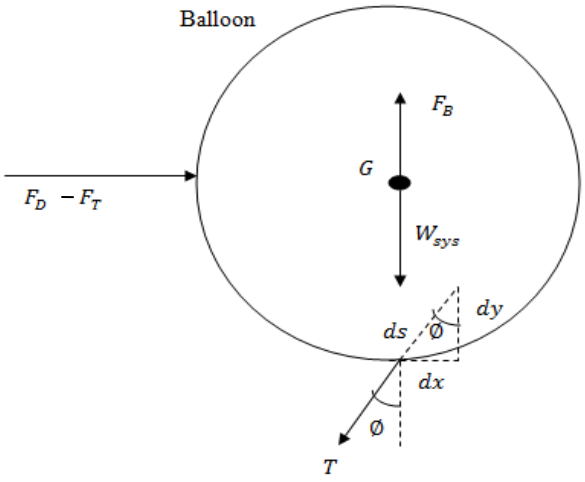

Figure 2: Dynamic model of system

In Figure 2, the center of mass of the simplified system is shown to be at the center of the spherical balloon and is represented by the designation G. The weight of the system is designated W_{sys}, the tension in the tethering capable is T, the buoyant force exerted on the balloon is F_B, the drag force is F_D, and the thrust force generated by the propellers is F_T. The tension in the cable is along the direction of the cable, which is inclined an angle $\emptyset$. The buoyant force acts through the centroid of the balloon, which in this simplified case also corresponds to the center of gravity, G. The drag force F_D acts through the centroid, and the line of action of the thrust force is assumed to act through the center of gravity (this assumption is valid since the center of gravity can always be shifted to a desired location by adding an appropriate amount of mass at the required distance).

From Figure 2, the differential arc length ds can be related to the differential lengths of the coordinate axes by the following relation:

$$ds = \sqrt{dx^2 + dy^2} = \sqrt{1 + \left(\frac{dy}{dx}\right)^2}\, dx\,. \qquad \text{Eq. 1}$$

To determine the deflection angle $\emptyset$ of the cable, it is first necessary to sum forces in the x and y directions. The sum of the forces in the x direction is

$$F_D - F_T - Tsin(\emptyset) = 0 \qquad \text{Eq. 2}$$

and the sum of the forces in the y direction is

$$F_B - W_{sys} - Tcos(\emptyset) = 0. \qquad \text{Eq. 3}$$

The above expressions can be simplified by realizing that $\sin(\emptyset) = \frac{dx}{ds}$ and $\cos(\emptyset) = \frac{dy}{ds}$. Setting $\frac{dy}{dx} = p$ and inserting the latter expressions and also Eq. 1 into the force balance equations yields the following simplified results for the force balance equations:

$$F_D - F_T - \frac{T}{\sqrt{1+p^2}} = 0 \qquad \text{Eq. 4}$$

$$F_B - W_{sys} - \frac{Tp}{\sqrt{1+p^2}} = 0. \qquad \text{Eq. 5}$$

Once F_D, F_T, F_B, and W_{sys} are quantified, the above nonlinear expressions can be solved in MATLAB using the code provided in Appendix B.

The goal of the simulation is to check the response of the tilt $\emptyset$ and the cable tension T to variations in thrust force and to ensure that the addition of a stabilization system is justified by significant reductions in both tilt and cable tension. Large values of tilt in the cable cause large angular deflections of the balloon, which contribute to decreased image stability. Large tension values decrease the total weight the balloon can lift, as the buoyant force has to then counter both the system weight and the tension. The values generated by the MATLAB code for tilt versus thrust force and tension versus thrust force are provided in Figures 3 and 4, respectively.

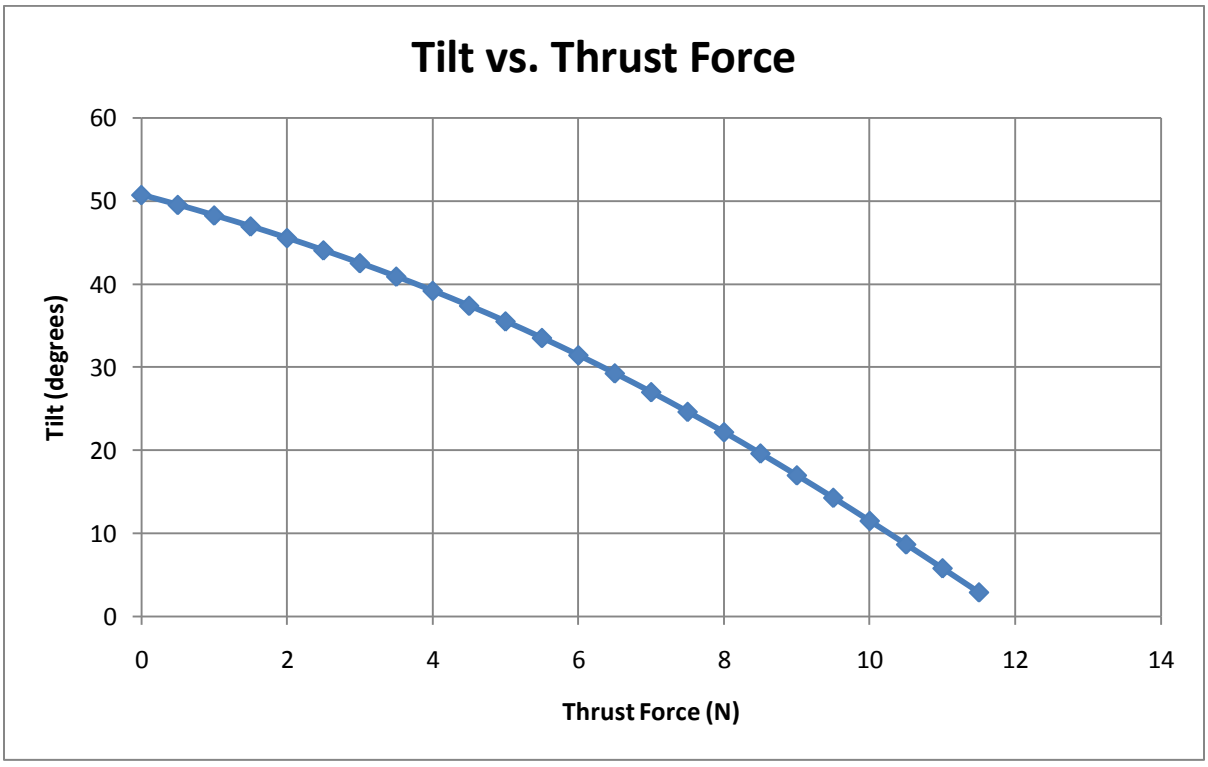

Figure 3: Tilt vs. Thrust Force

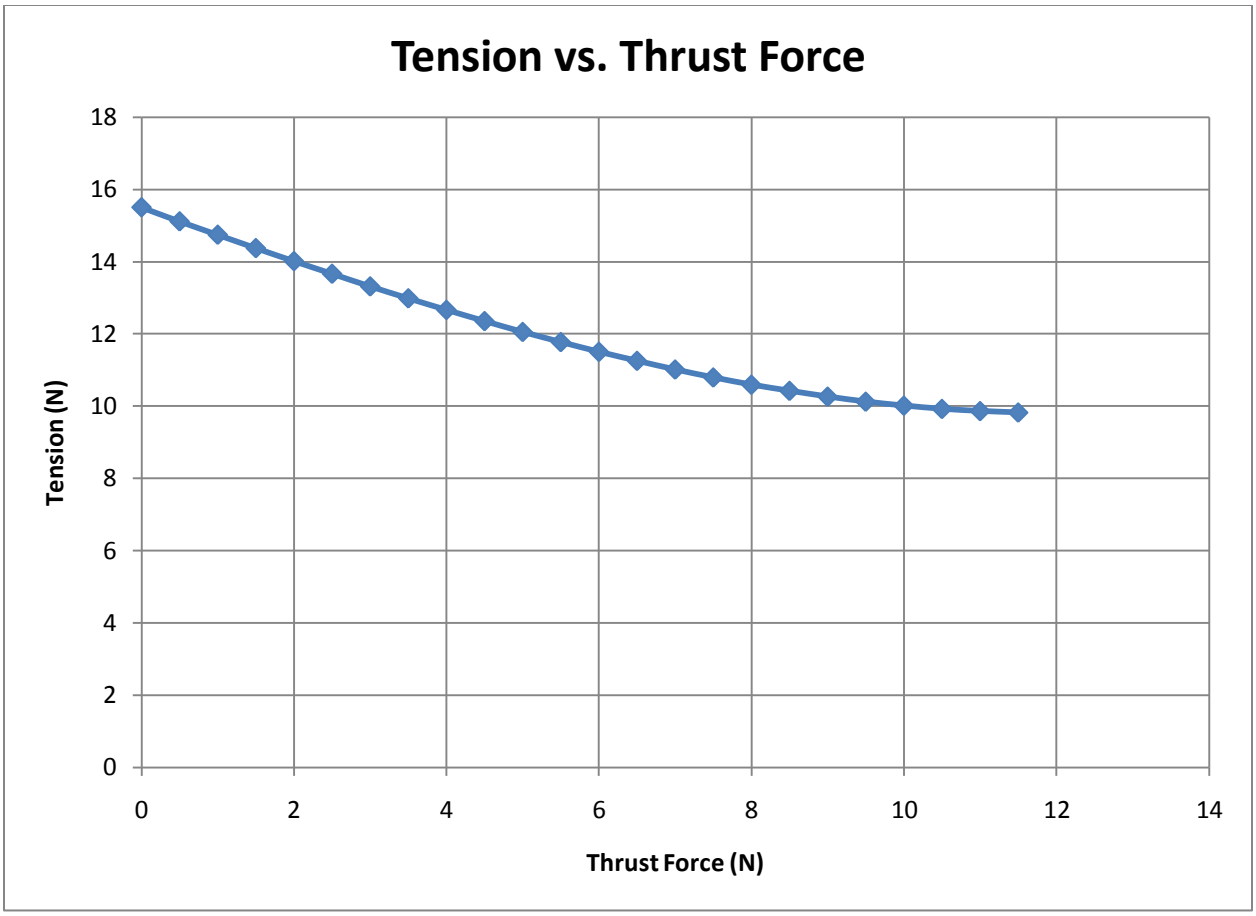

Figure 4: Tension vs. Thrust Force

Figures 3 and 4 were created by holding the wind force constant at 12 N (worst case scenario corresponding to wind value exceeding the maximum value specified), the system weight constant at 49 N, and the buoyant force constant at 59 N and varying the thrust force from 0 to 12 N. From Figures 3 and 4, it is clear that as thrust force is increased, the tilt decreased exponentially and the tension in the cable decreases towards a constant value equal to the difference between the system weight and buoyant force. It is evident from the above simulation that the addition of thrust force decreases the cable tilt from a large value to a much smaller value, and also decreases the tension in the cable to a lesser value, thus justifying the use of a dedicated stabilization system.

Wind Force Calculation

In order to determine the necessary thrust force to stabilize against wind, the drag force caused by the wind must be quantified. The Requirements Specification document dictates that the system must be capable of providing a stabilized image in wind speeds up to 5 m/s. Drag force is caused by fluid flow external to the body over which the fluid is flowing. Assuming that

the flow over the body can be modeled as incompressible (accurate assumption since the free stream fluid velocity is very low), the drag force can be quantified by the following expression:

$$F_D = \frac{1}{2} C_D \rho V^2 A. \qquad \text{Eq. 6}$$

The coefficient of drag is C_D, the density of the free stream is ρ, the velocity of the free stream is V, and the projected frontal area of the body is A. The projected frontal area of a spherical body is $A = \frac{1}{4}\pi D^2$, where the diameter of the body is D. The drag coefficient for a spherical body depends on the Reynolds number of the fluid flow, and can only be determined empirically. The Reynolds number for external flow over a spherical body is

$$Re = \frac{VD}{\nu}, \qquad \text{Eq. 7}$$

where ν is the kinematic viscosity of the fluid flow. The critical Reynolds number for the flow is approximately $2(10)^5$ (Cengel and Cimbala 2006). At the critical Reynolds number, the flow over the sphere sharply transitions from laminar flow to turbulent flow, causing a commensurate reduction in drag force. Corresponding to the change in the flow regime of the fluid is a proportionate change in the drag coefficient across the sphere; in the laminar regime, $C_D \cong 0.5$, and in the turbulent regime $C_D \cong 0.2$ (Cengel and Cimbala 2006). For the discussion to be useful, it is necessary to determine the sensitivity of the drag force to changes in air temperature, as kinematic viscosity varies greatly with temperature variation.

An analytical expression for the change in kinematic viscosity with temperature change was obtained by plotting empirical data points in Microsoft Excel and then performing a regression analysis on the data points. The data for kinematic viscosity of air was obtained from the properties charts provided by Cengel and Cimbala, 2006. The results of the regression are shown below in Figure 5.

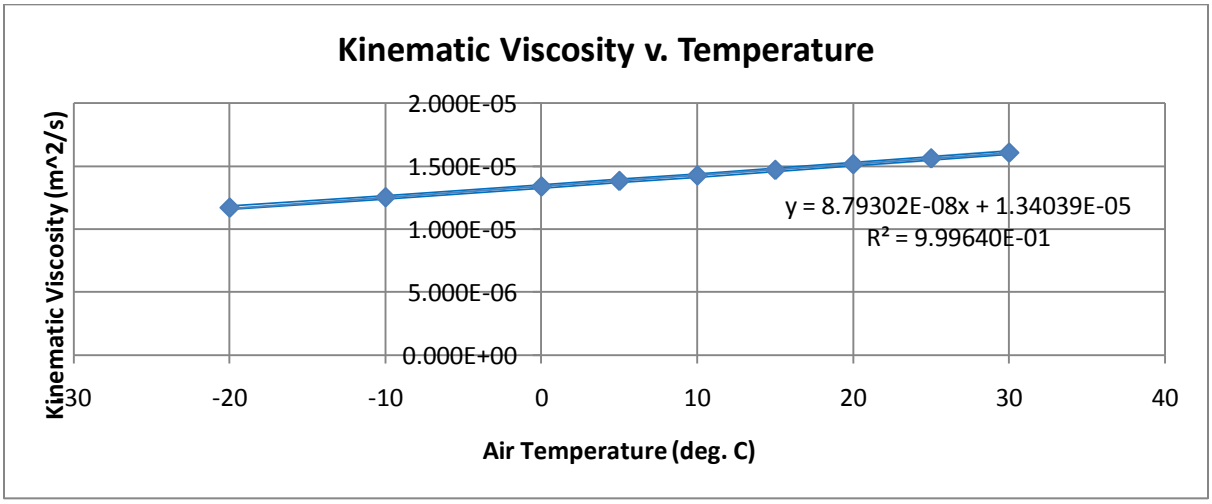

Figure 5: Kinematic Viscosity vs. Temperature

It is evident from Figure 5 that kinematic viscosity of air at a pressure of 1 atm varies linearly with temperature changes. The linear regression equation obtained in Excel is shown in the upper right corner of Figure 5. The regression analysis was very accurate, as the squared correlation coefficient (R^2) was very close to 1. Entering the regression equation shown in Figure 5 into the MATLAB code in Appendix C yielded the data for maximum wind force vs. temperature provided in Table 2. The wind velocity values in Table 2 were selected based upon wind values inducing the maximum drag on the system; an explanation is provided in the following pages.

Table 2: Maximum wind force

Air Temperature (°C)	Max Wind Force (N)	Velocity (m/s)
-20	5.09	2.32
-15	5.49	2.41
-10	5.91	2.50
-5	6.34	2.59
0	6.79	2.68
5	7.20	2.76
10	7.68	2.85
15	8.17	2.94
20	8.68	3.03
25	9.21	3.12
30	9.68	3.20

A sample wind force vs. wind velocity plot is shown below in Figure 6 for a temperature of 30 °C and a 1 m diameter balloon.

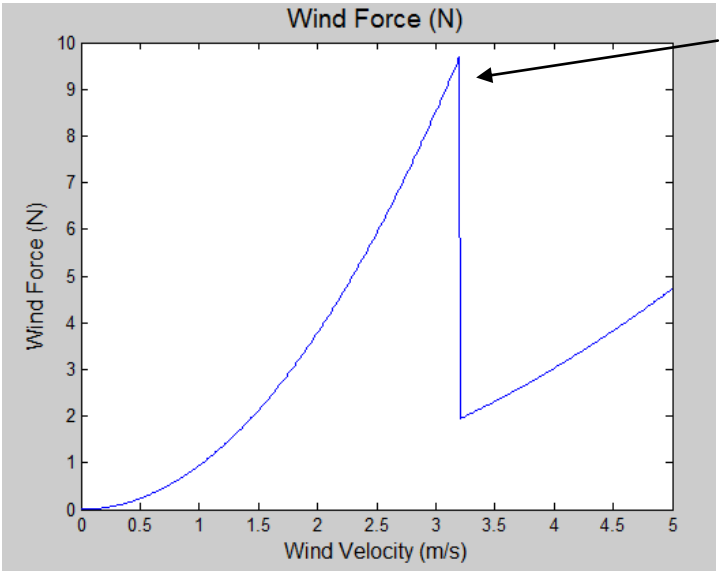

Abrupt transition due to change in fluid flow from laminar to turbulent

Figure 6: Wind Force vs. Wind Velocity

It is interesting to note that the critical Reynolds number is reached at approximately 3 m/s. This causes the drag coefficient to drop significantly, causing the maximum drag force to occur at a velocity between 0 and 5 m/s. For this reason, Table 2 also contains data showing at what velocity the maximum wind force occurs at. Evident from Table 2 is the observation that drag force increases with air temperature. From Table 2, it was determined that the stabilization units needed to produce a combined value of at least 10 N to successfully stabilize against wind speeds from 0 – 5 m/s.

Note, however, that the transition from laminar to turbulent flow is not as abrupt a phenomenon as Figure 6 portrays. In order to approximate the drag over a wide range of wind velocities, the drag coefficient had to be approximated as being either laminar or turbulent, with no intermediary values. In reality, Figure 6 is a smoother curve, with a lower maximum peak. The approximation used above is therefore a very liberal approximation of wind drag.

Stabilization Unit Selection

The next step in the stabilization system design was to select appropriate stabilization units to generate the required minimum of 10 N of thrust. Two options were initially considered: ducted fans and open-air propellers. Ducted fans consist of a motor and propeller blade surrounded by a low clearance cylindrical duct (see Figure 7). Open-air propellers, however, do not have the cylindrical duct encasing the propeller blade.

Figure 7: Ducted fan (www.ductedfans.com)

These two options were considered because a large market (radio-controlled aircraft) already existed which relied on the use of those two forms of stabilization units. Open-air propellers were chosen over ducted fans for two primary reasons. First of all, ducted fans producing the same thrust as an open-air propeller consumed much more power (upwards of 900

W for the Fury EDF ducted fan on www.ductedfans.com). Second, ducted fans were generally much more expensive and also heavier than open-air propellers producing the same thrust. Ducted fans are used in the remote controlled aircraft market because they are capable of producing values of thrust which could only be obtained otherwise by using very large conventional propellers.

Predicting the thrust generated by an open-air propeller is a very complex problem. The thrust force generated by the propeller is due to a pressure difference between the inlet and outlet surfaces of the propeller. The pressure difference is due to some very complicated effects. The pressure change is essentially generated because the propeller blade is a rotating wing with a varying angle of attack and changing airfoil shape. Using Bernoulli's Law in combination with the fact that force is equal to change in pressure times area yields the following result for a rotating blade modeled as a thin disk:

$$F_T = \frac{\pi}{8}\rho D^2(V_e^2 - V_o^2). \qquad \text{Eq. 8}$$

where C_D and ρ were defined previously. The complication arises in that neither the exit velocity V_e nor the inlet velocity V_o are known. The only other known method for analytically determining the thrust force generated by a certain propeller is to use a finite element fluid dynamics simulation based upon advanced airfoil theory. However, this analysis has been performed by radio-control enthusiasts with knowledge of aerospace engineering and placed online in the form of 'thrust calculators'. In order to validate the thrust calculators, two different thrust calculators were used and the same numbers were input into each calculator. The results were compared and found to be reasonably close in magnitude; they are presented in Figures 8 and 9 below. The results obtained from the online calculators seem to be reasonable, considering the large pitch and diameter of the blades.

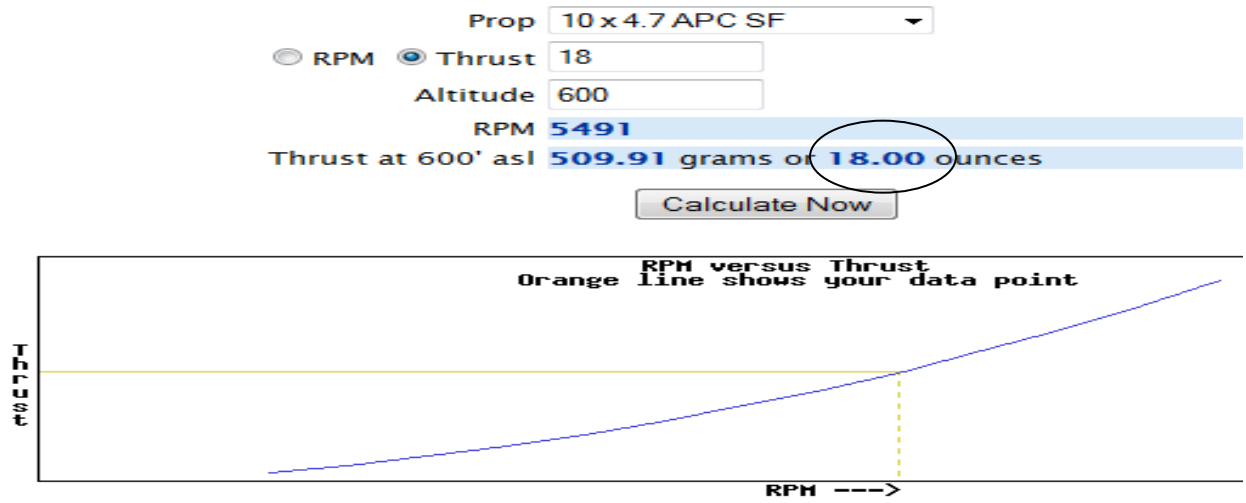

Figure 8: Thrust calculator #1 (http://www.gobrushless.com/testing/thrust_calculator)

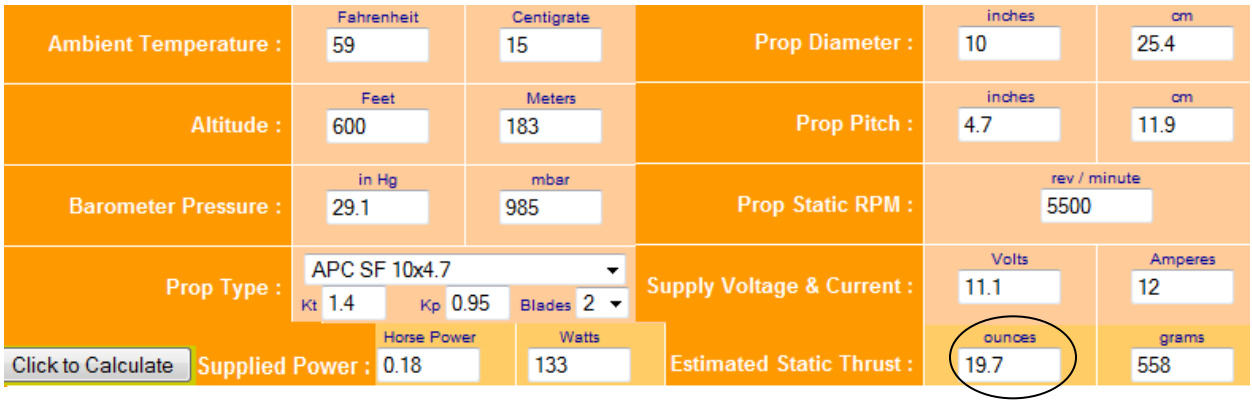

Figure 9: Thrust calculator #2 (http://adamone.rchomepage.com/calc_thrust.htm)

It is clear from Figures 8 and 9 that both the motor rpm and calculated thrust values (shown circled) are close in magnitude. Please note that 18 oz-force of thrust is equivalent to approximately 5 N of thrust, or half of the desired value of 10 N of thrust. For this reason, two propellers were chosen rather than one larger propeller, as to minimize power consumption.

The next step was to select stabilization system components (propeller blade as well as driving motor) to provide the necessary 10 N of stabilization thrust. Two attributes must be considered in the selection of a propeller blade. The first of these attributes is the diameter of the blade. A general rule can be gleaned from the observation that a propeller is nothing more than a momentum changing device; as the momentum of a control volume of air is changed, thrust is generated. So as diameter is increased, air flow is increased, which in turn increases thrust. The second attribute to consider is the pitch of the propeller. A propeller is essentially an 'air-screw', and as such the pitch of the propeller is defined as the distance the propeller would move through the air given one turn of the blade. So once again, as pitch is increased, more air is moved through the blade, resulting in increased thrust.

Taking into account the above observations on pitch and diameter, the thrust calculators were used to both estimate thrust generated by different propellers of varying dimensions and also to analyze how much power would need to be given to the propeller to provide the given thrust. It was found that the propeller which provided adequate thrust while remaining within reasonable power consumption limits (< 200 W) was an APC SF 10 x 4.7 propeller blade (10' x 4.7' (25.4 cm x 11.94 cm) corresponds to diameter x pitch). To provide the thrust, the motor driving the propeller would need to be supplied approximately 130 W of power and would also need to rotate at approximately 5500 rpm. Figure 10 below shows the APC SF 10 x 4.7 propeller blade (see Appendix D for more information).

Figure 10: APC SF 10 x 4.7 propeller blade

The next step was to select an appropriate motor to drive the propeller blade at the necessary angular speed. In order to achieve high values of rpm and stay within reasonable power supply limits, a brushless dc motor was chosen instead of a brushed motor, even though the brushed motors often have substantially lower costs. An important factor to consider in selecting the motor was a KV value high enough to allow the high rotation rates. The KV value of an electric motor is a measure of how many rpm the motor can rotate per volt supplied. Another important factor influencing motor selection was the weight of the motor. Since the balloon can only lift a specified weight, it is crucial that the weights of all the components be minimized. The last factor influencing motor selection was power demands. In order to produce at least 5 N of thrust per propeller/motor assembly, each motor must be capable of receiving at least 130 W of power.

The motor selected to meet the above criteria was a Hacker A20-20L Brushless out-runner motor. The mass of the motor is 55 g (1.94 oz), and the motor is capable of receiving 200 W of power at 11.1 V. The KV value of the motor is 1022 rpm/V; at 11.1 V the motor should therefore be more than capable of rotating at 5500 rpm. The motor can sustain a constant current of 6 – 15 A, with a maximum burst current of 19 A. It is interesting to note that the manufacturer of the motor recommends the same propeller blade as was selected earlier in order to prevent motor overload. The Hacker A20-20L brushless motor is shown below in Figure 11 (see Appendix E for more information and technical specifications).

Figure 11: Hacker A20-20L brushless motor

Wind Alignment Design

In order to stabilize against wind, the thrust force generated by the propellers must be equal and opposite when compared to the drag force caused by the wind. Since the drag force caused by the wind is in the same direction as the wind velocity, the propellers need to be aligned such that the thrust is generated in a direction opposite the wind velocity. The thrust

force generated by the propellers is perpendicular to the plane in which the propeller blade rotates (see Figure 12).

Figure 12: Direction of thrust force in relation to rotating propeller

A system or mechanism is therefore needed to align the plane of the rotating propeller perpendicular to the direction of the wind. Two options were considered to accomplish this task. The first option was differential thrust generated by the propellers. The differential thrust would be produced in one of two ways. The first method would be to cause one propeller to generate more thrust than the other, causing a net moment inducing rotation. The second method would be to cause the propellers to rotate in opposite directions, thus generating a couple moment causing rotation of the system. The second option to align the system was a wind alignment plate, which works in a fashion similar to a weather vane.

Differential thrust was eliminated as an option for two reasons. First, and most importantly, the alignment process would not be automatic and would have to be controlled by the user. The user would need to continuously adapt the differential thrust to compensate for randomly shifting wind velocity, a feat which would be much too complex for even the most skilled operator. Secondly, the differential thrust would need to be controlled electronically, thus significantly complicating the control circuitry design.

The first step in designing the wind alignment plate was generating a free-body diagram of the balloon and plate. The free-body diagram is shown below in Figure 12. The center of gravity and centroid of the balloon are labeled G and C, respectively. The drag force on the alignment plate is F_d and is directed in the same direction as the wind velocity, V_{wind}. The xyz axis is attached to the alignment plate axis shown in Figure 11 and rotates with the system at $\dot{\theta}$. The propellers are shown from the side, since the alignment plate and the propellers are perpendicular. The distance r is the moment arm of the drag force about point C.

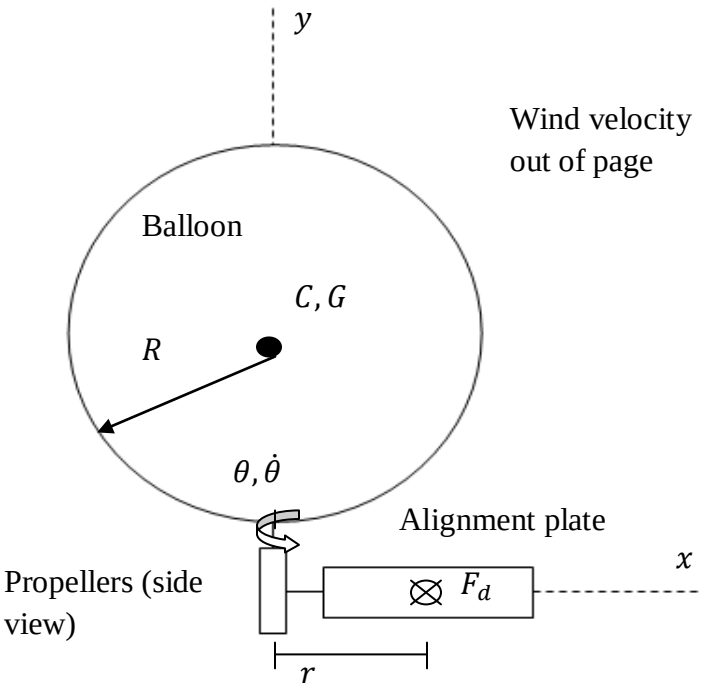

Figure 13: Wind alignment free-body diagram

For a preliminary analysis, the alignment plate will be designed as a rectangular rod. The drag force on the plate, F_d, is

$$F_d = C_D\left(\frac{1}{2}\rho_{air}V_{wind}^2 A_p\right), \qquad \text{Eq. 9}$$

where A_p is the projected frontal area of the plate. The coefficient of drag is C_D, and is dependent on the geometry of the alignment plate. Since a fast response is desired, the geometry will be chosen to provide a large coefficient of drag. The geometry providing the largest drag coefficient is a rod with a rectangular cross-section with a dimensional ratio of 0.5 (cross-section height divided by cross-section width) (Cengel and Cimbala 2006). For this geometry, the coefficient of drag is 2.5.

Since the wind velocity direction stays constant and the plate rotates, the projected frontal area A_p of the alignment plate also changes. A relation for the changing area was obtained by analyzing Figure 14.

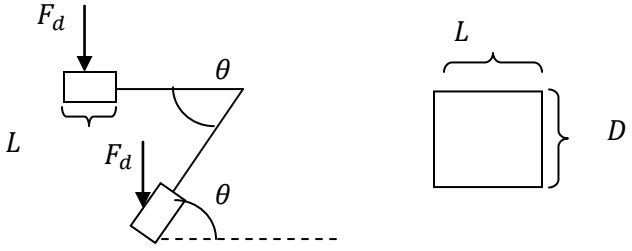

Figure 14: Projected frontal area

From Figure 14, the projected frontal area as a function of θ is

$$A_P = DL|\cos\theta|. \qquad \text{Eq. 10}$$

The absolute value of the cosine of θ is necessary because the projected frontal area is always a positive quantity. The initial equation of motion (EOM) obtained by summing the moments about the center of gravity was

$$\left(\frac{2}{5}m_bR^2 + \frac{1}{12}m_pD^2 + m_pr^2\right)\ddot{\theta} - 0.5C_dV_{wind}^2DL\,|\cos\theta|\cos\theta\, r = 0, \qquad \text{Eq. 11}$$

where m_p is the mass of the plate and m_b is the mass of the balloon. Two stability points are gleaned from the above EOM: $\theta = 90°$ and $\theta = 270°$. The first stability point, $90°$, is stable because small displacements from this point do not induce large deviations from $90°$. The second stability point, though, is only marginally stable since small disturbances from $270°$ cause large deviations from the stability point.

It is immediately evident from Equation 11 that there was no $\dot{\theta}$ term. Since there was no $\dot{\theta}$ term, the damping coefficient ζ is zero, and the response will not decay to the desired stability point of $90°$. The model initially developed and presented above was therefore inadequate, as a term inducing decay towards stability is not present.

The damping in the system arises because of relative velocity between the alignment plate and the surrounding air. The velocity of the air on the back of the plate causes a drag force which is proportional to the rotational rate $\dot{\theta}$ of the system. The drag is demonstrated below in Figure 15.

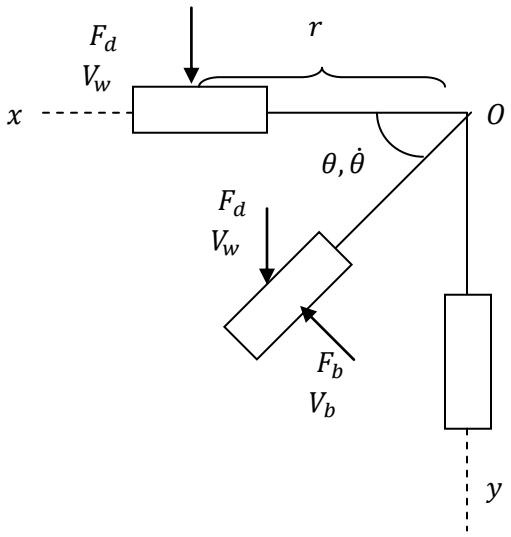

Figure 15: System damping

The back wind velocity and back drag on the alignment plate are represented by F_b and V_b, respectively. The distance to the point of action of both forces is r. The xyz frame rotates with the system. The velocity of the air at the back of the alignment plate is then

$$\bar{V}_b = \dot{\bar{\theta}} \times \bar{r} = \dot{\theta}\hat{k} \times r\hat{\imath} = \dot{\theta} r \hat{\jmath}. \qquad \text{Eq. 12}$$

The magnitude of the force F_b is therefore

$$F_b = \frac{1}{2}\rho_{air}\left(\dot{\theta} r\right)^2 A_P C_D. \qquad \text{Eq. 13}$$

Summing the moments about *O* yields the following result:

$$\left(\frac{2}{5}m_b R^2 + \frac{1}{12}m_p D^2 + m_p r^2\right)\ddot{\theta} - 0.5 C_d V_{wind}^2 DL\,|\cos\theta|\cos\theta\, r + \frac{1}{2}\rho_{air} r^3 \left|\dot{\theta}\right|\dot{\theta} A_P C_D = 0. \qquad \text{Eq. 14}$$

The absolute value term on the $\dot{\theta}$ term compensates for the fact that the direction of the moment caused by F_b changes when θ becomes greater then 90°. The time response of Equation 14 can be found by solving the equation using the ordinary differential equation solvers in MATLAB. The MATLAB code used to solve the EOM is provided in Appendix F. The time response is given below in Figure 16.

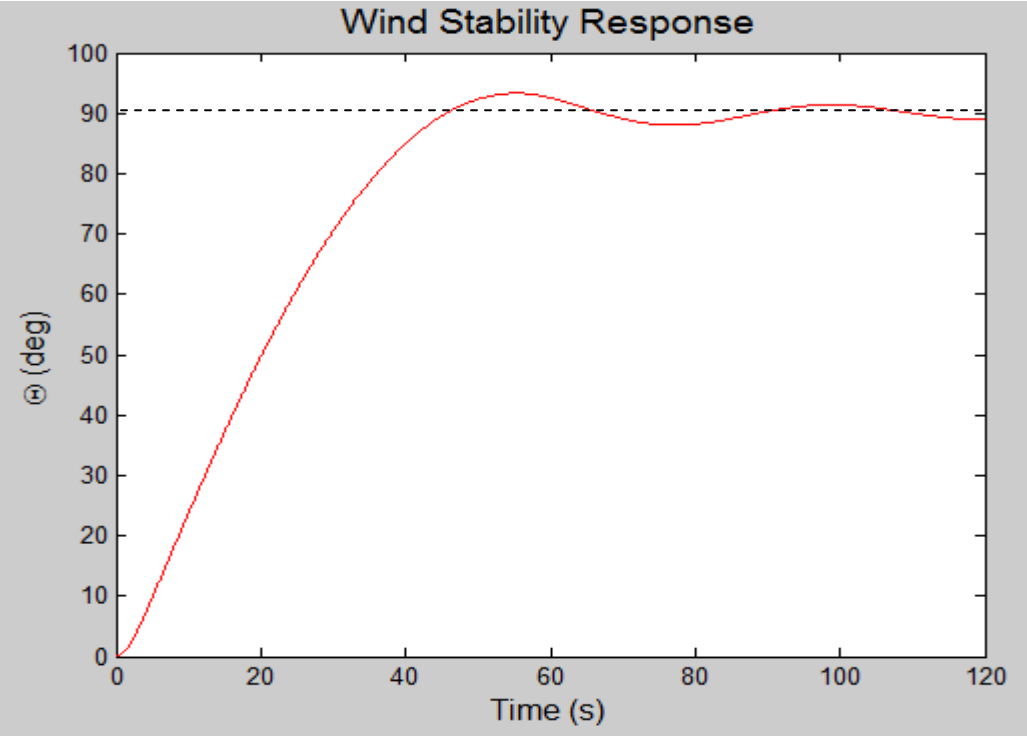

Figure 16: Time response of wind alignment plate

The wind alignment plate geometry used to generate Figure 16 is contained in the MATLAB code in Appendix F. After adjusting the geometries in the MATLAB code and observing the results, it was found that decreasing the moment arm r of the alignment plate decreased the time till the peak was reached, but increased the magnitude of the oscillations about equilibrium. A r value of one meter was found to provide the best balance between initial response time till peak and magnitude of oscillation about equilibrium.

The material used to construct the alignment plate needs to be as light-weight as possible; for this reason, Styrofoam will be used to create the alignment plate.

Image Stability: Stabilization Concerns

The effect of the motion of the system (particularly the oscillation about equilibrium) induced by the wind alignment plate must be addressed. In order to gage the effect of the motion on image stability, the response time of the $360°$ azimuth rotation motor of the imaging system (see Mechanical Imagine Design) must be compared to the angular velocity of the system, $\dot{\theta}$, because these two rotations occur about the same axis.

The largest angular velocity in the system response was found by plotting the angular velocity of the system versus time using the MATLAB code provided in Appendix F. The plot is provided below in Figure 17.

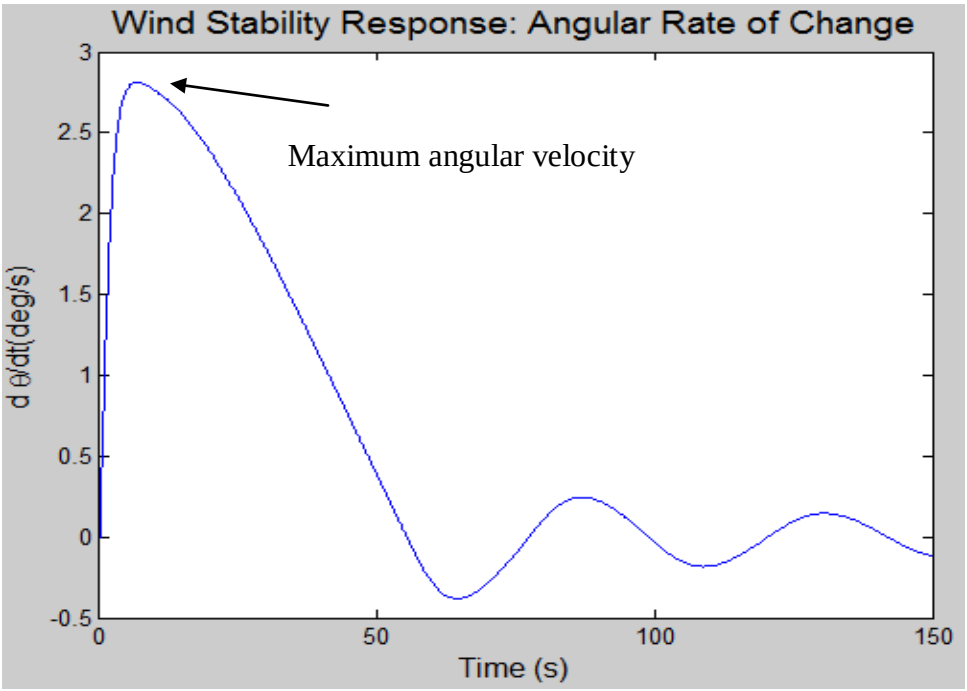

Figure 17: Angular velocity of system

Using MATLAB, the maximum angular velocity was found to be 2.81 degrees/s, or 0.05 rad/s. From the data sheet of the azimuth rotation servomotor (Appendix H), the angular speed of the servomotor has a maximum value of 9.52 rad/s. Since the angular speed of the servomotor is much greater than the maximum angular speed of the system, the user will be able to adjust the camera position manually to compensate for the very slow oscillation of the system. The slow oscillation of the system is also evident from the very large period of the system: 44 s.

In addition to modeling the rotation of the system due to the wind alignment plate, the system was also modeled as an inverted pendulum in order to quantify the rotation of the system about the base of the tethering system on the ground. To simplify the analysis, the tether cable was always assumed to be taut and straight (see free body diagram below in Figure 18).

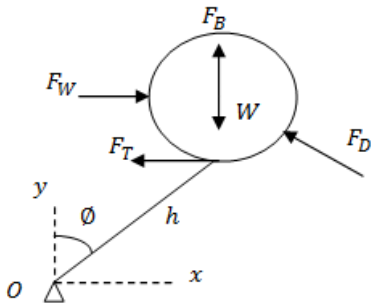

Figure 18: System modeled as inverted pendulum

In Figure 18, the length of the tethering cable is denoted by h, the rotation from the vertical position is $\emptyset$, the point of tether attachment is point O, F_D is the damping drag present in the system, F_T is the thrust force generated by both propellers, F_B is the buoyant force, W is the system weight, and F_w is the drag force induced by the wind. The system weight and buoyant force are both assumed to act through the centroid of the balloon of radius R.

Summing moments in the $z-$ direction about point O yielded the following equation of motion:

$$I_o\ddot{\emptyset} = -F_T(h\cos(\emptyset)) - F_D h + W\sin\emptyset\ h + F_w(R + h\cos\emptyset) - F_B h\sin\emptyset\ . \qquad \text{Eq. 15}$$

The inertia about point O is

$$I_O = \frac{2}{5}m_b R^2 + m_{sys}h^2 \approx m_{sys}h^2. \qquad \text{Eq. 16}$$

The mass of the entire system is m_{sys} and the mass of the balloon itself is m_b. Since the tether length $h \gg R$, the inertia of the balloon about its own center of gravity is negligible. The drag forces F_w and F_D can be obtained by inserting the proper terms for velocity (wind velocity and rotational velocity of balloon, respectively) into Equation 6. The thrust force is equal to the wind drag F_w in order to provide stability. The buoyant force is equal to the weight of the air

displaced by the balloon. Using an ordinary differential equation solver in MATLAB, the response to Equation 15 was obtained (see Appendix F - 1 for MATLAB code used) and shown below is Figure 19.

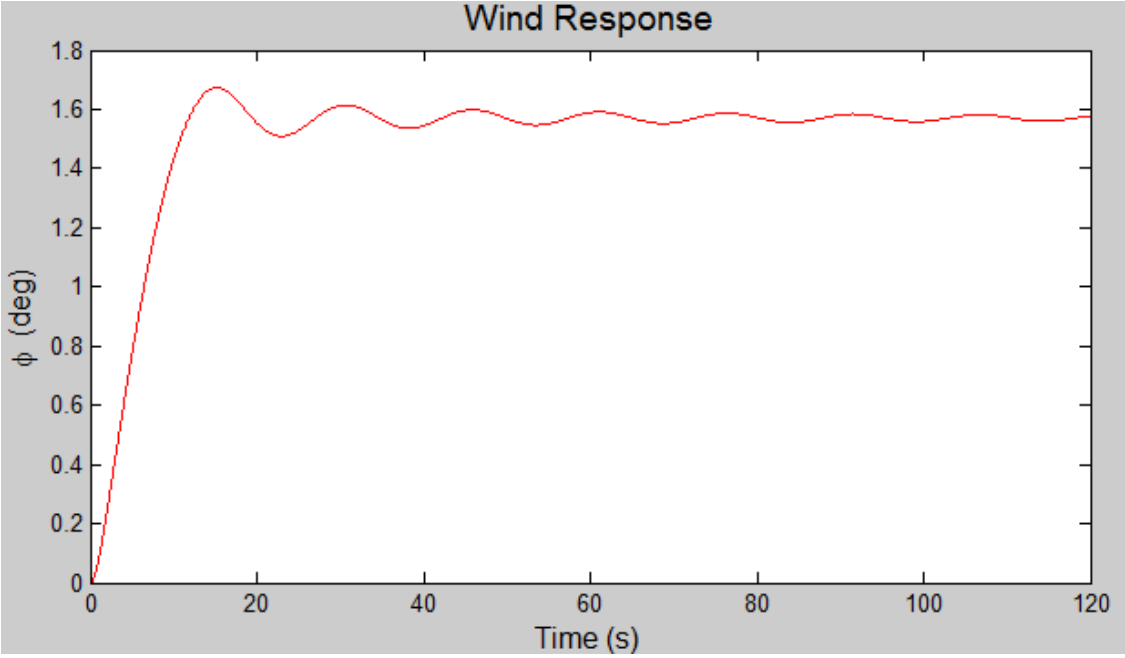

Figure 19: System response about tethering attachment

From Figure 19, it is clear that the period of the system is approximately 15 seconds, and that the maximum value of the angular displacement Ø is approximately 1.7°. Due to a combination of the slow response of the system (large period) and small angular displacement, the quick response time of the elevation rotation servomotor (see Appendix H) should suffice to allow the user to manually compensate for slow disturbances of the image.

Propeller Protection Casing Design

In order to protect both the integrity of the balloon and also the user from the rotating propeller blades, the propellers will each be surrounded by a cylindrical duct with wire mesh secured to the front and rear of the cylindrical duct. The diameter of the duct will be 12” (0.305 m), which is slightly larger than the diameter of the propellers.

Mechanical Imaging Design

Overview

The mechanical imaging system is responsible for two tasks: providing the 360° of azimuth rotation of the camera and also the 90° of elevation rotation of the camera. Azimuth rotation, or panning rotation, is defined as rotation about an axis which is perpendicular to the ground (horizontal) plane. Elevation rotation is defined as rotation of the camera from a position parallel to the ground to a position perpendicular to the ground and directed downwards. These rotations are better understood visually, and as such are presented below in Figure 20. Independent control of these two rotation angles will allow for the camera to essentially have a half sphere of visibility beneath the balloon.

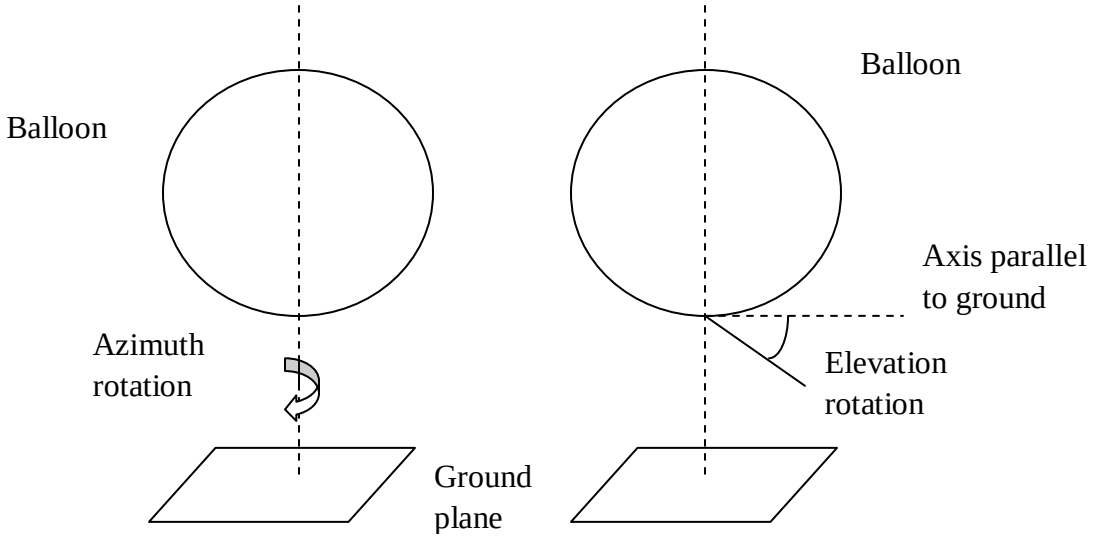

Figure 20: Azimuth and elevation rotation

The independent azimuth and elevation rotations satisfy the following requirement from the Requirements Specification:

> "The motion of the device and/or camera should allow for both 360° of azimuth rotation and 90° of elevation rotation of the camera in order to provide a stabilized image".

Elevation Rotation Motor Design

In order to select the motor to provide 90° of elevation rotation of the camera, the required holding torque of the motor is needed. The holding torque is the static torque required by the motor to keep the output shaft in the same location.

A simplified free-body diagram of the elevation rotation motor is shown below in Figure 21, with the camera modeled as a point mass on the end of the L-shaped shaft.

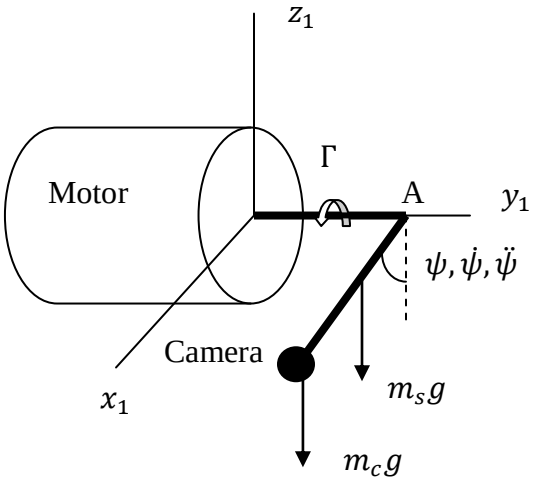

Figure 21: Free-body diagram of elevation rotation motor

In Figure 21, ψ represents the elevation rotation angle ($0 \leq \psi \leq 90°$), Γ is the torque generated by the motor output shaft, m_c is the mass of the camera components, m_s is the mass of the portion of the output shaft changing orientation, and the $x_1 y_1 z_1$ set of axes is fixed to the motor. Point *A* designates the joint between the two portions of the output shaft. A free-body diagram of the portion of the output shaft changing orientation is shown below in Figure 22.

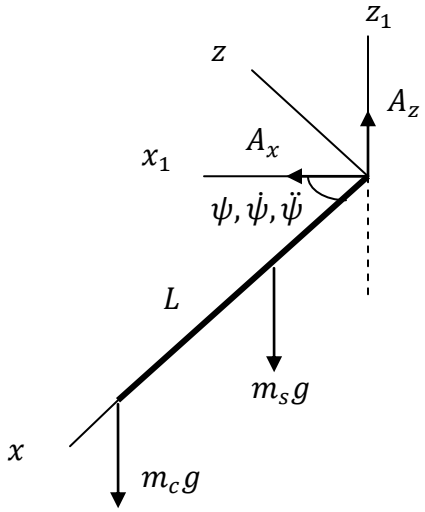

Figure 22: Elevation rotation shaft free-body diagram

The length of the output shaft is L, the force reactions at the fixed, permanent joint are A_x, A_y, and A_z, and the associated moments (not shown) are M_x, M_y, and M_z. The xyz axes are fixed to the rotating output shaft, and rotate at $\dot{\psi}$. For the sake of generality, a dynamic analysis will first be performed and then simplified to the static state by setting all time derivative terms to zero. The total angular rotation of the output shaft (assuming only elevation rotation) in the xyz frame is the following:

$$\{\omega\} = \begin{Bmatrix} 0 \\ \dot{\psi} \\ 0 \end{Bmatrix} rad/s. \qquad \text{Eq. 17}$$

In order to obtain the angular momentum, the inertia tensor in the xyz frame must be determined. The inertia tensor of the output shaft and camera in the xyz frame is the following:

$$\{I_A\}_{xyz} = \begin{bmatrix} 0 & 0 & 0 \\ 0 & \frac{1}{12}m_s L^2 + m_c L^2 & 0 \\ 0 & 0 & \frac{1}{12}m_s L^2 + m_c L^2 \end{bmatrix} \qquad \text{Eq. 18}$$

Since there are two planes of symmetry, all of the products of inertia drop out (xyz frame is principal set of axes). The angular momentum, $\bar{H}_A = I\bar{\omega}$, is

$$\bar{H}_A = \left(\frac{1}{12}m_s L^2 + m_c L^2\right)\dot{\psi}\,\hat{j} \qquad \text{Eq. 19}$$

To find the necessary motor torque Γ, the moments must be summed and set equal to the time derivative of the angular momentum. Point *A* is a valid location to sum moments since it is not accelerating (no longer acceptable when azimuth rotation is considered).

$$\dot{\bar{H}}_A = \{I_A\}\bar{\alpha} + \bar{\omega} \times \bar{H}_A = \left(\frac{1}{12}m_s L^2 + m_c L^2\right)\ddot{\psi}\,\hat{j} \qquad \text{Eq. 20}$$

$$\sum \bar{M}_A = M_x\hat{\imath} + \left(M_y + \frac{1}{2}Lm_s g\cos\psi + Lm_c g\cos\psi\right)\hat{j} + M_z\hat{k} \qquad \text{Eq. 21}$$

It can be determined from Figures 21 and 22 that $M_y = \Gamma$. Setting the latter two relations equal exposes the fact that $M_x = M_z = 0$. For the static situation ($\bar{\alpha} = \bar{\omega} = 0$), the moment balance degenerates into

$$\Gamma = -gL\,cos(\psi)\,(\tfrac{1}{2}m_s + m_c), \qquad \text{Eq. 22}$$

which is the static holding torque required by the elevation rotation motor. The maximum holding torque occurs at $\cos(\psi) = 1$, and is dependent on the mass of the shaft, length of the shaft, and mass of the camera. The MATLAB code provided in Appendix G calculates the holding torque across all values of ψ.

Mechanical Imaging System Component Selection

Three possible mechanisms for accomplishing the elevation and azimuth rotation are available: stepper motors, brushless DC (direct current) motors, and servomotors. Stepper motors are available in different angular step rotations per pulse. As step size decreases, control of the camera location increases in precision. Stepper motors seem to be heavier than servomotors, but also less complex. The next option for camera rotation is brushless DC motors;

these are less suitable for the task at hand since they offer the least amount of control over position. Also, there is no accurate way of measuring how far the output shaft has rotated. The last option, servomotors, are feedback controlled motors which receive a pulse-width modulation (PWM) signal instructing them to rotate the shaft to a specified angular position. Low torque servomotors are lightweight and generally low in cost, but are also the most complicated of the rotation mechanisms.

One concern with using a rotating motor is supplying the power to the second motor, which is rotating relative to the control signal and power supply (assuming power supply is placed apart from motor). In order to avoid excessive twisting of the signal/power wires, the rotation range of the azimuth rotation motor will be limited to $\pm 180°$. The two-motor system is shown below in Figure 23.

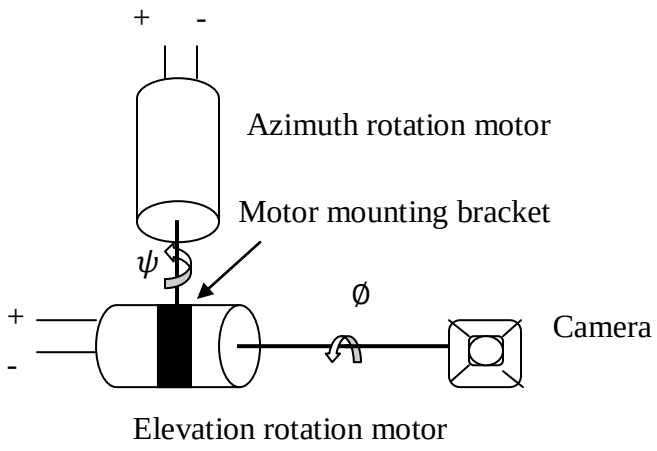

Figure 23: Motor attachment system

Elevation Rotation Motor Design

The first step in determining the torque requirement for the 90° elevation rotation servomotor was to determine the inertia of the load on the output shaft of the servomotor. A diagram of the system is shown below in Figure 24.

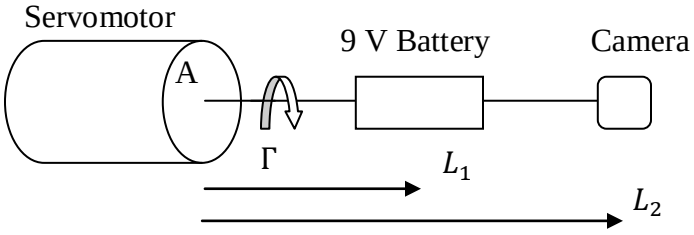

Figure 24: Elevation motor design

The torque of the motor is Γ, and the output shaft attaches to the servomotor at point *A*. The mass of a 9 V battery (m_b) is 45 g, and the dimensions are 48 mm x 25 mm x 15 mm, and the mass of the camera (m_c) is 14.2 g (see Appendix K). The camera was approximated as a cube with side length of 25 mm. Setting L_1 equal to 30 mm and L_2 equal to 70 mm yields a total inertia tensor about point A of

$$\{I_A\} = \begin{bmatrix} 7.2 & -10.13 & 0 \\ -10.13 & 133.9 & 0 \\ 0 & 0 & 133.9 \end{bmatrix} (10^{-6})\ kg\ \cdot m^2 \qquad \text{Eq. 23}$$

Summing the moments about the axis of the output shaft yields following relation, where $\dot{\beta}$ equals the angular acceleration of the output shaft:

$$\dot{\beta} = 138.9(10^3)\ \Gamma \qquad \text{Eq. 24}$$

Figure 25 demonstrates the relationship between angular acceleration of the output shaft and the required torque.

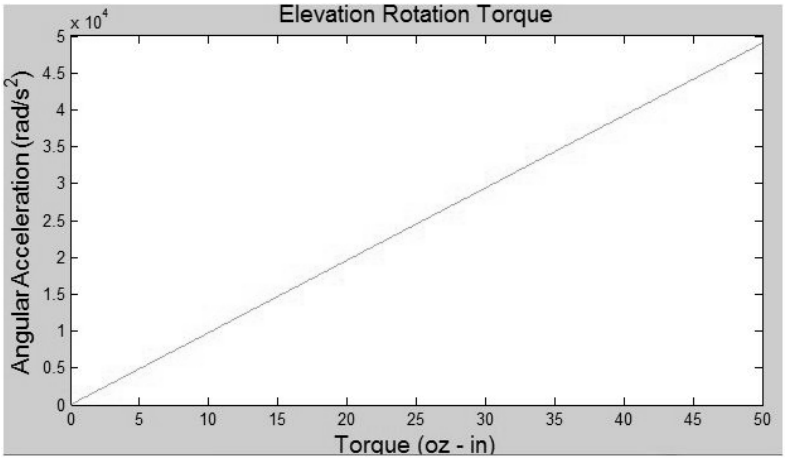

Figure 25: Elevation rotation torque

Using the above Figure, a servomotor was found which provided an output torque sufficient to generate a high angular acceleration (higher angular acceleration equates to faster user response time, and thus increases image stability). The servomotor selected was a Hitec HS-81 Standard Micro RC Servomotor (see Appendix H for data sheet).

Azimuth Rotation Motor Design

The next step in the design of the mechanical portion of the imaging system is the design of the azimuth rotation motor. The inertia that the azimuth rotation motor is required to rotate only differs by the inertia added by the elevation rotation servomotor (which is very small due to the small dimensions and mass of the servomotor) because the elevation rotation motor will be

connected directly onto the output shaft of the azimuth rotation motor. The additional inertia contributed by the elevation rotation servomotor is

$$I_{servo} = \frac{1}{12} m_{servo}(l^2 + d^2) = 1.79(10)^{-6}\, kg \cdot m^2 \qquad \text{Eq. 25}$$

where the mass of the servomotor is denoted by m_{servo}, and the dimensions relative to the inertia are $l = 30\ mm$ and $d = 20\ mm$.

Since the torque generated by the elevation rotation servomotor far exceeded the maximum (see discussion following Figure 25), and the load on the azimuth rotation motor only differs slightly

Image Stabilization

The problem of image stabilization can be broken into two categories: image noise due to high frequency vibration and image drift caused by oscillations of the balloon. The high frequency vibration of the system is caused by the high rate of rotation of the propellers. Slight imbalance in the propeller blade can transmit large vibration to the rest of the system. Oscillations of the balloon, however, are caused by displacement of the balloon due to varying, periodic, random wind force. The approach towards solving each of these problems is very different.

The task of eliminating high frequency vibration is simple in comparison to the task of maintaining image stability caused by oscillations of the platform. The problem of reducing high frequency vibration transmission can be visualized theoretically by modeling the camera and propeller assemblies (motor, propeller, and protective casing) as single degree of freedom (DOF) masses attached to ground by a joint with stiffness k and damping c. The simplified system is shown below in Figure 26.

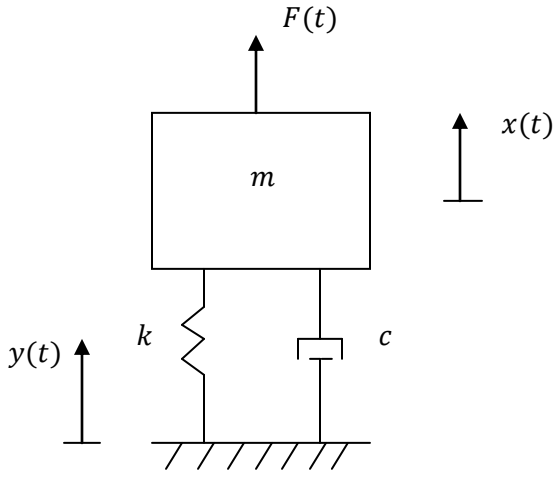

Figure 26: Simplified model for camera and propeller assemblies

The propeller assemblies can be modeled as a simple mass which is being forced by $F(t)$; the periodic forcing is caused by a rotating unbalanced mass. The frequency of the forcing can be modeled as approximately equal to the rotation rate of the propeller (the unbalanced mass). In this case, a vibration damping system can be added to remove mechanical energy from the vibration in the form of heat. The imaging system can be modeled as a mass having a moving base ($y(t)$). The damping system in both cases can be thought of as a vibration isolation system, where the goal is to minimize the force (F_{tr}) transmitted through to the base. Transmissibility is defined as

$$\frac{F_{tr}}{F_0} = \left(\frac{\left[1+\left(\frac{2\zeta\omega}{\omega_n}\right)^2\right]}{\left[1-\left(\frac{\omega}{\omega_n}\right)^2\right]^2+\left(\frac{2\zeta\omega}{\omega_n}\right)^2} \right)^{\frac{1}{2}} \qquad \text{Eq. 26}$$

The magnitude of the actual periodic force is F_0, which occurs at a frequency of ω. The damping ratio ζ depends on the mass of the system, the natural frequency ω_n, and the damping coefficient c. Important image stabilization attributes can be obtained from making observations of the frequency response of the transmissibility. The non-dimensional response of the system shown in Figure 26 is shown below in Figure 27 for varying values of ζ. See Appendix I for the MATLAB code used to generate Figure 27.

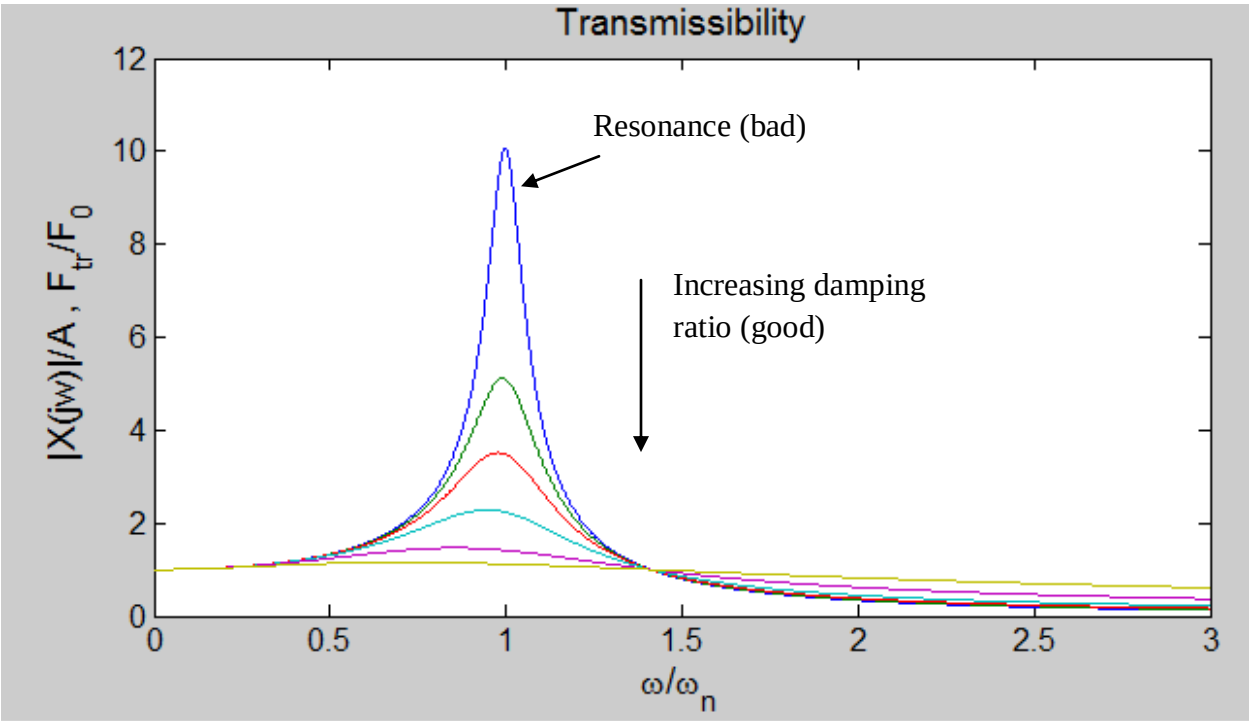

Figure 27: Transmissibility

Since the goal is to minimize transmissibility, it is desirable to have low damping coefficients and low natural frequencies. The worst possible scenario occurs when the natural frequency is equal to the driving frequency; at this point, the transmitted force becomes much larger than the actual driving force, causing large disturbances in the system. The solution to the high frequency vibration problem is therefore to change the system parameters to decrease the natural frequency and also change the damping to increase the value of ζ. This can be accomplished by changing the mounting infrastructure of the stabilization units and imaging system by using materials specifically designed for vibration isolation, such as Sorbothane (Appendix J).

The manufacturer of the Hitec HS-81 servomotor provides an accessory kit for attaching the servomotors to the supporting structure which comes with rubber dampers designed to mount onto the side bolt connections on the servomotor (see Appendix J – 1). Since the actual excitation frequency causing the high frequency vibration of the system is unknown and can only be measured via testing, matching material properties of a damper material to the characteristics of the excitation provides little useful design information. For this reason, the rubber dampers included in the servomotor accessory kit will be used to damp the high frequency vibration in the system. If it is discovered during testing that the dampers are not fulfilling their purpose, further analysis will be performed and a second material selected to provide damping. The simplicity and very low cost of rubber dampers permit the adaptation of the design at a late stage, during testing.

Electrical Imaging Design

Overview

The purpose of the electronic portion of the imaging system is to collect a live aerial video feed and transmit that feed to the ground to be made viewable on the user interface. The Requirements Specification document states that the video feed will have the capability to provide a minimum of 30 minutes of live video feed to the user interface.

System Components

The electronic component of the camera imaging system as a whole consists of three parts on the balloon and five parts on the ground. The parts in the air are the camera itself, a 2.4GHz PLL receiver, a 12 volt supply for the receiver, a SMA (sub millimeter array) antenna connector with rubber duck antenna, and two standard RCA audio/video cables that connect the video output to the user interface. Figure 28: **Imaging system** is a basic block diagram describing the internal interfacing of the system.

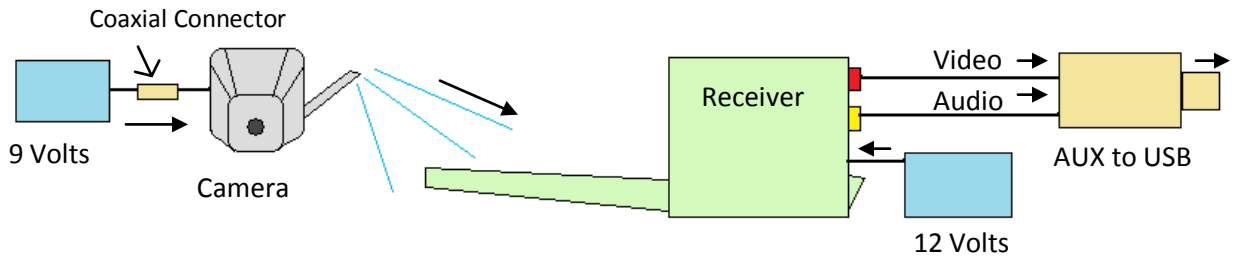

Figure 28: Imaging system

The bold black arrows indicate the direction of flow of data and power. The gray object represents the camera/transmitter, which wirelessly transmits the video feed to the user interface. The wireless broadcasting is represented by the blue lines. The green receiver collects the signal through the rubber encased antenna. Its video and audio outputs can be seen as the red and yellow connections. The blue boxes represent power supplies. The first is a 9 volt battery powering the camera, and the second is a 12 volt power supply powering the receiver. The tan boxes represent connectors and converters. The first is a coaxial connector fastening the battery to the camera. The second is called a video and audio grabber; it takes the auxiliary output from the receiver and converts it to a USB that can be plugged into a laptop.

Camera Selection

The specific camera chosen is provided by boostervision.com (see Appendix K). The criteria for camera selection consisted of factors of weight, size, image quality, wireless range, price, and availability. The following decision matrix demonstrates the justification for choosing the 2.4GHz BoosterVision GearCam.

Table 3: Decision matrix for camera selection

Category	Weight	BoosterVision	Pencil Eraser Cam	Zoom Cam	GearCam DVR
Price	0.4	4	2	1	3
Weight	0.2	5	5	2	4
Wireless Range	0.2	5	3	1	1
Video Quality	0.2	3	3	4	5
Totals:	1	4.2	3	1.8	3.2

The features include a small size and light weight 2.4 GHz wireless mini color camera. The camera also includes audio from a built in microphone. However, the audio feature will not be utilized by the system. The device has low power consumption and needs only a 9 volt battery for power. The size is 20 mm (W) by 20mm (H) by 20mm (D). These dimensions are equivalent to the size of a dime which makes the device small enough to be suitable for the aircraft. The field of view of the camera is 60 degrees, and it provides CMOS 380 TV lines of resolution. The range is said to be 91.44 to 213.36 meters (300 to 700 feet) in the air on an aircraft by the manufacturer. The camera transmission distance was successfully tested; the range was found to be greater than 45.72 meters (150 feet) outdoors on the ground. The zoom on the camera must be adjusted manually by twisting the lens with a small tool. The solution to the focusing complication is to focus the camera at infinity; this is the method used by cheap disposable cameras. This method will allow all objects at a significant distance to be in focus. Because objects from a distance of approximately 36.6 meters (120 feet) will be recorded, this method will provide adequate focus for the imaging system. The operation time of the camera was also tested using a new 9 volt battery; the operation time was found to be greater than one hour. These results surpass the requirement of 30 minutes of live video feed.

Receiver

The BoosterVision camera includes a no tuning needed PLL (Phase-locked Loop) receiver. A phase-locked loop is a control system that tries to generate an output signal whose phase is related to the phase of the input “reference” signal. The end goal of this control process is to keep the input phases matched. It has a SMA (Sub millimeter Array) antenna connector with rubber duck antenna. The input to this component is the wirelessly transmitted 2.4 GHz video and audio feed. It also requires a 12 volt power supply. The output is the auxiliary

connections. A USB video and audio grabber will be needed to convert these auxiliary connections into a format that can be used by the laptop portion of the user interface.

Platform Design

System Overview

The platform design consists of the infrastructure to secure the subsystems to the balloon and the balloon itself. The balloon must be a lighter-than-air system in order to rise on its own without the aid of the stabilization system. The main purpose of the balloon is to assist the user in getting the camera to the desired elevation specified by the user. Some of the factors that helped to determine the size of the balloon included the weights of the components needed on the infrastructure of the balloon and also the amount of helium gas needed in the balloon.

Helium Gas Design

Two potential choices for lifting gas were compared to decide which would be used to raise the balloon: hydrogen or helium. The principle governing the mass a certain body can lift when immersed in a fluid is determined by Archimedes' Principle, which states that the buoyant force exerted on a body is equal and opposite to the weight of the volume of fluid the body displaces (the buoyant force acts through the centroid of the displaced volume of fluid). After performing a dynamic analysis of a spherical balloon immersed in air, it was evident that the amount of mass the balloon could lift was proportional to the difference in density between the air ρ_{air} and the lifting gas ρ_{lg} (with the proportionality factor being the volume of the displaced air).

$$m_{sys} = V(\rho_{air} - \rho_{lg}). \qquad \text{Eq. 27}$$

Figure 29 shows a comparison of the densities of hydrogen, helium, and air over a wide temperature range. When the density of hydrogen and helium were compared to the density of air (shown in Figure 29), there was only a slight difference; therefore, for the same volume balloon, hydrogen and helium can lift almost the same mass (refer to this quantity as static lift potential). Figure 30 demonstrates the static lift potential for a spherical balloon with a one meter radius. It is clear from the figure that the lift potential of both gases is very similar.

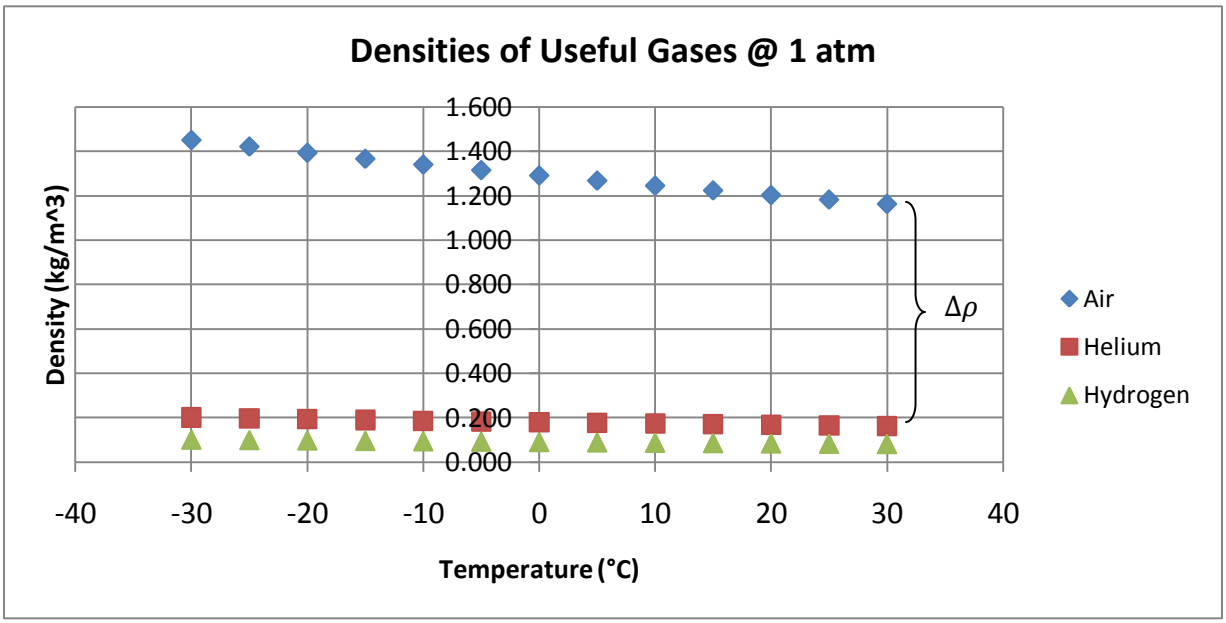

Figure 29: Densities of air, helium and hydrogen at 1 atm.

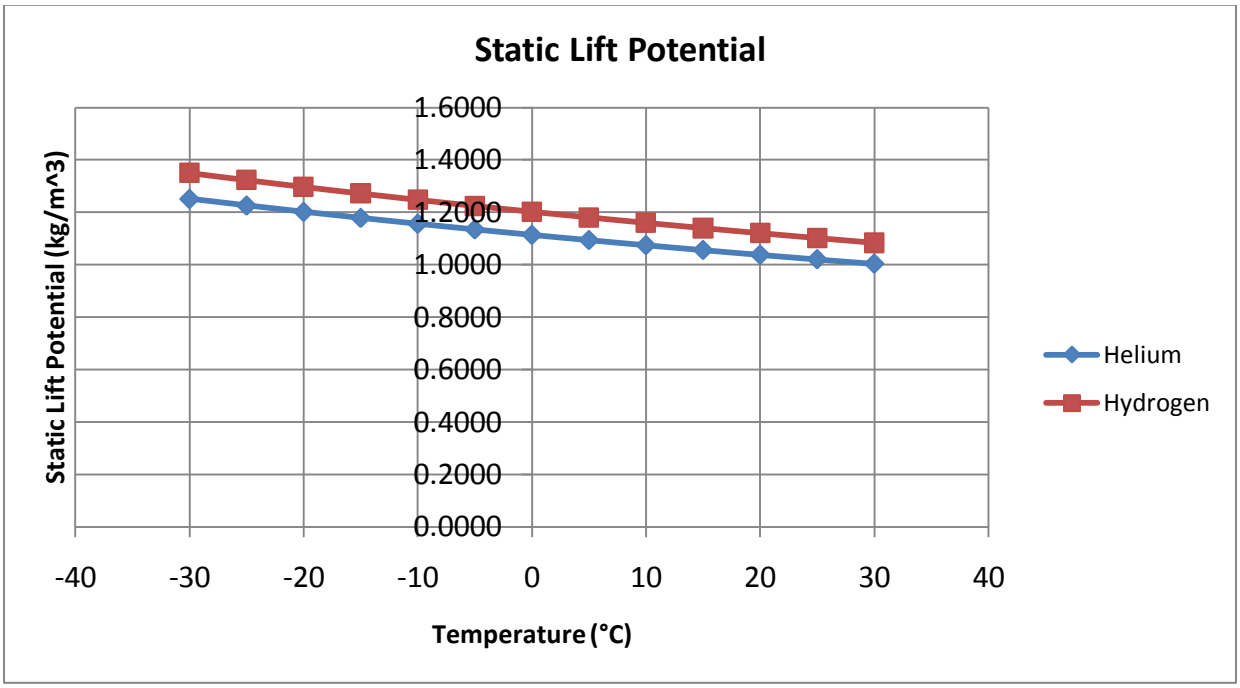

Figure 30: Static lift potential of helium and hydrogen.

Hydrogen is a highly inflammable gas, the presence of which creates substantial hazards when working with it. Helium, however, continues to increase in price for unknown reasons. Helium was chosen for use as the lifting gas because of the high safety concerns associated with

hydrogen. Airgas Company (located in Searcy, Arkansas) provided the best quote on helium at $104.00 per tank plus $0.40 per day of rental for a 220 cubic feet tank.

Platform Lift Potential

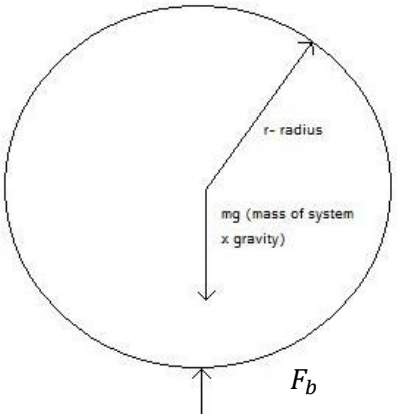

Figure 31: Balloon lift potential diagram

M_{sys} is the total mass of the system including the mass of the supporting and attachment infrastructure. The density of air (ρ_{air}) is proportional to the air temperature and pressure; the relationship is provided in Equation 28. The specific air constant (*R*), for air is 0.287 kJ/kg·K. The specific air constant for helium is 2.077 kJ/kg·K. The average temperature of Searcy, Arkansas in April, when the balloon will be tested, is 20° C (US Climate Data). It is assumed that since the system operates outdoors then the air pressure is the standard air pressure, or 101.325 kPa (1 atm). It can be inferred from Figure 32 and Equation 28 that the density of air does not significantly change as the temperature varies within reasonable environmental limits.

$$\rho = \frac{P}{R\,T} \qquad \text{Eq. 28}$$

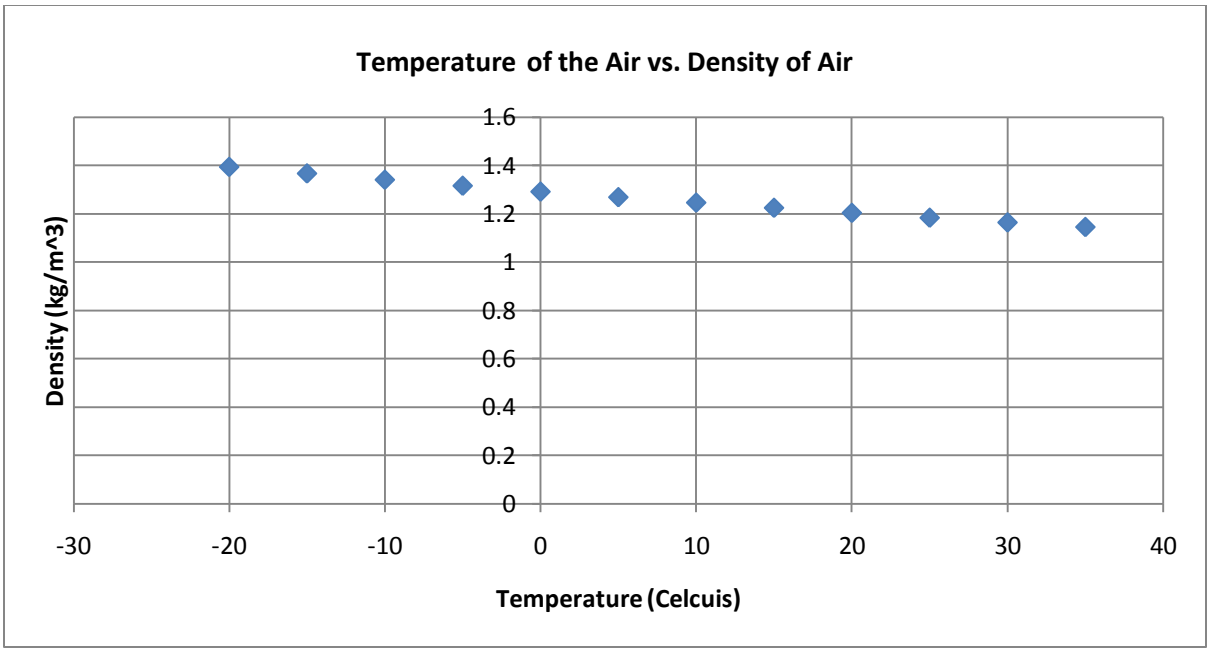

Figure 32: Graph of the density of air compared to the temperature of the air (Engineering Toolbox)

As shown in Figure 33, standard air pressure varies little between 0 m and approximately 152 meters above sea level. Searcy, Arkansas is at approximately 81 meters above sea level (www.usclimatedata.com). Since the system is only going to rise to a maximum elevation of 36.6 meters above ground (see Requirements Specification), the total elevation above sea level will be 127 meters. A significant deviation from the original standard air pressure does not occur until an elevation of 914 meters is reached; since the elevation of Searcy is much less than this, then it can be deduced that the effect of elevation change on lift capacity is negligible.

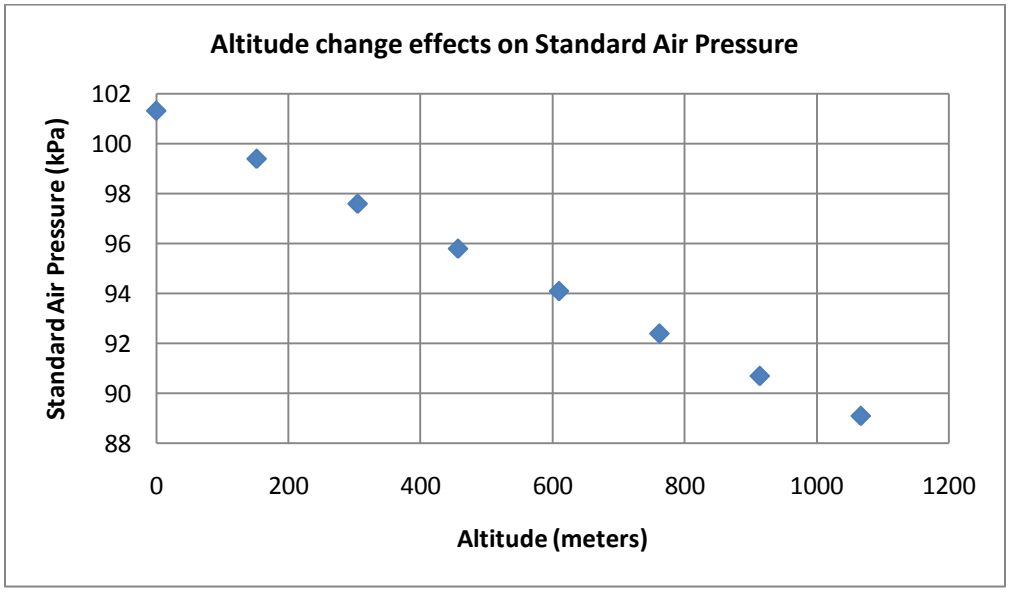

Figure 33: Altitude change vs. Standard Air Pressure

The amount of mass a spherical balloon can lift is proportional to the volume of the balloon. Since the volume of the balloon is a cubic function of the balloon radius, the amount of mass the system can lift increases exponentially as the balloon radius increases. Therefore, a slight increase in the diameter gives a large increase in lifting capabilities (shown in Figure 34).

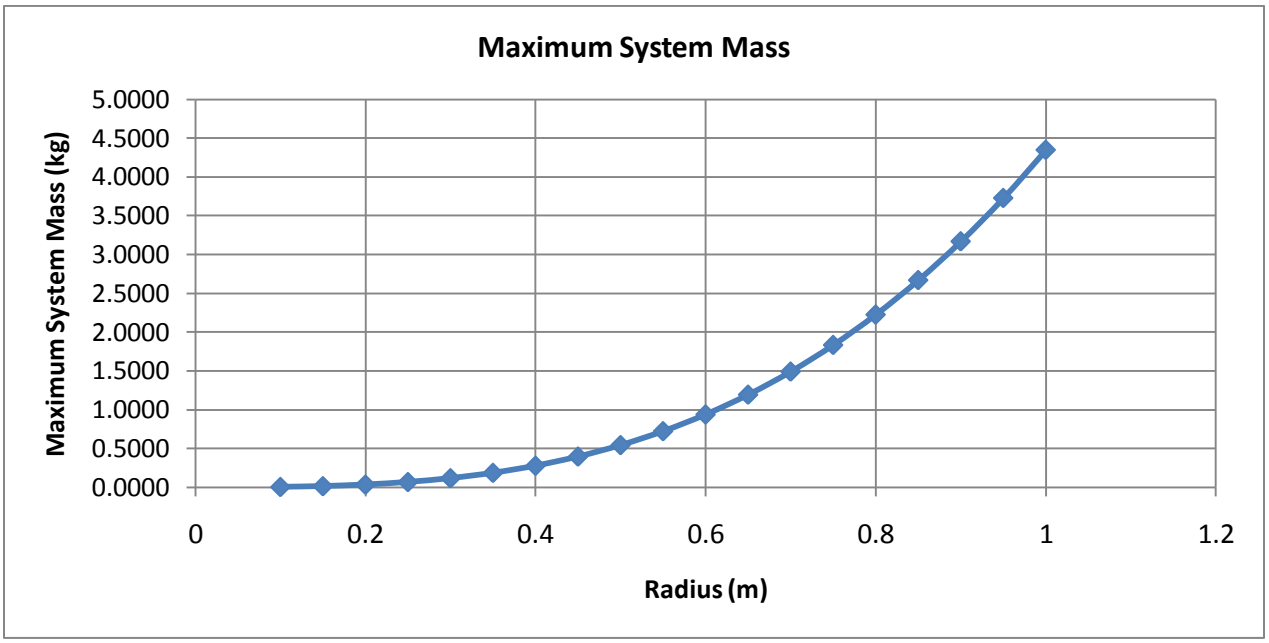

Figure 34: Maximum lifting capabilities determined by radius of balloon.

The equation to determine the required lifting capability of the balloon is:

$$r = \sqrt[3]{\frac{3M_{sys}}{4\pi(\rho_{air}-\rho_{He})}} \; or \; M_{sys} < \frac{4}{3}\pi r^3(\rho_{air}-\rho_{He}) \qquad \text{Eq. 29}$$

The mass of the system, M_{sys}, is all the components included on the infrastructure underneath the balloon. The balloon selected is 2.13 m in diameter (7 ft); see Appendix L. In order to reduce complexity and weight, the balloon will be designed to be lighter-than-air (rise on its own) rather than neutrally buoyant (buoyant force equal to system weight); this will eliminate the need for the propulsion system to lift the balloon, thus eliminating the motor needed to rotate the propellers to the vertical direction. Since the weight of the balloon itself is approximately 2.3 kg, the estimated lifting capability for the balloon is approximately 2.9 kg (a massless 1 meter radius helium balloon can lift 4.5 kg).

The system mass includes the mass of the imaging system, stabilization system, power system, wires, material to hold the components, shafts to move the camera and propellers, etc. The mass of the components are summarized in Table 4.

Table 4: System component weights.

Component	Mass (g)
Power Supply	763
Balloon	2268
Stabilization system	110
Camera	85
0.9144 meters (3 feet) PVC	218
Tethering cable	498
Other electrical components	300
Camera Motors	33.2

The combined mass of the system is therefore estimated to be 4275.2 grams. Equation 29 estimates a 2.13 m diameter balloon to be capable of lifting 5254 grams; since the system mass is predicted to be less than this value, the system will indeed be lighter-than-air.

Attachment Infrastructure Design

On the platform infrastructure, the two locations most important to consider are going to be where the tether is attached and where the propellers are attached. The infrastructure has to be able to support the combined 10 N thrust force generated by the propellers. Also, the infrastructure has to withstand the tethering force. These issues will be considered when choosing the material to construct the platform and also the methods of attachment. The material selected for the infrastructure is PVC. A finite element analysis (FEA) shows the connection to the tether and to the propeller assemblies will withstand the force from the propeller assemblies.

The results of the analysis are shown in Figures 35 and 36. The yield strength of PVC is approximately 55.15 MPa (Engineering Toolbox). The maximum stress on the infrastructure is shown in Figure 35 to be 3.8 MPa, yielding a factor of safety is 14. There is a 5 N force at each end of the pipe where the four bolts are connected to the PVC pipe. The stress could be reduced by shortening the length of the PVC, if needed. The PVC is 1.27 cm diameter (1/2 inch). The deflection of the infrastructure due to the 10 N force is minimal. The deflection is approximately 0.00716 meters, as shown in Figure 36.

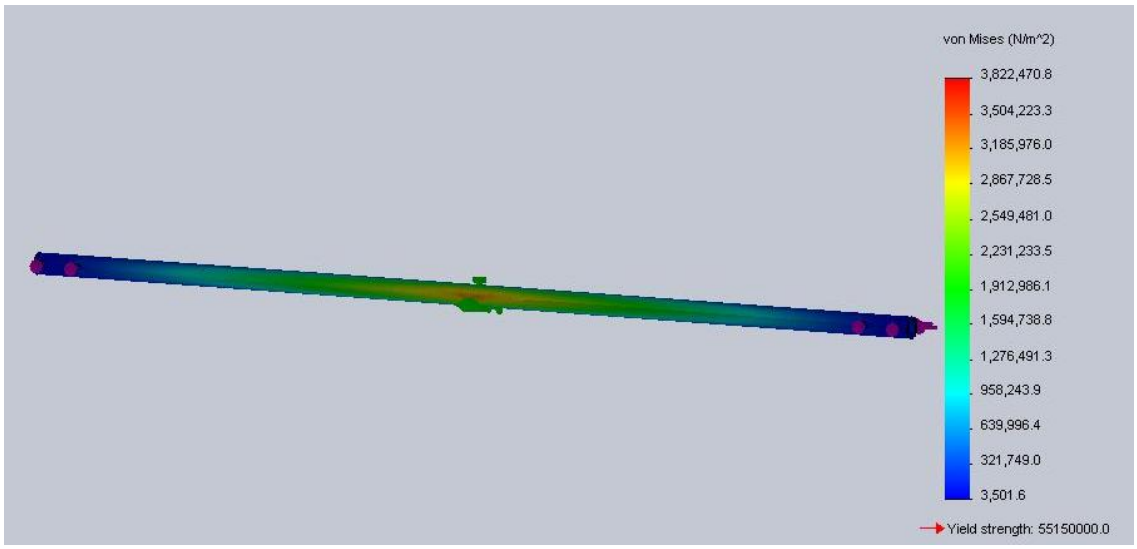

Figure 35: Stress analysis of the PVC pipe.

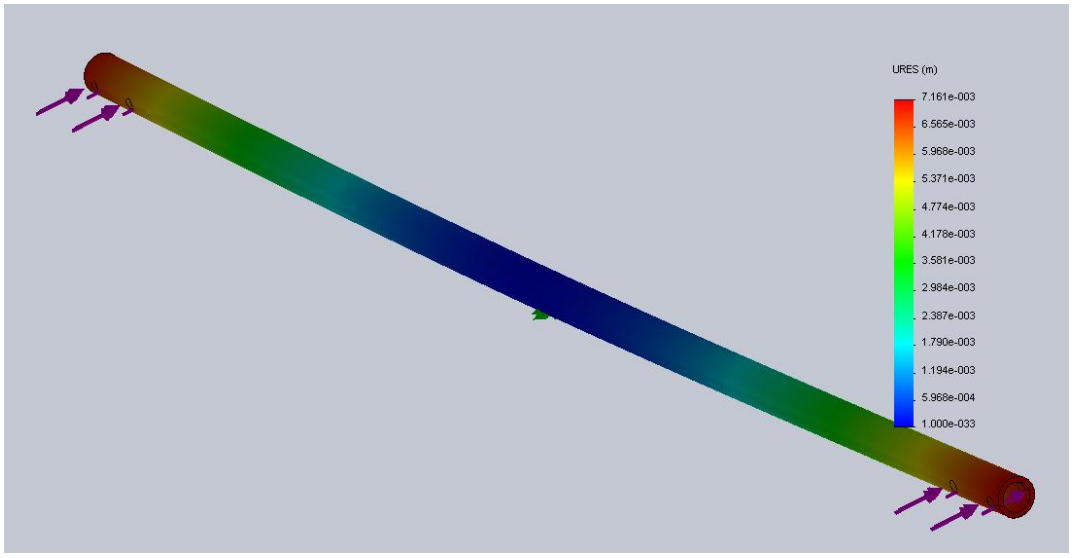

Figure 36: Deflection of the pipe from the 10 N force.

The actual attachment of the motor and propeller combination to the PVC is accomplished using bolts. There is a bracket attached to the back of the motor (see Appendix E) for Hacker A20-20L motor) which then can be attached with four screws onto an aluminum circle cut-out. Two bolts will hold the aluminum to the PVC. The attachment is shown in Figures 37 and 38.

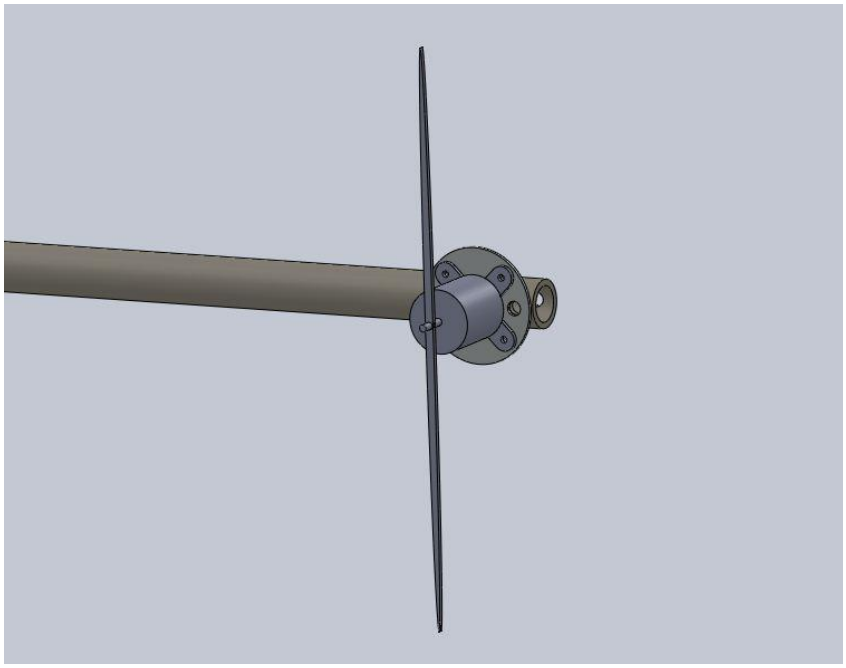

Figure 37: Propeller and Motor attachment to the PVC.

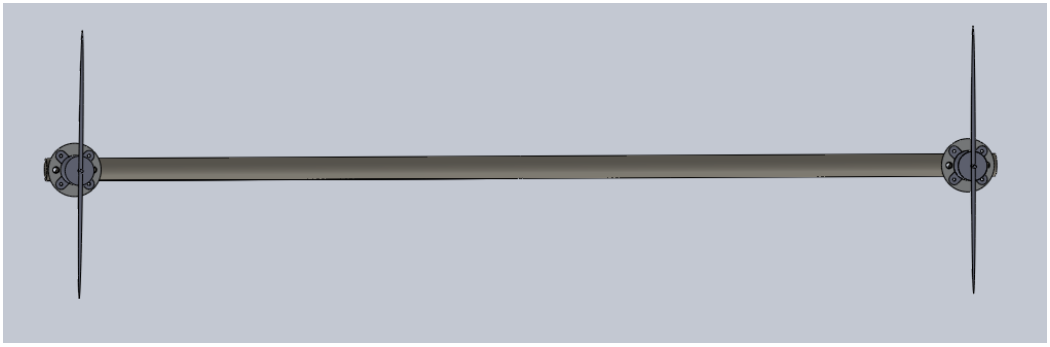

Figure 38: Attachment of stabilization system.

The bottom of the balloon has four connections for a payload attachment; these attachments are a feature of the balloon purchased. The four attachments are shown in Figure 39 The mounting rings will be connected onto the balloon infrastructure via a rigid attachment.

Figure 39: Infrastructure attachment to balloon.

The camera will be attached to a system of two motors. The first motor will be bolted to the PVC with two screws. The second motor will be attached with a bracket to the first motor, and the camera itself will be glued to the rotating arm attached to the second motor's output shaft. The 9 V battery will be attached via a battery case for the purpose of changing the battery once the battery loses charge. These connections are shown in Figure 40.

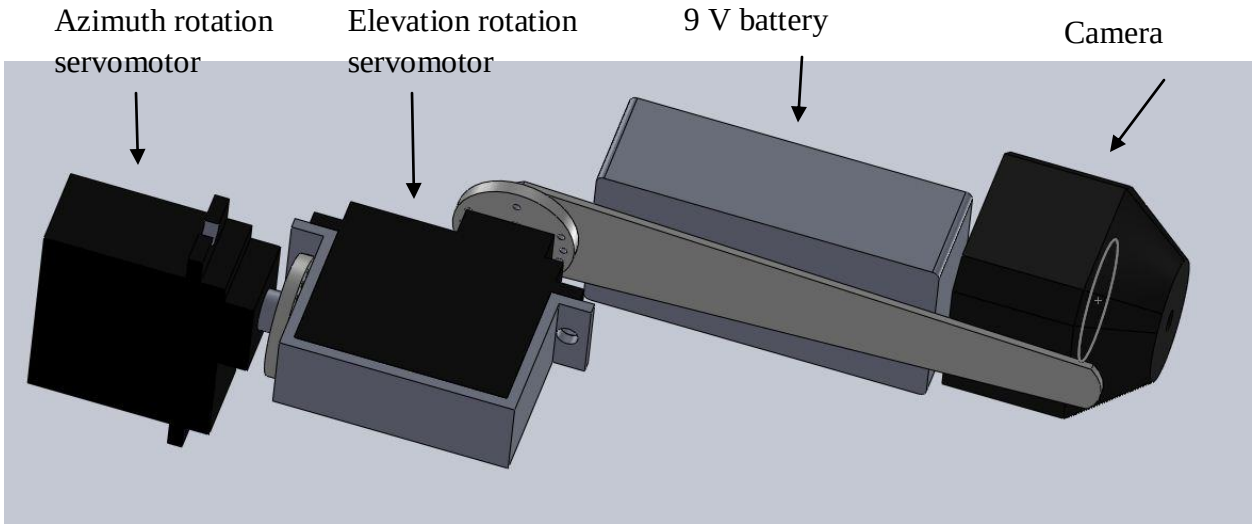

Figure 40: Attachment of camera and 9 V battery to the second motor.

There are also five lithium polymer batteries that will be attached to the PVC infrastructure. Each battery will be placed into a metal case to fit the battery. The case will be screwed into the PVC; this is shown in Figures 41 and 42 .

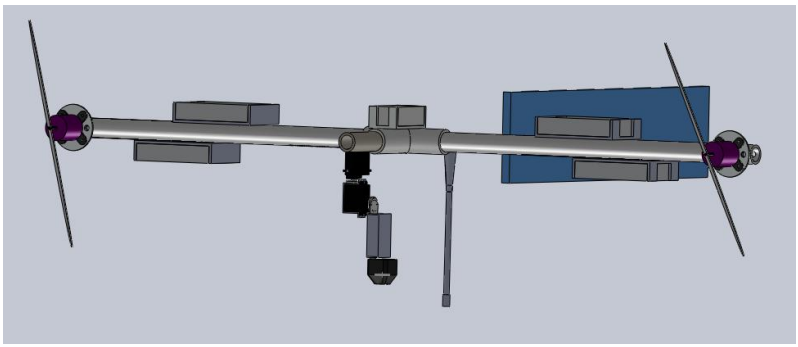

Figure 41: Placement of five lithium polymer batteries.

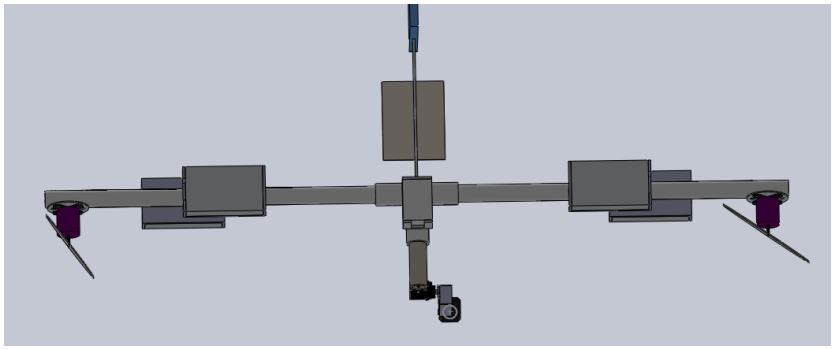

Figure 42: Another view of the placement of the batteries.

The entire system design of the platform infrastructure is shown in Figures 43, 44, and 45. These figures show where the placements of the components are going to be. Also, the symmetry of the design is evident; symmetry is beneficial, as it keeps the center of gravity along the center of the balloon.

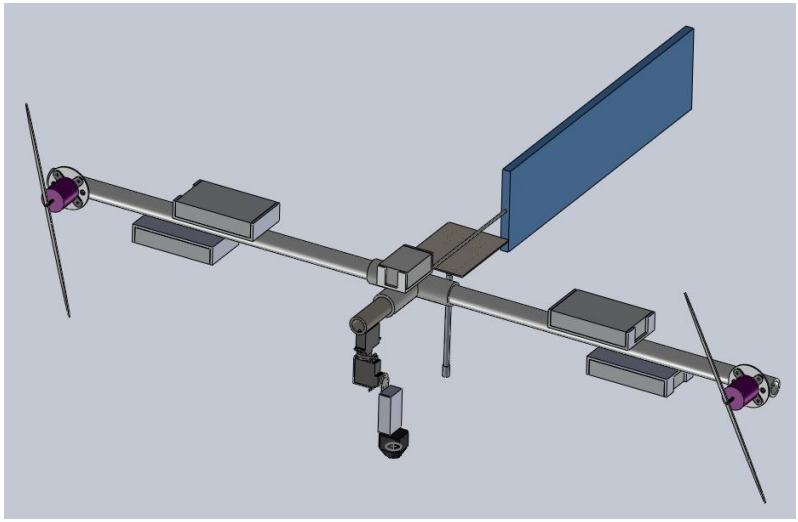

Figure 43: Attachment of major subsystems.

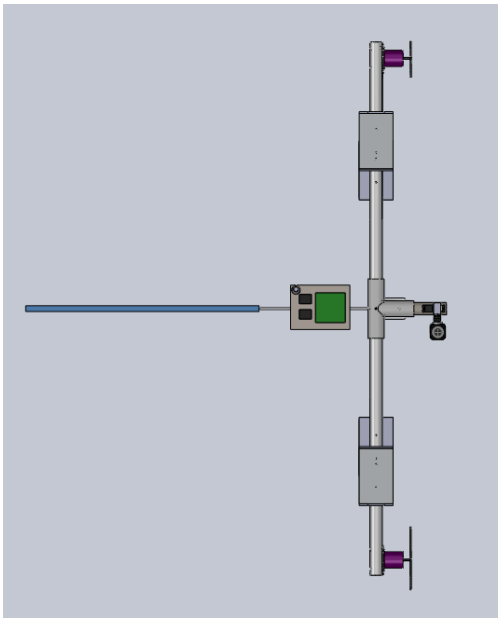

Figure 44: Bottom view of the infrastructure design.

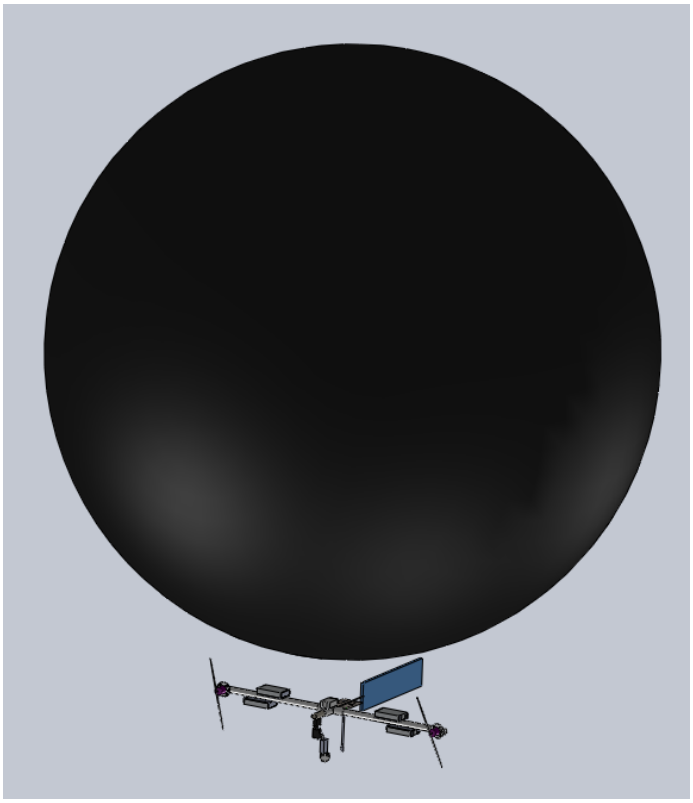

Figure 45: Comparison between platform infrastructure and balloon dimensions.

Tethering Design

Overview

The purpose of the tethering system is to secure the system to the ground and also to reel in the platform from the desired elevation. The two factors primarily affecting the design of the tethering system are how much the entire system will weigh and also ensuring the system is small enough to fit in the 0.425 meters (15 cubic feet) requirement. The tethering cable must be able to support the stress generated by the balloon pulling upwards and the user reeling the system in. It can be assumed that the vertical acceleration of the system is negligible, since the user can dictate the rate at which the balloon rises by adjusting how much tethering cable is released.

System Components

1. Tethering cable
2. Reeling mechanism and supporting infrastructure

Tethering Cable Tension

The relation to determine the needed strength of the tethering cable is shown in Equation 30. Since the acceleration of the system is negligible when the system has reached the desired height, the system can be modeled as a static system, where the sum of the forces is zero. The tension, T, determines the required strength of the tethering cable material.

$$T = \left[(\rho_{air} - \rho_{He})\frac{4}{3}\pi r^3 + M_{sys}\right]\left(9.81\frac{m}{s^2}\right) \quad \text{Eq. 30}$$

The mass of the system, provided in the platform design, is 4037.2 grams and the radius of the balloon chosen is 1.065 meters. Also, the density of air is 1.204 kg/m^3 and the density of helium is 0.1664 kg/m^3. With this equation, the tension in the cable is 91.1 N. The material selected for the tethering cable is 6.35 mm diameter (0.25 inch) hollow braid polypropylene. This material can withstand up to 4404 N (990 lbf).

The force on the reeling system is calculated by subtracting the system weight from the buoyant force cause by the displacement of air by the balloon. Equations 31 and 32 show the required reeling force calculations:

$$F_{net} = F_{buoyancy} - M_{He}\, g - M_{sys}\, g \quad \text{Eq. 31}$$

$$F_{net} = (\rho_{air}\, g\, V_{balloon}) - \rho_{He}\, V_{balloon}\, g - M_{sys}\, g \quad \text{Eq. 32}$$

From Equations 31 and 32, the net force on the reeling system is 11.9 N; this is also the required force of the user to reel in the system. A Bayco deluxe reel with stand will be used as the structure; it is shown in Figure 46.

Figure 46. Reeling system for tether rope.

As stated in the FAA regulations provided in Appendix A, a bright colored flag must be attached for every 15.24 meters (50 feet) of tethering cable released. Plastic pennant flags will be attached to the tethering cable to fulfill this requirement, and since only 36.6 m of cable is required, only two pennants will be needed. The mass of the plastic pennant flags is negligible.

Power Supply Design

Overview

The objective of the power supply is to fulfill the following requirement from the Requirements Specification document:

> "The power system should allow for a minimum of 1 hour flight time and also a minimum of 30 minutes of live video, not necessarily continuous, from the imaging system."

The components of the system requiring power are the brushless motors driving the propellers, the servomotors providing mechanical imaging rotation, the microprocessor, the receiver, and the decoder which transforms the user input signal from the receiver to a form useable by the microprocessor.

The components consuming the largest amount of power are the motors of the stabilization system. The servomotors providing the 360° azimuth rotation and 90° elevation rotation of the imaging system consume the next highest amount of power. The microprocessor, receiver, and decoder all consume far less power than either of the previously mentioned components. Note that the interface between the power supply and the communication system is referenced in the Communication System Design.

Selection of Power Supply for Propeller Motors

The motors driving the propellers of the stabilization system require large amounts of power due to the high rotation rates of the motor output shafts. The battery required to provide power to the motors must be capable of meeting the power requirements necessary to generate the required amount of thrust.

The primary concern in the selection of the power supply for the propeller motors was the need for a battery capable of providing substantial amounts of current (in the range of 10 - 12 A). To address this concern, two options were available; the first option was to utilize a conventional battery with a high capacity, on the order of approximately $10 - 12\ A\ h$. The second option was to use a battery with a high discharge rate. Due to concern over the maximum weight of the system, it was deemed more feasible to use a battery with a high discharge rate rather than a large capacity. Also, a battery with a high discharge rate can provide large bursts of current only when large gusts of winds demand it. In order to keep operating costs low for the users of *Sky Vision*, the batteries selected to provide power must be rechargeable.

Several alternatives were examined in order to select the design which best fit the needs presented in the prior discussion. The first alternative was to provide power through the

tethering cable and utilize a lead-acid battery on the ground to provide the required power. However, it was found that the weight of 36.3 m of wire of a gage large enough to handle 10 – 12 A of current was substantially large, and far exceeded the lift capabilities of the balloon. Also, the cost of both the cable and the lead acid battery exceeded the cost of batteries light enough to be mounted on the balloon.

The next option for power supply was lithium polymer batteries. Lithium polymer batteries were selected to provide power to the stabilization system for several primary reasons. First, lithium polymer batteries have a high energy density: they can provide large amounts of power for small battery weights. Due to this, the weight of the lithium polymer batteries was smaller than any of the aforementioned options. Next, the batteries are capable of being easily recharged. Also, the manufacturer of the propeller motors recommends using an 11.1 V, 3 cell lithium polymer battery pack for providing power to the motors.

The specific battery selected to provide power to the stabilization system is an 11.1 V, 3 cell (3S) lithium polymer battery with a battery capacity of 2.5 $A\ h$ and a maximum discharge rate of 10 – 12 C (this is discussed in relation to the worst case scenario for power requirements and run time in the following pages). The mass of each battery is 175 g. The 3S lithium polymer battery is shown below in Figure 47. The dimensions of each battery pack are 58mm x 95mm x 19mm.

Figure 47: 11.1 V, 3S lithium polymer battery

The next step in the design of the power supply was to determine the quantity of 11.1 V, 3S lithium polymer battery packs needed to provide the correct amount of power to the stabilization system

Estimating Required Power of Propeller Motors

The power consumed by each motor driving the propellers in order to generate 5 N of thrust each is 130 W (see thrust calculators on in Stabilization System Design). 5 N of thrust corresponds to the worst case scenario corresponding to the wind speed causing the maximum drag on the balloon (wind speed of approximately 3 m/s).

The first step in determining battery life was to determine a relationship between supplied power and battery longevity. Battery longevity for a 2.5 $A\ h$ battery can be obtained via the following formula:

$$Battery\ Longevity = \frac{(11.1\ V)(2.5\ Ah)}{P_{supplied}}\left(60\frac{min}{h}\right) \qquad \text{Eq. 33}$$

In Equation 33, $P_{supplied}$ is the power supplied by the battery to the motors (dependent on thrust force needed), the voltage of the batteries is constant at 11.1 V, and the capacity of the batteries is 2.5 $A\ h$. Table 5 provides data for battery longevity versus wind speed, where the power supplied to each motor is proportional to the wind speed on the balloon.

Table 5: Battery longevity

Wind Speed (m/s)	Battery Longevity for one 2.5 A h batteries per motor (minutes)	Battery Longevity for two 2.5 A h batteries per motor (minutes)
3.0	12.5	25.0
2.8	13.6	27.3
2.5	15.0	30.0
2.3	16.7	33.3
2.0	18.8	37.5
1.8	21.4	42.9
1.5	25.0	50.0
1.3	30.0	60.0
1.0	37.5	75.0
0.8	50.0	100.0
0.5	75.0	150.0
0.3	150.0	300.0
0.0	NA	NA

It is evident from Table 5 that a runtime of 60 minutes (as specified in the Requirements Specification) can only be obtained via a single 2.5 $A\ h$ battery when the average wind speed over the entire hour is approximately 0.7 m/s (1.5 mi/h).

Table 6 contains average wind speed data per month for Little Rock, Arkansas. It is clear from the table that the average wind speed in March thru April (when testing occurs) is approximately 4.0 m/s.

Table 6: Average wind speed for Little Rock, AR

	Average Wind Speed (mph)	Average Wind Speed (m/s)
January	8.4	3.8
February	8.9	4.0
March	9.6	4.3
April	9	4.0
May	7.6	3.4
June	7.1	3.2
July	6.7	3.0
August	6.3	2.8
September	6.6	3.0
October	6.8	3.0
November	8	3.6
December	8.1	3.6

Though the average wind speed in the aforementioned months is approximately 4.0 m/s, the actual wind speed varies about the average speed according to the Rayleigh distribution (Gipe 2004). The Rayleigh distribution for wind speed is

$$f(V) = dV\ \left(\frac{\pi}{2}\right)\left(\frac{V}{V_{avg}^2}\right)e^{\left(-\frac{\pi}{4}\left(\frac{V}{V_{avg}}\right)^2\right)} \quad \text{Eq. 34}$$

where dV is the wind speed bin width, V is the speed of the wind speed bin, and V_{avg} is the average wind speed. Plotting the above function in MATLAB for a wind speed of 4 m/s yields the following distribution for Little Rock, Arkansas.

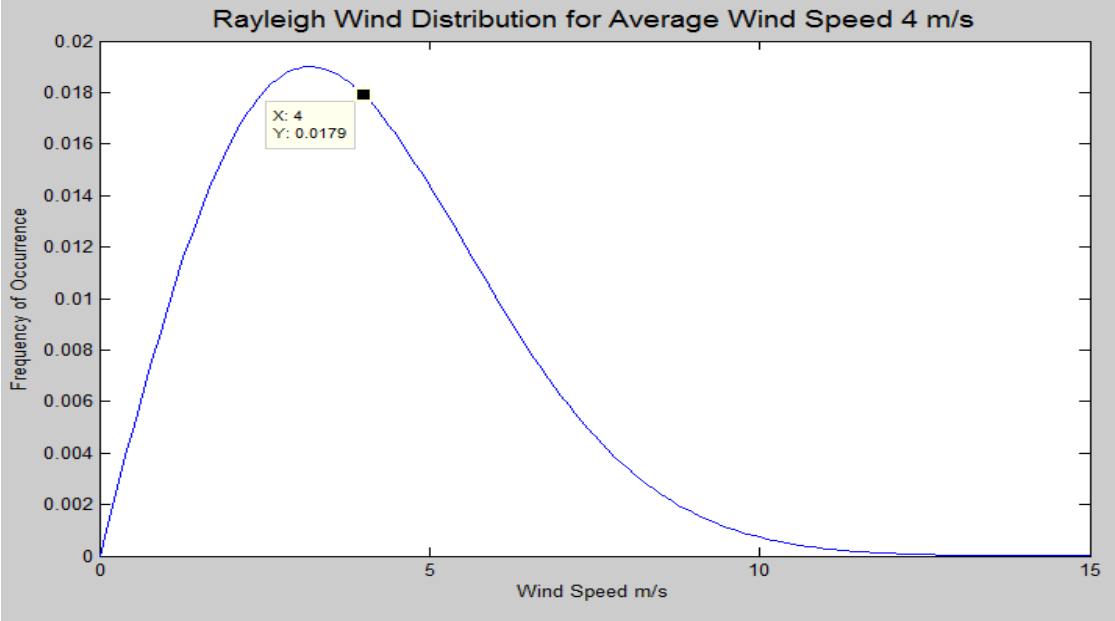

Figure 48: Rayleigh wind distribution for average wind speed of 4 m/s

Summing the frequency of occurrences of a range of wind speed bins provides the frequency of occurrence of a range of wind speeds. Since 3 m/s is a worst case scenario, summing from 2.5 m/s to 3 m/s will give a frequency of occurrence of the worst case wind speed range. The frequency of occurrence for a range 2.5 m/s to 3 m/s is 11% (found using MATLAB). Therefore, even on a day with an average wind speed of 4 m/s, the worst case range occurs only 11% of the total time. Since the drag force of the wind on the balloon drops drastically at 3 m/s, wind values between 4 and 5 m/s only require low values of power to the propeller motors to stabilize against wind. Dividing the runtime calculated in Table 5 for a worst case scenario of 3 m/s winds by the frequency of occurrence for the worst case range of 2.5 – 3 m/s wind range gives an approximate expected runtime of 112.6 minutes.

The approximation, however, assumed that the propeller motors are not running except when the wind speed is in the worst case scenario range and also that each propeller motor is connected to a single 11.1 V, 2.5 $A\,h$ battery. To account for compensating for wind speeds at all times (not merely the worst case scenario), it is assumed that the influence of all other wind speeds on battery longevity is equal to the influence on battery longevity of the worst case wind speed range. Since both wind speed ranges have the same effect, the prior mentioned run time accounting for only the worst case range is essentially halved, causing a run time of 56.3 minutes.

Since the projected run time is less than that dictated by the Requirements Specification (60 min.), further capacity must be added to the power supply system. The further capacity will be accomplished by adding another battery of equal capacity to each propeller motor. The addition of more power than necessary will incorporate a factor of safety into the power supply

system, which will allow for days on which the wind speed distribution does not fit the Rayleigh probability density function curve and instead has a higher frequency of occurrence of the worst case wind speed range.

Estimating Power Required by Other Power Consuming Systems

The four other systems requiring power (other than the camera, which operates on its own 9 V power supply) are the two servomotors providing imaging rotation (6 V and 0.5 A, see Appendix H), the microprocessor (5 V and 48 mA, see Appendix N), the decoder for the controller receiver (5 V and 670 μA, see Appendix T), and the controller receiver itself (5 V and 5.2 mA, see Appendix T). The combined power of all the aforementioned components is 6.3 W; therefore, 30 minutes of run time for the system requires 3.15 $W\ h$.

Due to the light weight of the lithium polymer batteries, a lithium polymer battery will also be used to provide power to all other power consuming components. Since only 3.15 $W\ h$. are needed, another 3 cell lithium polymer battery with lower energy (11.1 V 830 mAh) will be used, as opposed to the 3 cell lithium polymer batteries used by the stabilization system. The battery selected for providing power to all other power consuming systems is a 3 cell 11.1 V, 830 mAh lithium polymer battery with the following capacity in $W\ h$:

$$Capacity = 11.1\ V\ (0.83\ A\ h) = 9.21\ W\ h \qquad \text{Eq.}$$

Since the required capacity was 3.15 $W\ h$, the 3 cell 11.1 V 830 mAh lithium polymer battery will be capable of providing power for the required 30 minutes of run time. The battery selected is shown below in Figure 49.

Figure 49: 11.1 V 830 mAh, 3S lithium polymer battery

The mass of the battery is 63 g and the dimensions are 36 x 53 x 21 mm. The cost of the battery is $10.00.

Power Supply Schematics

The advantage of wiring batteries in parallel is an increase in the $A\,h$ capacity of the batteries while preserving the same voltage of just one of the batteries. Since the motors require 11.1 V and a high battery capacity, it is judicious to wire the batteries providing power to the stabilization system in parallel. Another advantage of wiring the batteries in parallel is that it removes the possibility of one propeller motor running out of power before the other propeller; this situation would cause a net moment about the system's center of gravity, causing unwanted azimuth rotation of the system. The output of 11.1 V will be connected to the power supply of the propeller motor's control circuits. Note that that the 'central power system' refers to the power supply of the microprocessor, decoder, receiver, and imaging rotation servomotors.

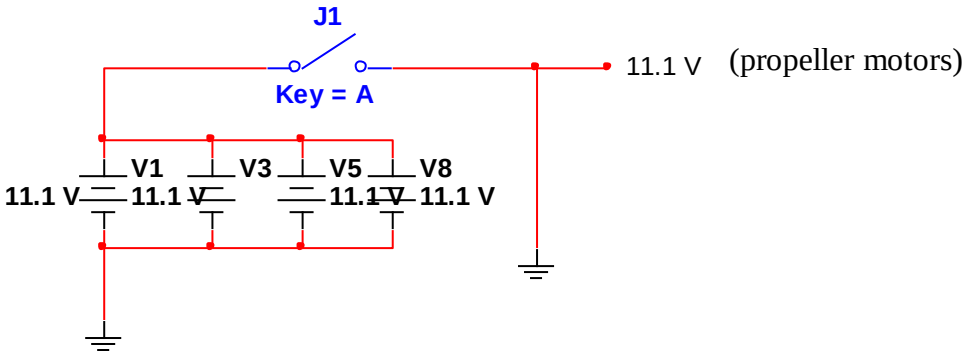

Figure 50: Schematic of four 11.1 V 2.5 Ah batteries

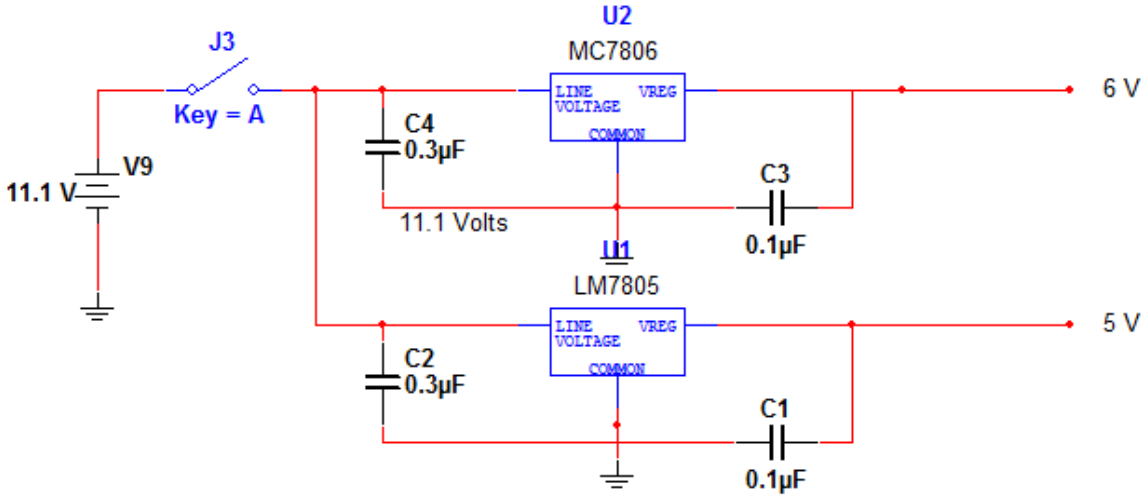

Figure 51: Schematic of central power system

Voltage regulators will be used to drop the 11.1 V down to 6 V and 5 V. Voltage regulator MC7806 will be used to drop the voltage from 11.1 V to 6 V, and voltage regulator LM7805 will be used to drop the voltage from 11.1 V to 5 V (see Appendix P for data sheets of voltage regulators). .The two servomotors providing imaging rotation will draw the 6 V from the power supply circuit (Figure 51). The output of 6V will connect to the power supply of servomotors control circuit. The 5 V power branch will provide the necessary power to microprocessor and the decoder for the controller receiver. The output will connect with the power supply pin of microprocessor and the decoder.

The reason that the smaller capacity battery will not be in parallel with the other four batteries was obtained by analyzing the work down by the previous blimp senior design group. The prior group found that electrical interference noise from the propeller motors is significant, and will interfere with the camera: to minimize this noise, the power supply of the imaging rotation motors and microprocessor will be separated from the power supply of the propeller motors.

Although the central battery can also provide the surplus power to the propeller motors when they are in parallel, the surplus power of (9.21Wh-3.15Wh)/2=3.03Wh for each propeller motors is insignificant when compared to the maximum of 130W drawn by each propeller motor. Therefore, the best scenario is to provide power to the central power system from a source independent of the propulsion motor's power supply.

Wiring Selection

One issue with using large amounts of current is that conventionally available 18 gage wire cannot withstand the current required to drive the stabilization motors. A lower gage of wire is therefore needed for use in the stabilization system. Selecting an appropriate gage for the wiring depends on several factors. The first factor is the type of wiring desired, as the type of wiring dictates how much current the wire gage can withstand before failure. The two types of wiring are power transmission wiring and chassis wiring. Power transmission wiring is wiring in which open air is allowed to dissipate the heat generated by the wire. Chassis wiring, however, is wiring in which the space is enclosed and the heat is not dissipated, leading to increased wire temperatures and corresponding increases in internal wire resistance. Since the system will be in the air and the wiring external, the wire gage should be selected based on the current estimates for power transmission wiring.

The next criteria influencing wiring selection is the internal resistance of the wire gage. Higher gage of wire (smaller diameter wiring) typically involves higher values of resistance per unit length. Large values of resistance per unit length are undesirable, as they introduce transmitted power loss through conversion of electrical energy to thermal energy.

The last criteria influencing wiring selection is the weight of the wire. A lower gage of wire is much heavier than a higher gage, due to the increased diameter of the wire. It is therefore beneficial, for the sake of weight, to select the wire which meets a large current requirement, without far exceeding the necessary gage.

The current requirement for the wire gage was set at a value exceeding the maximum burst current from the lithium polymer batteries supplying power to the stabilization system. The maximum current draw of each propeller motor is specified by the manufacturer to be 15 A continuous current, though the projected maximum draw of the propeller motors in this application is 12 A (to generate 5 N of thrust per motor). Since the power supply of batteries is in parallel, the maximum current through the wire is 30A. From the American Wire Gage Table, a wire gage of 7 will be selected. The maximum power transmission current of 7 gage wire is 30 A, the internal resistance is 1.634 ohms/km, and the wire diameter is 3.7 mm.

Communication System Design

Overview

The purpose of the communication system is to maneuver the balloon and camera positioning according to user inputs from the ground. The communication process begins when the user manipulates a hand held controller. These movements are converted to a signal that is wirelessly transmitted at a frequency originally planned to be 2.4GHz. This signal is picked up by a receiver mounted on the system. This receiver is interfaced with a microprocessor which interprets the signal from the ground. The microprocessor outputs the appropriate pulse width modulated signal to the motor control circuit. The motor control circuit sends power in the correct direction through the propeller motors and camera rotation motors causing the system and camera to respond according to the user's instruction.

System Components

The communication system can be broken down into three major components. The first component consists of the hand held radio controller and includes both the transmitter and receiver. A microprocessor makes up the second major component. It must be programmed to interface with the receiver and interpret the input signal into outputs that can be used by the motors. The third major component consists of all the necessary motor control circuitry which sends the necessary power to the motors. The figure below is a basic block diagram describing the original internal interfacing of this system before significant design changes were made.

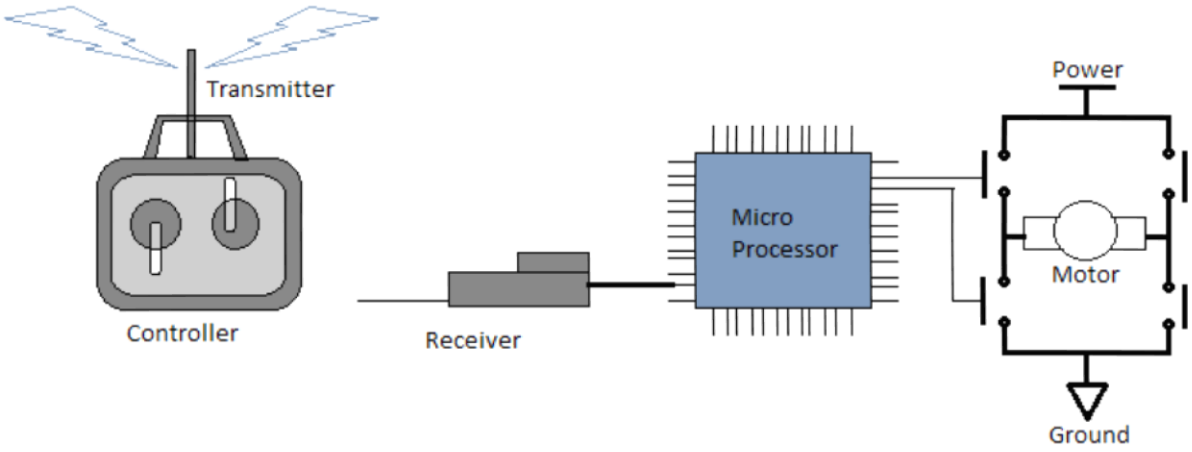

Figure 52: Communication system

Controller

The original controller chosen is the Exceed RC 2.4GHz Radio Control System. This programmable device was thought to be perfect for the system because it is typically used for small RC helicopters. The low cost of approximately 45 dollars made it financially attractive as well. This component will take the user manipulations and transmit them to the system.

Figure 53: Initial RC controller

Features include a six channel transmitter complete set with receiver. Controls allow for complete forward/backward, left/right, up/down, and pitch control. It uses a rotor head for precision and smooth movements; it claims it can display great stability and precision for 3D flight; this stability may aid the system greatly with the task locking the camera onto a stationary object on the ground particularly during windy situations. The system uses frequency modulation and a frequency of 2.4GHz. It is capable of simultaneously controlling three servo motors. A main concern is whether it will be possible to control all four motors with the device. If only three motors can be controlled at a time, then perhaps one of the three signals can be utilized as a "switching" signal. If this signal was set one way, then the other two signals could control the propeller motors. If the signal were set the other way, then the remaining signals could control the camera motion. Because the device is programmable, it will be possible to modify the signal output to conform to the system needs. Another solution to having three outputs would be to control both propeller motors using the same signal.

All of the above assumptions made it seem that the communication system was basically designed except for the programming of the device. This assumption turned out to be false upon further research. First of all, upon contacting the manufacturer of the camera, it was made clear that some 2.4GHz RC controllers interfere with the 2.4GHz GearCam. Upon researching the

non-interfering 2.4GHz radios, it was discovered that one would cost between three and five hundred dollars. Second of all, research lead to the realization that the device was designed for a very specific application. The tutorials for programming the device made it evident that user manipulation of a single control would cause outputs on multiple receiver channels. For the sake of simplicity in programming balloon control, it is desirable for each input from the user to affect one output. However, with the Exceed RC, each input will necessarily produce multiple outputs. The fact that the device was programmable led to the false conclusion that it could be conveniently modified to fit the needs of *Sky Vision*. Therefore, a new control option needed to be chosen for the project.

Alternative Controller Selection

The following decision matrix was formulated after extensive research of available transmitters and receivers. The main factors considered in the purchasing decision included adequate number of transmission channels, adequate transmission range, and a price low enough to fit within *Sky Vision's* budget.

Table 7: Decision Matrix for transmitter

Decision Matrix for Transmitter							
		Firefly	Fireblade	205 Trans	204 Trans	OTX-315-HH-LR8	CMD HHLR MD-315
Manufacturer		Rfsolutions	Rfsolutions	Rfsolutions	Rfsolutions	Linx Tech	Linx Tech
Receiver Size	0.2	1	1	2	2	5	5
Receiver Price	0.2	2	2	2	2	5	5
Price	0.2	3	2	3	2	4	5
Range	0.2	2	5	3	3	4	4
Channel #	0.2	5	5	5	5	5	2
		2.6	3	3	2.8	4.6	4.2

The OTX by Linx Technologies was selected as the replacement transmitter for the system (see Appendix S); it is also called the MS long range handheld transmitter. The handheld transmitter cost less than $40.00, had a transmission range of 304 m (1000 ft), and comes with an eight button option. This device is available to purchase in a number of different available frequencies. The linxtechnologies.com website gives a very helpful recommendation for this exact topic. The website says 315MHz is primarily used for remote keyless entry and garage door openers. As a result, this frequency is somewhat crowded. In addition, the FCC allowed power is lower than for other frequencies, and selection of antennas is limited. 418MHz is a good to use in the U.S. as it is not very crowed. Therefore, it has less chance of encountering interference and performs better. 433.92MHz is not good in the U.S. due to the chance of interference from amateur radio and the nearby pager band. 902-928MHz modules are more expensive due to the more complex filtering and modulation required for link reliability at these higher frequencies. The option of 2.4GHz was immediately ruled out due to the risk of camera

interference. Based on the website recommendations, the 418MHz version of the transmitter was selected.

Figure 54: Transmitter

The MS Long-Range Handheld transmitter is ideal for general-purpose remote control and command applications that require longer transmission distances. It will be configured with 8 buttons to meet *Sky Vision* control needs. It contains an on-board MS Series encoder. This encoder enhances ease of use and security and allows instant creation of up to 2^{24} unique addresses without cumbersome dip switches. When paired with a MS Series decoder, transmitter identity can be determined and button functions can be established. The unit is powered by a single 3V CR2032 lithium button cell. The below diagram illustrates the internal wiring and organization of the handheld device.

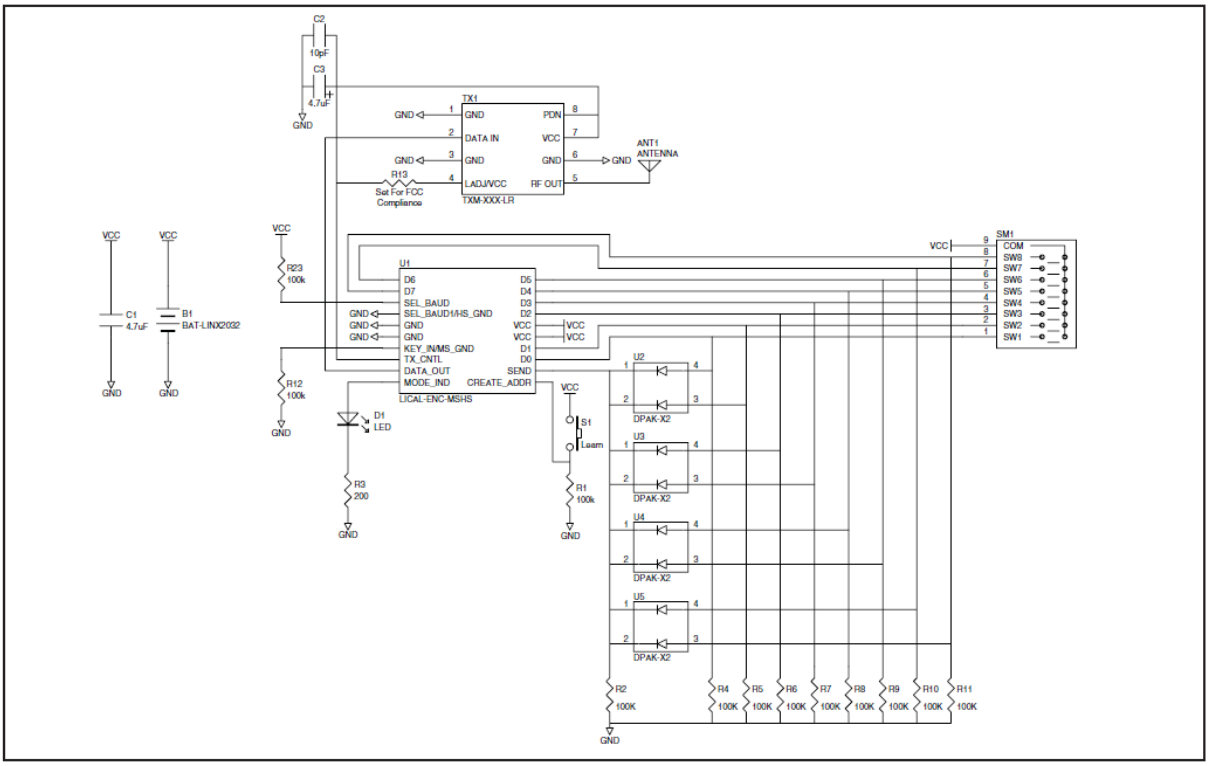

Figure 55: Wiring diagram of transmitter

In addition to the transmitter, a corresponding receiver and decoder are necessary to pick up and utilize the transmitted signal. The selected transmitter was available to purchase in a full kit. The kit in the below figure cost approximately $150.00 USD, which unfortunately does not fall within budget limitations.

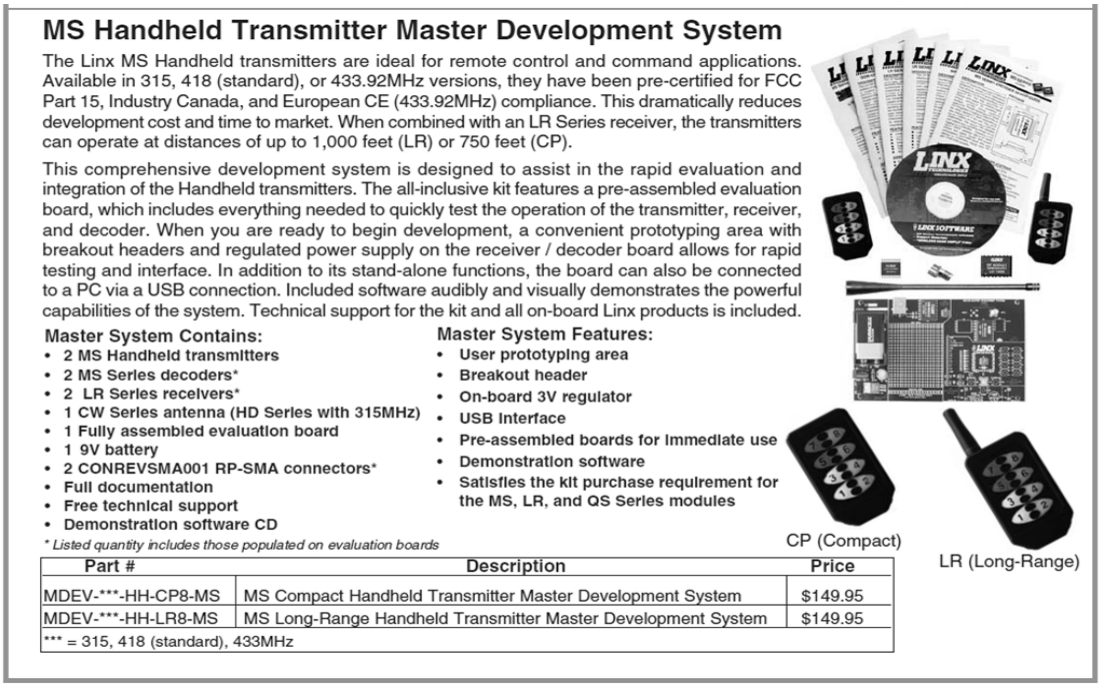

MS Handheld Transmitter Master Development System

The Linx MS Handheld transmitters are ideal for remote control and command applications. Available in 315, 418 (standard), or 433.92MHz versions, they have been pre-certified for FCC Part 15, Industry Canada, and European CE (433.92MHz) compliance. This dramatically reduces development cost and time to market. When combined with an LR Series receiver, the transmitters can operate at distances of up to 1,000 feet (LR) or 750 feet (CP).

This comprehensive development system is designed to assist in the rapid evaluation and integration of the Handheld transmitters. The all-inclusive kit features a pre-assembled evaluation board, which includes everything needed to quickly test the operation of the transmitter, receiver, and decoder. When you are ready to begin development, a convenient prototyping area with breakout headers and regulated power supply on the receiver / decoder board allows for rapid testing and interface. In addition to its stand-alone functions, the board can also be connected to a PC via a USB connection. Included software audibly and visually demonstrates the powerful capabilities of the system. Technical support for the kit and all on-board Linx products is included.

Master System Contains:
- 2 MS Handheld transmitters
- 2 MS Series decoders*
- 2 LR Series receivers*
- 1 CW Series antenna (HD Series with 315MHz)
- 1 Fully assembled evaluation board
- 1 9V battery
- 2 CONREVSMA001 RP-SMA connectors*
- Full documentation
- Free technical support
- Demonstration software CD

Master System Features:
- User prototyping area
- Breakout header
- On-board 3V regulator
- USB interface
- Pre-assembled boards for immediate use
- Demonstration software
- Satisfies the kit purchase requirement for the MS, LR, and QS Series modules

** Listed quantity includes those populated on evaluation boards*

CP (Compact)

LR (Long-Range)

Part #	Description	Price
MDEV-***-HH-CP8-MS	MS Compact Handheld Transmitter Master Development System	$149.95
MDEV-***-HH-LR8-MS	MS Long-Range Handheld Transmitter Master Development System	$149.95

*** = 315, 418 (standard), 433MHz

Figure 56: Transmitter master development kit

Even though this all inclusive kit is not within budget, it did allow for an efficient way of selecting compatible components. The necessary parts were selected based on the recommendations laid out in both this development system and also on the website. First of all, a LR series receiver and MS series decoder were selected. They are shown below along with a wiring schematic of the pins.

Features:
- Secure 2^{24} possible addresses
- 8 data lines
- Low 2.0-5.5V operating voltage
- Low supply current (370µA @ 3V)
- Ultra-low 0.1µA standby current
- Definable recognition authority
- True serial encoding
- Excellent noise immunity
- Selectable baud rates
- No programmer required
- Direct serial interface
- Small SMD package
- Latched or momentary outputs
- Encoder ID output by decoder

Applications Include:
- Keyless Entry
- Door and Gate Openers
- Security Systems
- Remote Device Control
- Car Alarms / Starters
- Remote Status Monitoring
- Call / Paging Systems

Figure 57: Decoder features (left) and receiver IC (right)

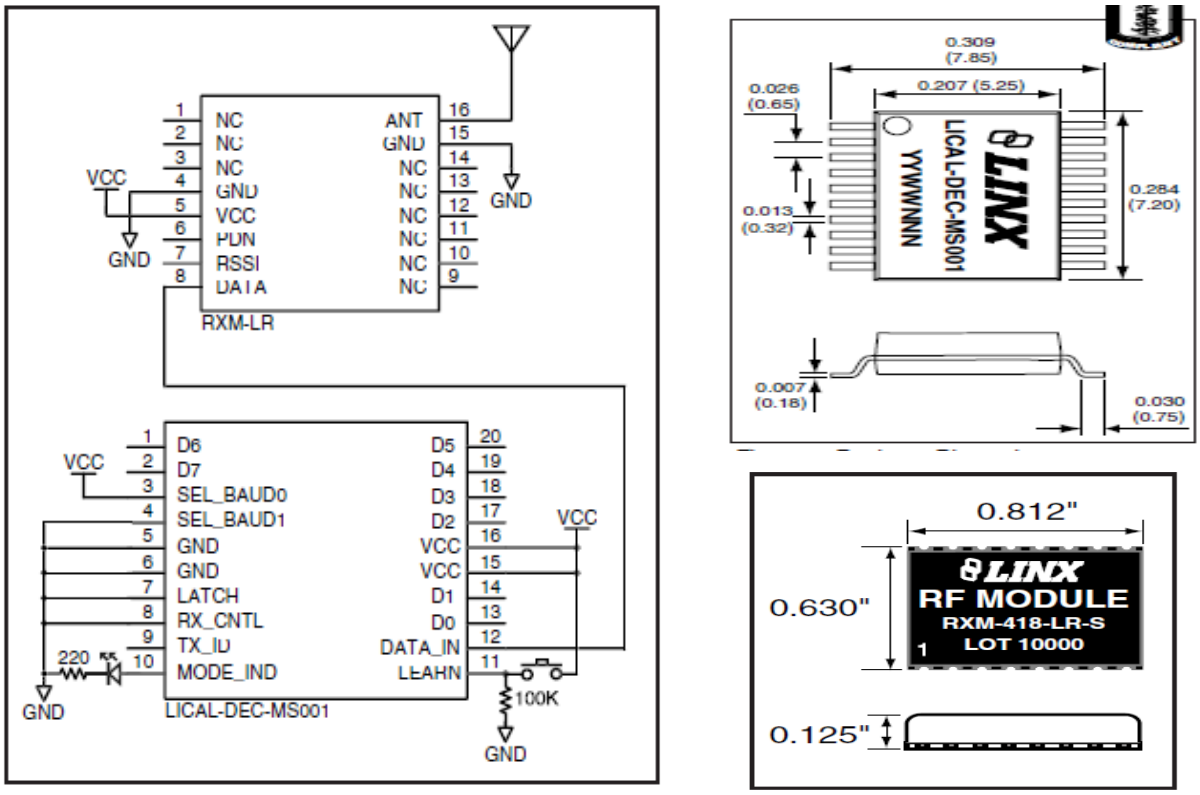

Figure 58: Wiring schematic and IC dimensions for receiver and decoder

This wiring schematic will allow for simple integration of the receiver with the control circuitry. The dimensions show that the receiver chip will be large enough to solder by hand. The LR series receiver features long range, low cost, and low power consumption. It uses a direct serial interface and can detect data at rates up to 10,000 bps. The only external RF component required is the antenna, which will be described at a later point. This allows for simple integration of the system even by engineers without previous RF experience. The receiver's advanced synthesized architecture achieves a sensitivity of -112dBm, which provides a 5-10 times improvement in range over previous solutions. When paired with the selected long range transmitter, a reliable wireless link is formed. This link is capable of transferring over distances of up to 3000 feet. Applications operating at slower transmission speeds and shorter distances will still benefit from the increased reliability and noise immunity. The receiver has an operating voltage of 5 volts and current of 5.2 milliamps.

The MS series decoder is designed to function alongside the encoder already embedded in the handheld controller. It is ideal for remote control and command, keyless entry, and many other similar applications. As shown in the wiring schematic above, the decoder has eight outputs. On each of these outputs the decoder reproduces the button states on its outputs. Each output then becomes an input into the microprocessor chip. The fact that there is one output per control button will greatly simplify the programming needed on the microprocessor. This decoder, unlike those made by many competitors, includes the ability to assign user groups to

individual output lines. It can recognize up to 40 different encoders, but only one encoder will be utilized by the *Sky Vision* system. Outputs can be either latched or momentary. Like the receiver, the decoder features low voltage supply of 5 volts and low current consumption of only 670 micro amps.

An antenna is a necessary part of the communication system. The specific type recommended for the 418 transmitter is a CW Series Whip Antenna. The dimensions of this part are shown below.

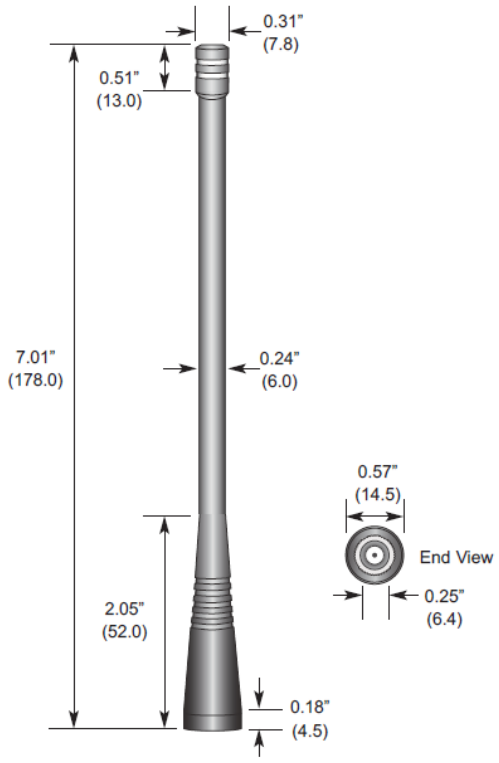

Figure 59: CW Series Whip Antenna

This ¼-wave antenna delivers good performance in a rugged and attractive package. It comes available with standard SMA (sub millimeter array) connectors or RP-SMA (reverse polarity SMA) connectors. It detects a center frequency of 418MHz and is recommended for frequencies in the range of 380 to 450MHz. A wide variety of matching connectors make numerous mounting options possible. This antenna's output is connected to the input on pin 16 of the LR series receiver IC.

The figure below represents an updated block diagram for the communication system.

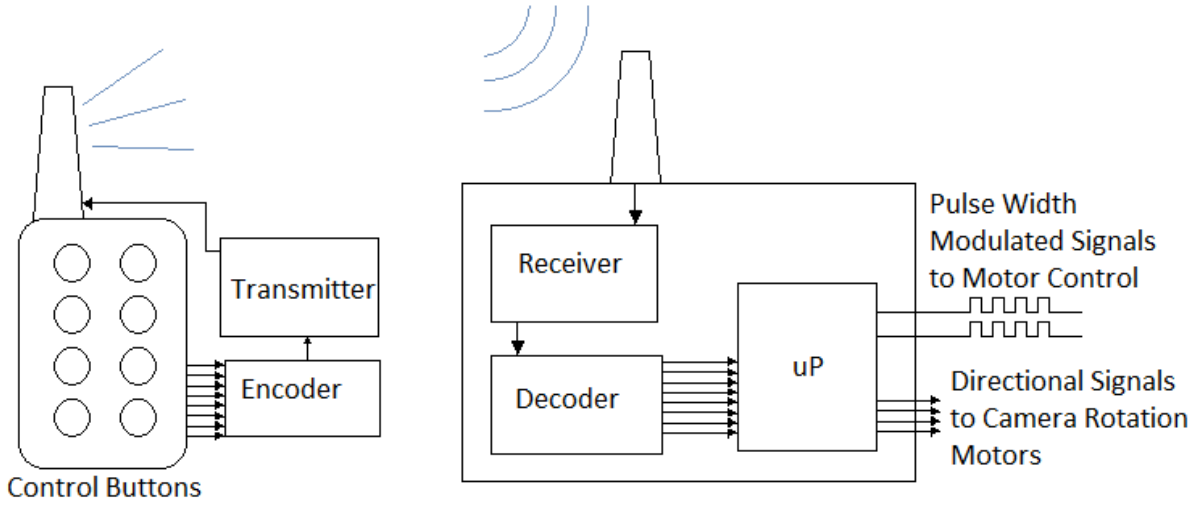

Figure 60: Updated communication system

Microprocessor Selection

The microprocessor selection process was very simple for the project. There were a number of convincing factors that led to the final choice of the DSPIC30F6015. The main factors considered were the availability of a programmer, the benefit of working together with other teams, and the functionality of the microprocessor in regards to motor control. The following figure outlines this decision process.

Microchip Decision Matrix				
		DSPIC30F6015	68HC12	DSPIC24F
Programmer Availability	0.2	5	3	5
Interteam Colaboration	0.2	5	2	4
Free Sample Availability	0.2	5	2	5
Motor Control Functionality	0.2	5	4	2
Past Experience	0.2	2	5	2
		4.4	3.2	3.6

Figure 61: Microprocessor decision matrix

The final goal is that the microprocessor will have two main functions. Both functions will be a direct result of user inputs onto the handheld transmitter device. The first function will control the output sent to the stabilization motors. The signal sent to the stabilization motors will be a pulse width modulated signal. This signal will be sent to a power MOSFET to allow current

to flow to the stabilization servo motors. Different duty cycles will be selected to allow high, medium, or low power supply levels to be sent to these motors. The level to be sent to the motor will be determined by the user based on the amount of wind drag on the balloon. The second function will be to control the direction the camera is pointing. These outputs will be sent into an H-bridge to allow for changes in the direction of camera rotation. The microprocessor will be programmed using the PIC programmer owned by the Harding Engineering Department. It will be mounted on a Schmart-board prototyping board (see Appendix O) for ease in interfacing with the other communication components.

A flow chart describing the operation of the microprocessor is shown below in Figure 62, and a pin-out diagram of the microprocessor is provided in Figure 63.

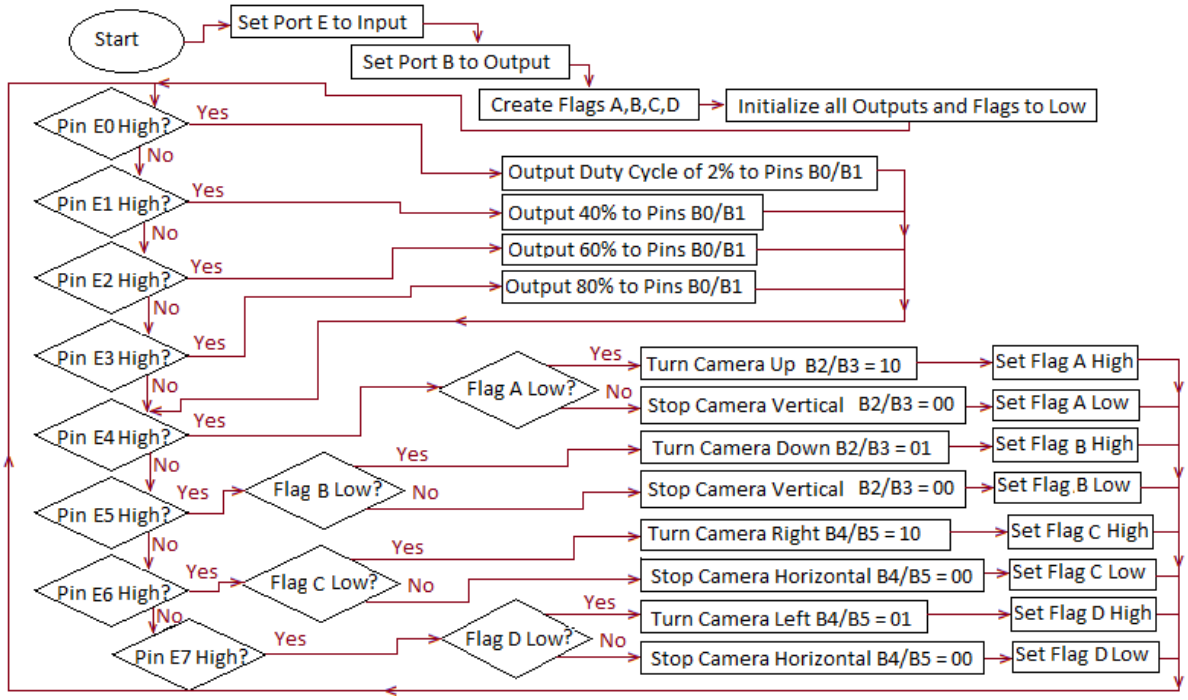
Start
Set Port E to Input
Set Port B to Output
Create Flags A,B,C,D
Initialize all Outputs and Flags to Low
Pin E0 High?
Yes
No
Output Duty Cycle of 2% to Pins B0/B1
Pin E1 High?
Output 40% to Pins B0/B1
Pin E2 High?
Output 60% to Pins B0/B1
Pin E3 High?
Output 80% to Pins B0/B1
Pin E4 High?
Flag A Low?
Turn Camera Up B2/B3 = 10
Stop Camera Vertical B2/B3 = 00
Set Flag A High
Set Flag A Low
Pin E5 High?
Flag B Low?
Turn Camera Down B2/B3 = 01
Stop Camera Vertical B2/B3 = 00
Set Flag B High
Set Flag B Low
Pin E6 High?
Flag C Low?
Turn Camera Right B4/B5 = 10
Stop Camera Horizontal B4/B5 = 00
Set Flag C High
Set Flag C Low
Pin E7 High?
Flag D Low?
Turn Camera Left B4/B5 = 01
Stop Camera Horizontal B4/B5 = 00
Set Flag D High
Set Flag D Low

Figure 62: Microprocessor flow chart

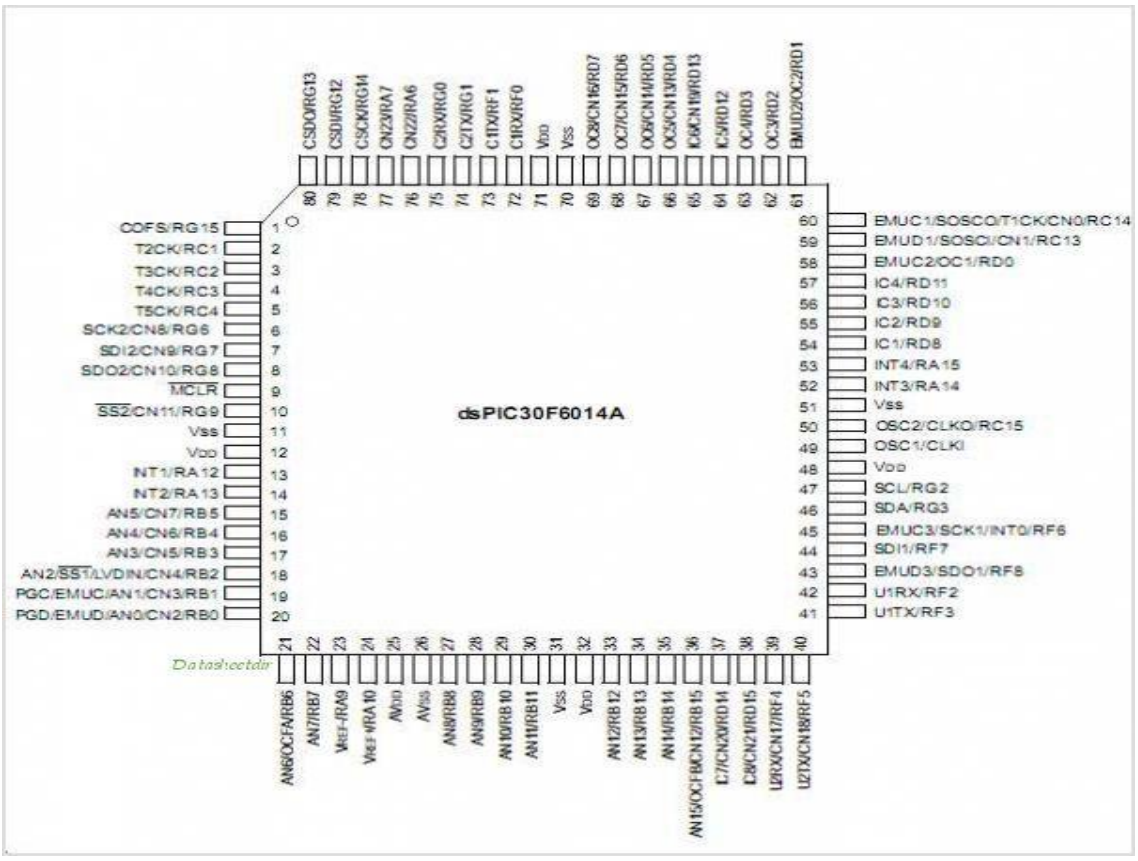

Figure 63: Microprocessor pin out diagram

Motor Control

The simplicity and familiarity of an H-Bridge to control the motors powering the stabilization system makes the use of an H-Bridge an attractive option for motor control. The issue with the H-Bridge circuit is that the propellers in the stabilization system require as much as 10 Amps. As of yet, two H-Bridge circuits that claim to handle 10 A have been found. Though using an IC version of an H-Bridge would simplify the design, no IC versions of an H-Bridge have been found which can handle the current requirements of the system. A generic H-Bridge circuit is shown below in Figure 64.

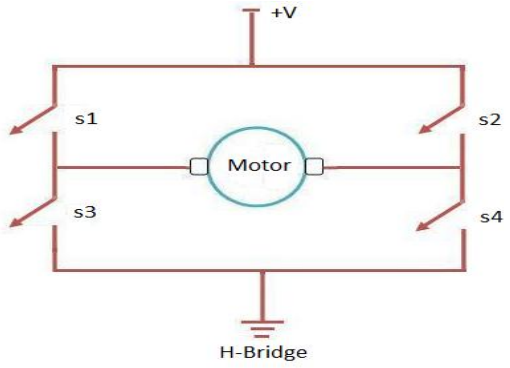

Figure 64: Generic H-Bridge circuit

The reason an H-Bridge is attractive for component control is that it allows for the propellers and imaging motors to be turned in either direction based on the state of the H-Bridge. The control system for this application will need four of H-Bridge circuits, as four motors are on the system. Two H-Bridge circuits will send power to the propeller motors, and two will send power to the camera rotation motors.

The following truth table demonstrates the result of various switch configurations. A warning must be made against ever closing S1 and S3 simultaneously (see Figure 64 for labeling of S1 and S3), since this results in a complete short of the power supply to ground.

Table 8: Truth table

S1	S2	S3	S4	Result
1	0	0	1	motor moves right
0	1	1	0	motor moves left
0	0	0	0	motor runs free - slows to stop
0	1	0	1	motor brakes
1	0	1	0	motor brakes
1	1	x	x	not allowed - short circuit
x	x	1	1	not allowed - short circuit

Key	
1	switch closed
0	switch open
x	doesn't matter

The following diagram shows an H bridge that is designed to handle 10 A. This feature is crucial to our project because the propellers must be able to provide adequate thrust against the wind. In order to provide this thrust, adequate power must be provided to the motors driving the propellers. In order to deliver adequate power, the control circuitry must be able to handle 10 A of current.

TTL type Q and inverted Q inputs control a classic H-bridge circuit, rated at 50 volts and about 10 amps. The circuit can control power and direction of a DC motor.

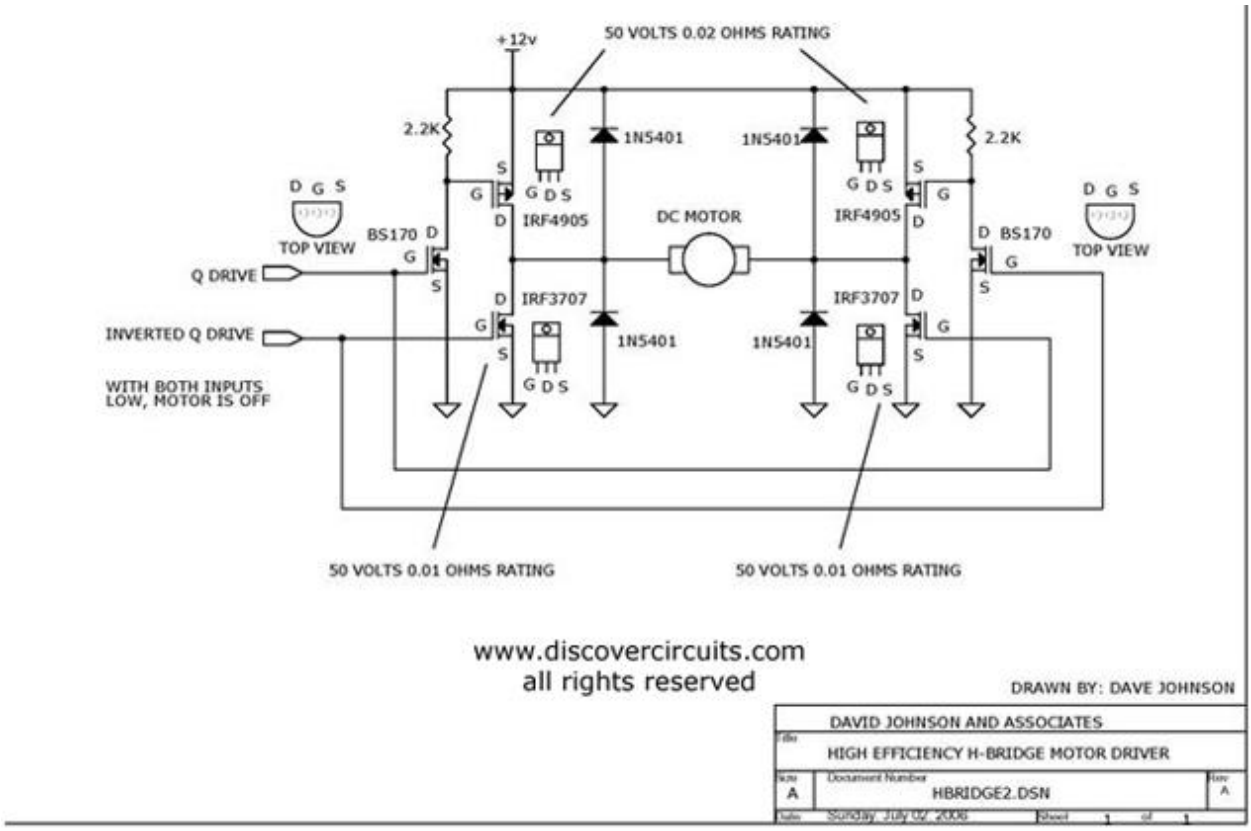

Figure 65: H-Bridge circuit to be used

User Interface Design

The user interface consists of a device on which the user can view the live video feed transmitted from the imaging system on the balloon. Initially, it was thought that an LCD screen and corresponding circuitry would be used to view the live video feed. However, it was found that analog output to USB output connectors were cost effective, simple to use, and readily available (see Appendix Q); see Figure 66 below.

Figure 66: Analog to USB connector

The USB connector supports video formatting and high quality video resolution, and complies with USB Specification Rev. 2.0 (see Appendix Q). Due to the ease with which the video format will be converted to USB, a user supplied laptop computer will be used to view the live video feed.

The handheld radio controller utilized by the user to send control signals to the system is described in detail in the Communication System Design.

Budget

Budget Overview

Table 9. Budget overview table.

	Initial Projected	Current Projected	Spent
Stabilization	$110.00	$107.80	$107.80
Imaging System	$82.00	$124.13	$124.13
Main Power Supply	$135.00	$103.95	$73.95
Tether	$50.00	$19.98	$11.50
Platform	$350.00	$395.90	$286.30
Communication	$50.00	$69.82	$69.82
User Interface	$48.00	$9.00	
MicroProcessor and Circuitry	$40.00	$51.09	$51.09
Contingency	$135.00	$118.33	**Percent Spent**
			78.78%
Total	$1,000.00	$1,000.00	$724.59

The initial budget estimate of the stabilization system was a fairly accurate estimate, as the difference between the funds spent and funds estimated was only $3. The estimated camera budget was inaccurate, because the imaging rotation servomotor costs were not included in the initial budget estimate. The power supply was approximately $30 under the initial amount estimated, because lithium polymer batteries were found to be cheaper than initially expected. The tethering system had a much less cost than that anticipated, because the decision was made to power the system using batteries on the balloon rather than sending power through the tethering cable. The platform was approximately $50 more than anticipated, for two primary reasons: helium was more expensive than estimated, and also the cost of the balloon was increased due to selecting a balloon with premade load attachments. The communication budget is approximately the same as that initially estimated. The user interface was much cheaper than initially estimated, because a user-supplied laptop will be used as the user interface, eliminating the need for an LCD display.

The estimated budget for the control circuitry (combination microprocessor and transmitter) was very inaccurate, due to the decision to use a microprocessor to control the stabilization system and mechanical imaging system.

Subsystem Budgets

Imaging System

Component	Item to Purchase	Quantity	Total	Vendor
Camera	2.4 ghz Mini GearCam	1	$69.95	boostervision.com
Camera	shipping	1	$8.95	boostervision.com
Receiver	no tuning needed PLL receiver	1	$0.00	boostervision.com
Receiver	12 volt ac/dc supply	1	$0.00	boostervision.com
Camera	9 volt battery clip	1	$0.00	boostervision.com
Connector	Mini Coaxial Plug (size H)	1	$3.23	Radio Shack
Motors	Hitec HS-81	2	$34.00	rctoys.com
Motor Attachment	Hitec HS-81 Kit	2	$8.00	rctoys.com
		Total	$124.13	

Stabilization System

Component	Item to Purchase	Quantity	Total	Vendor
Motors	Hacker A20-20L	2	$89.90	rctoys.com
Propeller	APC SF 10 x 4.7 inch	2	$7.90	rctoys.com
Casing		2		undecided
Mounting				undecided
Motors	shipping	1	$10.00	rctoys.com
Propellers	shipping included above	1	$0.00	rctoys.com
		Total	$107.80	

Main Power Supply

Component	Item to Purchase	Quantity	Total	Vendor
Camera Pwr	9 Volt Battery	2	$6.00	Kroger
Motor Pwr	Lipo; 11.1V / 2500mah; 10-12C;	4	$80.00	maxxprod.com
Motor Pwr	Shipping	1	$7.95	maxxprod.com
Receiver Pwr	12 Volt AC/DC Supply	1	$0.00	boostervision.com
Motor Pwr	Lipo; 11.1V / 830mah; 10-12C;	1	$10.00	maxxprod.com
		Total	$103.95	

Tether System

Component	Item to Purchase	Quantity	Total	Vendor
Reel	Bayco Deluxe 150' Reel with Stand	1	$8.48	Lowes
Tether Cord	1/4 polypropylene (120 feet)	1	$6.00	knotandrope.com
Tether Cord	shipping	1	$5.50	knotandrope.com
		Total	$19.98	

Platform System

Mounting	PVC Pipe 0.5 inch by 5 feet	1	$1.30	Lowes
Balloon	7 feet Urethane Balloon	1	$265.00	southernballoonworks.com
Balloon	shipping	1	$20.00	southernballoonworks.com
Helium	220 cubic feet tank	1	$104.00	AirGas
Helium	Rental fee per day	14	$5.60	AirGas
		Total	$395.90	

Communication System

Component	Item to Purchase	Quantity	Total	Vendor
Transmitter	MS Long Rang Handheld Transmitter	1	$32.80	linxtechnologies.com
Decoder	MS series decoder	2	$6.20	linxtechnologies.com
Receiver	LR Series Receiver	2	$19.60	linxtechnologies.com
Attena	CW series whip attena	1	$5.74	linxtechnologies.com
Connector	Attena connector	1	$2.30	linxtechnologies.com
Connector	Attena connector	1	$3.18	linxtechnologies.com
		Total	$69.82	

User Interface System

Component	Item to Purchase	Quantity	Total	Vendor
AUX to USB	EasyCAP (captures video & audio)	1	$9.00	dealextreme.com
AUS to USB	free shipping	1	$0.00	dealextreme.com
screen	user's own laptop	1	$0.00	user
		Total	$9.00	

Microprocessor and Control Circuitry

Component	Item to Purchase	Quantity	Total	Vendor
Microprocessor	free sample DSPIC30F6015	3	$0.00	microchip.com
Evaluation Board	SchmartBoard 202 - 0011 - 01	2	$51.09	schmartboard.com
		Total	$51.09	

Project Management

Fall 2010 Schedule Analysis

Many unanticipated elements influenced the realization of the Fall 2010 Schedule (Gantt Chart, Work-Breakdown Schedule, and Network Diagram). The primary factor influencing the realization of the Fall 2010 Schedule was the influence of recursive design elements and system interdependencies.

The main design of all of the subsystems was directly influenced by the design of at least one other subsystem. For example, the power system relied on the design of the stabilization system. However, the thrust generated by the propellers hinged upon how much power they were supplied.

Many system interdependencies, such as the example provided above, shifted the design from a linear process to a recursive process. The design had to be based on estimates of other systems, the influencing system design was then edited, and those edits were factored into the design of the systems contingent on the edited system. For this reason, the Network Diagram was changed to add an arrow leaving the 'System Design and Analysis' and into the beginning of the subsystem designs. The addition of the recursive element of design caused the estimated times for design to be drastically altered.

Another primary change was the addition of an Image Stabilization task. Image stabilization was a factor in the design of most of the subsystems; no one single subsystem existed which cured the problem of image stability. Therefore, a separate task was added which addressed the problem of image stability as a task inherent to all subsystem designs. Also, the task of designing the tether cable to transmit power was removed from the Work-Breakdown Schedule.

The schedule analysis for the Spring Semester appears to still remain unchanged, as image stability has been designed into all the other subsystems to be built, rather than being built as its own physical/electrical system. Changes to the schedules for the Spring Semester are a reflection of design decision changes; ex., powering the system via system mounted batteries rather than the tethering cable transmitting power.

Gantt Chart

Fall 2010

ID	Task Name	Start	Finish	Duration
1	Project Management	8/23/2010	12/9/2010	79d
2	Documentation	8/23/2010	12/9/2010	79d
3	Project Choice	8/23/2010	9/7/2010	12d
4	Requirements Specification	9/7/2010	9/28/2010	16d
5	System Design and Project Plan	9/28/2010	10/12/2010	11d
6	Device Design	10/5/2010	11/16/2010	31d
7	Propulsion Design	10/12/2010	10/26/2010	11d
8	Camera System	10/12/2010	10/26/2010	11d
9	Platform Design	10/12/2010	11/2/2010	16d
10	Communication Design	10/26/2010	11/9/2010	11d
11	User Interface	10/26/2010	11/9/2010	11d
12	Tethering Design	11/2/2010	11/16/2010	11d
13	Power Design	11/2/2010	11/16/2010	11d
14	Thanksgiving Break	11/22/2010	11/26/2010	5d
15	System Design and Analysis	11/9/2010	12/7/2010	21d
16	Final Design	11/9/2010	12/9/2010	23d

Fall 2010 Work-Breakdown Schedule

ID	Activity	Description	Deliverables/ Checkpoints	Duration (days)	People
F1.0	**Project Management**	Ensure project is completed correctly and on time	Description of team member task completion	Aug. 23rd – Dec. 9th	Ph
F 2.0	**Documentation**	Ensure changes and progress is recorded	Engineering notebooks, A3 reports, and design reports	Aug. 23rd – Dec. 9th	Ph, P, J, C
F 3.0	**Project Choice**	Decide on which problem solution to pursue	Problem specification report	Aug. 23rd – Sept. 7th	Ph, P, J, C
F4.0	**Requirements Specification**	Complete set of all system requirements	Requirements specification document	Sept. 7th – Sept 28th	Ph, P, J, C
F 5.0	**System Design & Project Plan**	Report of semester goals and deadlines, along with functional descriptions of subsystems	System Design and Project Plan final report	Sept. 28th – Oct. 12th	Ph, P, J, C
F6.0	**Device Design**	Complete design of subsystems	Component selection and performance specifications. of subsystems	Oct. 12th – Nov. 16th	Ph, P, J, C
F6.1	Platform Design	Design of balloon and mounting infrastructure	Type of balloon; performance specifications of balloon; design of mounting brackets	Oct. 12th – Nov. 2nd	C (1), Ph (2)
F6.2	Camera Design	Design of imaging system and camera rotation system	Camera selection; camera rotation design	Oct. 12th – Oct. 26th	J, Ph
F 6.2.1	Imaging Design	Design of camera system to provide live video feed	Camera selection and performance specifications; data transmitter and receiver	Oct. 12th – Oct. 26th	J
F 6.2.2	Camera Rotation Design	Design of system to rotate camera 90°	Motor and mounting system selection; performance specifications	Oct. 12th – Oct. 26th	Ph
F6.3	Stabilization Design	Stabilize, rotate, and translate device	Stabilization unit design and selection; movement specifications; mounting design; performance specifications	Oct. 12th - Oct. 26th	Ph (1), C (2)
F6.4	Power Design	Design power system to power device	Battery selection; power distribution design; performance specifications	Nov. 2nd – Nov. 16th	P (1), J (2)
F6.5	Communication Design	Design system to transmit user inputs/outputs to/from device	Communication method selected; control circuitry design; performance specifications	Oct. 26th – Nov. 9th	J (1), P (2)
F6.6	Tether Design	Design system to secure device	Selection of tethering cord; reeling device design; performance specifications	Nov. 2nd – Nov. 16th	C (1), Ph (2)
F6.7	User Interface Design	Design system to receive inputs and display live video feed	User interface control circuitry designed; performance specifications	Oct. 22nd – Nov. 9th	P (1), J (2)
F7.0	**System Design and Analysis**	Ensure correct integration of subsystems and order parts	Final system design and documentation of parts ordering	Nov. 9th – Dec. 7th	Ph, P, J, C
F8.0	**Final Design**	The final design of system and subsystems	Final Design Report (includes schematics and project model)	Nov. 9th – Dec. 9th	Ph, P, J, C

- **Please note that 'performance specifications' includes test results**

Network Diagram

Fall 2010

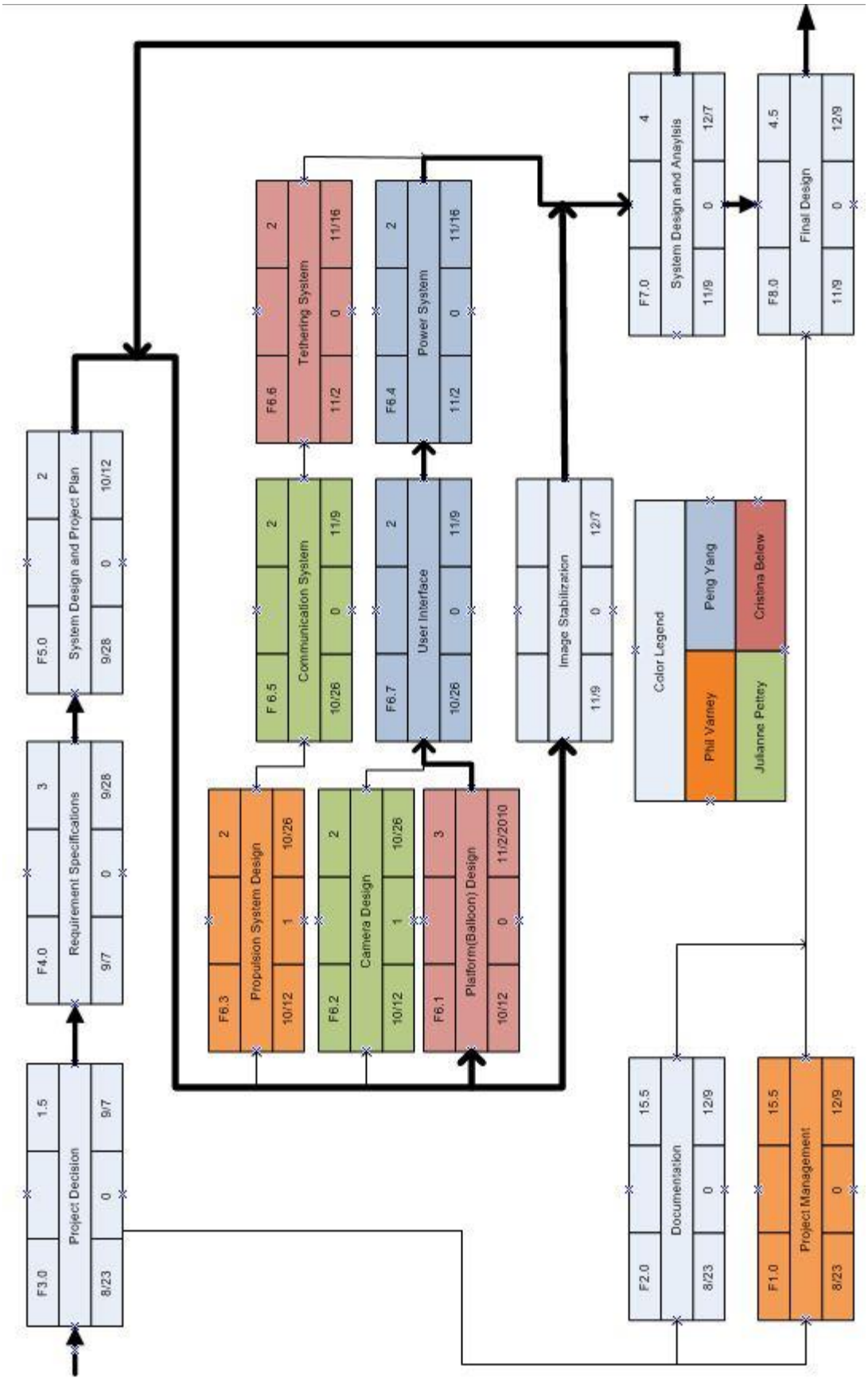

Gantt Chart

Spring 2011

ID	Task Name	Start	Finish	Duration
1	Project Management	1/18/2011	5/5/2011	78d
2	Documentation	1/18/2011	5/5/2011	78d
3	Device Build	1/18/2011	2/22/2011	26d
4	Platform Build	1/18/2011	2/8/2011	16d
5	Camera Build	1/18/2011	2/1/2011	11d
6	Propulsion Build	1/18/2011	2/1/2011	11d
7	Device Testing	2/1/2011	3/8/2011	26d
8	Propulsion Testing	2/1/2011	2/15/2011	11d
9	Camera Testing	2/1/2011	2/15/2011	11d
10	Communication Build	2/1/2011	2/15/2011	11d
11	User Interface Program	2/1/2011	2/15/2011	11d
12	Power Build	2/8/2011	2/22/2011	11d
13	Tether Build	2/8/2011	2/22/2011	11d
14	Platform Testing	2/8/2011	2/22/2011	11d
15	Communication Testing	2/15/2011	3/1/2011	11d
16	User Interface Testing	2/15/2011	3/1/2011	11d
17	Project Status Report	2/15/2011	4/5/2011	36d
18	Power Testing	2/22/2011	3/8/2011	11d
19	Tether Testing	2/22/2011	3/8/2011	11d
20	System Integration	3/1/2011	3/29/2011	21d
21	Spring Break	3/14/2011	3/18/2011	5d
22	System Testing and Modifications	3/22/2011	4/12/2011	16d
23	User's Manual	4/19/2011	5/3/2011	11d
24	Final Report	4/12/2011	5/3/2011	16d

Spring 2011 Work-Breakdown Schedule

ID	Activity	Description	Deliverables/ Checkpoints	Duration (days)	People
S 1.0	**Project Management**	Ensure project is completed correctly and on time	Description of team member task completion	Jan. 18th – May 5th	Ph
S 2.0	**Documentation**	Ensure changes and progress is recorded	Engineering notebooks, A3 reports, design reports	Jan 18th – May 5th	Ph, P, J, C
S 3.0	**Device Build**	Complete builds of subsystems	All of subsystems connected as specified by design	Jan. 18th – Feb. 22nd	Ph, P, J, C
S 3.1	Platform Build	Connect mounting infrastructure to balloon	Mounting brackets for tether, stabilization system, and imaging system attached to balloon	Jan. 18th – Feb. 8th	C (1), Ph (2)
S 3.2	Camera Build	Build imaging system and camera rotation system	Imaging and camera rotation subsystems connected. Camera control circuitry built for both imaging and camera rotation	Jan. 18th – Feb. 1st	J, Ph
S 3.2.1	Imaging Build	Build camera system	Receiver/transmitting circuitry built and connected to camera	Jan. 18th – Jan. 25th	J
S 3.2.2	Camera Rotation Build	Build of camera rotation system	Camera mounted to elevation rotation shaft and motor. Motor connected to control circuitry	Jan 25th – Feb. 1st	Ph
S 3.3	Stabilization Build	Build of stabilization system to stabilize device	Stabilization units built, assembled, and mounted to platform frame	Jan 18th – Feb. 1st	Ph (1), C (2)
S 3.4	Power Build	Build power system to power device	Power distribution system and voltage regulating system built and connected to battery	Feb. 8th – Feb. 22nd	P (1), J (2)
S 3.5	Communication Build	Build system to transmit user inputs/outputs to/from device	Remote control circuitry built and ready to be mounted to user interface and aerial portion of platform	Feb. 1st – Feb. 15th	J (1), P (2)
S 3.6	Tether Build	Build system to secure device to ground	Reeling mechanism connected to rope. Rope attachment to balloon mechanism built	Feb. 8th – Feb. 22nd	C (1), Ph (2)
S 3.7	User Interface Program	Program software to receive inputs and display live video feed	Laptop displays live video feed and records.	Feb. 1st – Feb. 15th	P (1), J (2)
S 4.0	**Device Testing**	Complete testing of each subsystem	Test results of subsystems; modification recommendations	Feb. 1st – Mar. 8th	Ph, P, J, C
S 4.1	Platform Testing	Test the platform to ensure it can support subsystems	Results of balloon lift and stability tests; modification recommendations	Feb. 8th – Feb. 22nd	C (1), Ph (2)
S 4.2	Camera Testing	Ensure camera can provide live feed and rotate through specified angle	Results of camera imaging and rotation tests; modification recommendations	Feb. 1st – Feb. 15th	J, Ph
S 4.2.1	Imaging Testing	Ensure the camera can provide satisfactory video feed	Results of imaging testing; modification recommendations	Feb. 1st – Feb. 15th	J
S	Camera	Ensure camera can rotate	Actual range of rotation	Feb. 1st –	Ph

4.2.2	Rotation Testing	specified elevation range	specified; modification recommendations	Feb. 15th	
S 4.3	Stabilization Testing	Ensure stabilization units compensate for wind drag and angular deflection	Actual thrust output quantified; modification recommendations	Feb. 1st – Feb. 15th	P (1), C (2)
S 4.4	Power Testing	Ensure power outputs can provide power for all subsystems	Actual power output quantified; modification recommendations	Feb. 22nd – Mar. 8th	P (1), J (2)
S 4.5	Communication Testing	Ensure system can communicate to device at max. altitude and receive/transmit user signals	Actual communication range quantified; modification recommendations	Feb. 15th – Mar. 1st	J (1), P (2)
S 4.6	Tether Testing	Ensure tether can support system	Actual reeling force quantified; modification recommendations	Feb. 22nd – Mar. 8th	C (1), Ph (2)
S 4.7	User Interface Testing	Ensure user interface can transmit/receive signal from/to communication system	Test proper response of balloon to user input on the user interface. Verify live video feed; modification recommendations	Feb 15th – Mar. 1st	P (1), J (2)
S 5.0	**Project Status**	Statement of project status	Project status report	Feb. 15th – April 5th	Ph, P, J, C
S 6.0	**System Integration**	Integrate subsystems to ensure correct functionality	Provides fully integrated prototype to test	Mar 1st – Mar. 29th	Ph, P, J, C
S 7.0	**System Testing and Modifications**	Testing of total integrated system and corresponding modifications	Complete system prototype	Mar. 22nd – April 12th	Ph, P, J, C
S 8.0	**User's Manual**	Instructions to user on how to operate system	User's manual report	April 19th – May 3rd	Ph, P, J, C
S 9.0	**Final Report**	Presentation of final device and system capabilities	Final report document	April 12th – May 3rd	Ph, P, J, C

Network Diagram Spring 2011

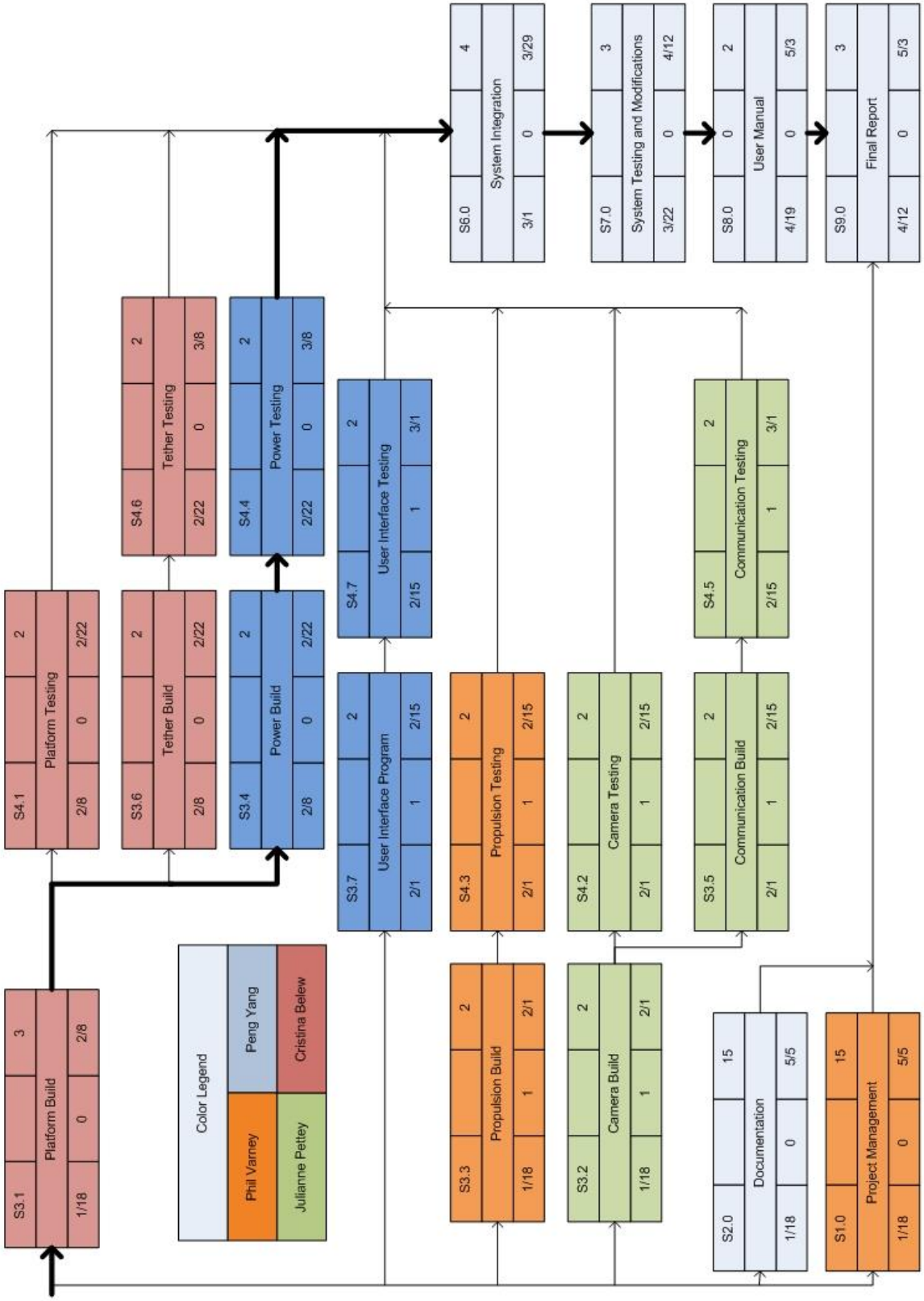

References

"Air - Altitude, Density, and Specific Volume." *Engineering Toolbox*. Web. 25 Nov. 2010. <http://www.engineeringtoolbox.com/air-altitude-density-volume-d_195.html>.

"American Wire Gauge Table and AWG Electrical Current Load Limits with Skin Depth Frequencies." *PowerStream Power Supplies and Chargers for OEMs in a Hurry*. Web. 06 Dec. 2010. <http://www.powerstream.com/Wire_Size.htm>.

"Climate Searcy - Arkansas - Climate Graph." *Climate - United States - Monthly Averages*. Web. 25 Nov. 2010. <http://www.usclimatedata.com/climate.php?location=USAR0508>.

Gipe, Paul. *Wind Power: Renewable Energy for Home, Farm, and Business.* 1st Edition, Chelsea Green Publishing Company

Y.A. Cengel, Cimbala, *Fluid Mechanics: A Practical Approach*, Third Edition, McGraw Hill.

Appendices

Appendix A

FAA Regulations

Subpart A - General

101.1 Applicability.

(a) This part prescribes rules governing the operation in the United States, of the following:

(1) Except as provided for in 101.7, any balloon that is moored to the surface of the earth or an object thereon and that has a diameter of more than 6 feet or a gas capacity of more than 115 cubic feet.

(2) Except as provided for in 101.7, any kite that weighs more than 5 pounds and is intended to be flown at the end of a rope or cable.

(3) Any unmanned rocket except:

(i) Aerial firework displays; and,

(ii) Model rockets:

(a) Using not more than four ounces of propellant;

(b) Using a slow-burning propellant;

(c) Made of paper, wood, or breakable plastic, containing no substantial metal parts and weighing not more than 16 ounces, including the propellant; and

(d) Operated in a manner that does not create a hazard to persons, property, or other aircraft.

(4) Except as provided for in 101.7, any unmanned free balloon that-

(i) Carries a payload package that weighs more than four pounds and has a weight/size ratio of more than three ounces per square inch on any surface of the package, determined by dividing the total weight in ounces of the payload package by the area in square inches of its smallest surface;

(ii) Carries a payload package that weighs more than six pounds;

(iii) Carries a payload, of two or more packages, that weighs more than 12 pounds; or

(iv) Uses a rope or other device for suspension of the payload that requires an impact force of more than 50 pounds to separate the suspended payload from the balloon.

(b) For the purposes of this part, a gyroglider attached to a vehicle on the surface of the earth is considered to be a kite.

[Doc. No. 1580, 28 FR 6721, June 29, 1963, as amended by Amdt. 101-1,

29 FR 46, Jan. 3, 1964; Amdt. 101-3, 35 FR 8213, May 26, 1970]

101.3 Waivers.

No person may conduct operations that require a deviation from this part except under a certificate of waiver issued by the Administrator.

[Doc. No. 1580, 28 FR 6721, June 29, 1963]

101.5 Operations in prohibited or restricted areas.

No person may operate a moored balloon, kite, unmanned rocket, or unmanned free balloon in a prohibited or restricted area unless he has permission from the using or controlling agency, as appropriate.

[Amdt. 101-1, 29 FR 46, Jan. 3, 1964]

101.7 Hazardous operations.

(a) No person may operate any moored balloon, kite, unmanned rocket, or unmanned free balloon in a manner that creates a hazard to other persons, or their property.

(b) No person operating any moored balloon, kite, unmanned rocket, or unmanned free balloon may allow an object to be dropped there from, if such action creates a hazard to other persons or their property.

(Sec. 6(c), Department of Transportation Act (49 U.S.C. 1655(c)))

[Doc. No. 12800, Amdt. 101-4, 39 FR 22252, June 21, 1974]

Subpart B - Moored Balloons and Kites

Source: Docket No. 1580, 28 FR 6722 June 29, 1963, unless otherwise noted.

101.11 Applicability.

This subpart applies to the operation of moored balloons and kites. However, a person operating a moored balloon or kite within a restricted area must comply only with 101.19 and with additional
limitations imposed by the using or controlling agency, as appropriate.

101.13 Operating limitations.

(a) Except as provided in paragraph (b) of this section, no person may operate a moored balloon or kite-

(1) Less than 500 feet from the base of any cloud;

(2) More than 500 feet above the surface of the earth;

(3) From an area where the ground visibility is less than three miles; or

(4) Within five miles of the boundary of any airport.

(b) Paragraph (a) of this section does not apply to the operation of a balloon or kite below the top of any structure and within 250 feet of it, if that shielded operation does not obscure any lighting on the structure.

101.15 Notice requirements.

No person may operate an unshielded moored balloon or kite more than 150 feet above the surface of the earth unless, at least 24 hours before beginning the operation, he gives the following information to
the FAA ATC facility that is nearest to the place of intended operation:

(a) The names and addresses of the owners and operators.

(b) The size of the balloon or the size and weight of the kite.

(c) The location of the operation.

(d) The height above the surface of the earth at which the balloon or kite is to be operated.

(e) The date, time, and duration of the operation.

101.17 Lighting and marking requirements.

(a) No person may operate a moored balloon or kite, between sunset and sunrise unless the balloon or kite, and its mooring lines, are lighted so as to give a visual warning equal to that required for obstructions to air navigation in the FAA publication "Obstruction Marking and Lighting" .

(b) No person may operate a moored balloon or kite between sunrise and sunset unless its mooring lines have colored pennants or streamers attached at not more than 50 foot intervals beginning at 150 feet above the surface of the earth and visible for at least one mile.

(Sec. 6(c), Department of Transportation Act (49 U.S.C. 1655(c)))

[Doc. No. 1580, 28 FR 6722, June 29, 1963, as amended by Amdt. 101-4,
39 FR 22252, June 21, 1974]

101.19 Rapid deflation device.

No person may operate a moored balloon unless it has a device that will automatically and rapidly deflate the balloon if it escapes from its moorings. If the device does not function properly, the operator shall immediately notify the nearest ATC facility of the location and time of the escape and the estimated flight path of the balloon.

Appendix B

Propeller Justification MATLAB Code

```
% Balloon pitch deflection

syms T p real

Ft = 11.99; % Thrust force from propulsion units (N)
Fd = 12; % Wind force (N)
w = 5*9.81; % system weight (N)
Fb = 6*9.81; % Bouyant force (N)

eq1 = -Ft + Fd - T/sqrt(1 + p^2);  % Sum of forces in x-direction
eq2 = Fb - w - T*p/sqrt(1 + p^2);  % Sum of forces in y-direction

S=solve(eq1,eq2,'T,p');
Tension = vpa(S.T,4);
slope = vpa(S.p,4);

disp(sprintf('Thrust         = %8.2f N',double(Ft)))
disp(sprintf('Wind Force     = %8.2f N',double(Fd)))
disp(sprintf('System Weight  = %8.2f N',double(w)))
disp(sprintf('Bouyant Force  = %8.2f N',double(Fb)))
disp('    ')
disp(sprintf('Tension        = %8.2f N',double(Tension)))
disp(sprintf('Tilt           = %8.2f degrees',double(90-atand(slope))))
disp(' ')

phi = 90 - atand(slope);

rising_force = Fb - w - Tension*cos(phi);  % Lifting force
```

Appendix C

Maximum Wind Force MATLAB Code

```
%%%  Wind Force Calculation
%%%
%%%     This program calculates the average wind force exerted on the
%%%     balloon by a constant wind velocity
%%%
%%%     C_d = drag coefficient
%%%
%%%     F_wind = 0.5*C_d*p*V^2*A
%%%
%%%     Assumption: Balloon is spherical
%%%     Assumption: P = 1 atm and T = 20 C

clear

T = -20:5:30;                    % Air temperature (C)
F_max = zeros(length(T),1);  V_max = zeros(length(T),1);

for i = 1:length(T)

    rho = 1.204;                    % Density of air (kg/m^3)
    v = 8.79302e-8*T(i) + 1.34039e-5; % Kinematic viscosity of air (m^2/s)
    V_wind = [0:0.01:5];        % Relative wind speed range on balloon (m/s)
    C_d = zeros(length(V_wind),1);
    r = 1;                          % Radius of balloon (assume spherical (m)

    Re = V_wind*2*r/v;              % Reynolds number for flow over a sphere
    A = pi*r^2;                % Projected frontal area of spherical balloon

    for j = 1:length(V_wind)
        if Re(j) <= 4e5             % 4 x 10^5 slightly larger than Re_cr
            C_d(j) = 0.5;           % C_d for flow Re < Re_cr
        elseif Re(j) > 4e5 && Re(j) < 1e6
            C_d(j) = 0.1;           % C_d for flow Re > Re_cr
        else
            C_d(j) = 0.2;           % C_d for Re > 1e6
        end

        V_wind_2(j) = V_wind(j)^2;                % Wind speed squared
        F_wind(j) = 0.5*C_d(j)*rho*V_wind_2(j)*A; % Wind force (N)

    end

    [F_max(i), k] = max(F_wind);
    V_max(i) = V_wind(k);

end

plot(V_wind,F_wind)
title('Wind Force (N)','fontsize',14)
xlabel('Wind Velocity (m/s)','fontsize',12)
ylabel('Wind Force (N)','fontsize',12)
```

Appendix D

APC10 x 4.7 Propeller Data Sheet

APC 10x4.7 SF Slow Flyer Electric RC Airplane Composite Propeller

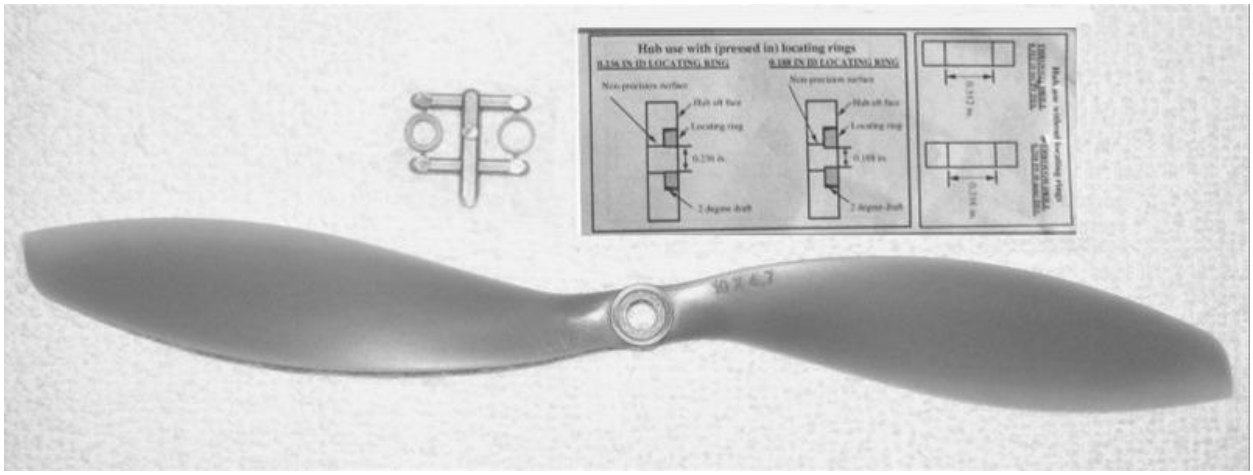

Product Description:

APC Landing Products Slow Flyer RC electric composite model airplane propeller A10047SF / LP 10047SF is designed for use with electric rc airplanes. APC Slow Flyer props are not for high power applications but are specifically crafted for low power use. Includes locating rings in various sizes and instructions on adaptation procedures.

APC Landing Products electric model airplane propellers have enjoyed strong acceptance and growth since their introduction in 1989. They are especially popular in rc pattern flying and rc airplane racing events. The performance and low noise advantages are largely spawned by the precision methods APC - Landing Products uses to design and manufacture APC electric rc airplane propellers.

APC 10x4.7 SF Slow Flyer Electric RC Airplane Composite Propeller Specifications

- Length: 10 inches
- Pitch: 4.7 inches per revolution
- Type: Slow Flyer Electric
- Material: 1 Piece Composite
- Use: Electric RC Airplanes

APC - Landing Products preserves a close rapport with the rc aircraft competition community to benefit from technical interchange so important to improved rc airplane propeller designs. There is continuous evolution in rc aircraft design and engine performance. Consequently, propeller design must continuously evolve as well to keep pace with these improving technologies.

Due to APC's excellent quality and consistent performance APC - Landing Products' rc airplane propellers are perfect for any electric rc application from parkflyers to 3D aerobatics to scale rc aircraft.

Note: This rc airplane propeller is designed only for use with electric motors. Do not attempt to use this propeller with glo or gas powered engines.

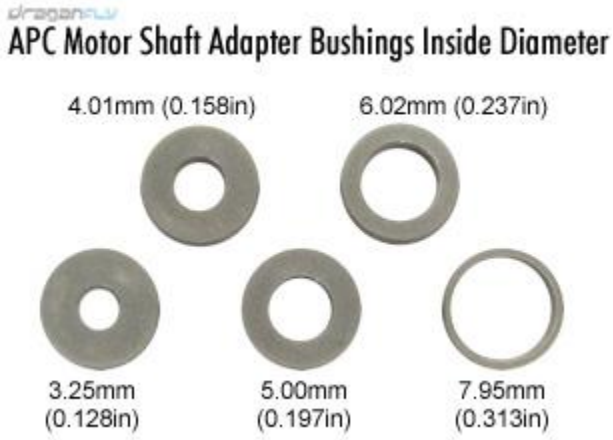

Appendix E

Hacker A20-20L Motor Data Sheet

Hacker A20 – 20L Motor

The A20 motors are small outrunner of our series and provides great efficiency and light weight. They're ideal for small electric airplanes up to 600g (21oz). Featuring a Slotted 14-pole outrunner design. The Curved Neodym-Magnets offer a perfect gap from the inside of the rotor for optimal power and efficiency. Spare shafts, Backmount, Prop adapter and all screws are included. 3,5mm gold bullet connectors are provided (not with A20-S) The motors are available in different Lengths and Windings. Please refer data the data tables to find the right motor for your application.

Motor	***A20-S***		***A20-M***		***A20-L***		***Motor***
Leistungsbereich	max. 100W (15sec.)		max. 150W (15sec.)		max. 200W (15sec.)		Powerrange
E-Segler	bis 500g / up to 19oz		bis 800g / up to 28oz		bis 1100g / up to 39oz		Electric-Sailplane
Sport- und Scale	bis 400g / up to 14oz		bis 600g / up to 21oz		bis 800g / up to 28oz		Sport and Scale
Kunstflug und 3D	bis 250g / 8,8oz		bis 400g / up to 14oz		bis 550g / 19oz		Pattern and 3D
Hubschrauber	bis 250g / 8,8oz		bis 400g / up to 14oz		bis 550g / 19oz		Helicopter
Windungszahl	***34***	***50***	***26***	***30***	***20***	***22***	***Turns***
Leerlaufstrom (Io) @8,4V [A]	0,75A	0,4A	0,7A	0,6A	0,85A	0,75A	Idle Current (Io) @8,4 V [A]
Innenwiderstand (Ri) [Ohm]	0,147	0,232	0,117	0,174	0,109	0,089	Resistance (Ri) [Ohm]
RPM/Volt (Kv)	1500	1088	1130	980	1022	924	RPM/Volt (Kv)
Wellendurchmesser D2	3,0 mm(0,118")						Shaft Diameter D2
Wellenlänge L2	12mm / 0,47"						
Gewicht	29g / 1,0oz		42g / 1,48oz		55g / 1,93oz		Weight
Aussendurchmesser D1	28 mm (1,1")						Diameter D1
Länge L1	24mm / 0,94"		30mm / 1,18"		34mm / 1,33"		Length L1
Befestigungslöcher	16mm + 19mm, 4 x M3						Mountingscrew diam.
Typ	14-Poliger Aussenläufer						Type
Drehzahlsteller	4..7Amp Brushless		12..20 Amp Brushless		20..30 Amp Brushless		Speed Control
empf. Timing	20° - 25°						recomm. Timing
Schaltfrequenz	8 - 16 kHz						Switching Frequency

A20-20L

Leichter und leistungsstarker Motor für 3D-Modelle bis ca. 550g und 3S-Setup
Lightweight Motor for 3D-Airplanes up to 19oz for 3S-Setup

Prop	10x4,7 APC-Slow	10x6 ACC
LiPo	3 S	3 S
Volt	10,5 V	10,5 V
Amp.	17,1 A	14,5 A
RPM	7221	8408
Power	180 W	153 W
Contr.	X-20	X-20

Motor	***A20-XL***			***Motor***
Leistungsbereich	max. 300W (15sec.)			Powerrange
E-Segler	bis1500g / up to 53g			Electric-Sailplane
Sport- und Scale	bis 1100g / up to 39oz			Sport and Scale
Kunstflug und 3D	bis 800g / up to 28oz			Pattern and 3D
Hubschrauber	bis 800g / up to 28oz			Helicopter
Windungszahl	***6***	***6***	***12***	***Turns***
Leerlaufstrom (Io) @8,4V [A]	3,5A	3,4A	1,2A	Idle Current (Io) @8,4 V [A]
Innenwiderstand (Ri) [Ohm]	0,014	0,020	0,075	Resistance (Ri) [Ohm]
RPM/Volt (Kv)	3500	2500	1039	RPM/Volt (Kv)
Wellendurchmesser D2	3,175 mm / 0,125"			Shaft Diameter D2
Wellenlänge L2	15mm / 0,59"			
Gewicht	78g / 2,73oz			Weight
Aussendurchmesser D1	28mm / 1,1"			Diameter D1
Länge L1	40mm / 1,57"			Length L1
Befestigungslöcher	16mm + 19mm, 4 x M3			Mountingscrew diam.
Typ	8-Poliger AL	10-Poliger AL	14-Poliger AL	Type
Drehzahlsteller	30..40 Amp Brushless			Speed Control
empf. Timing	8° - 15°	15° - 20°	20° - 25°	recomm. Timing
Schaltfrequenz	8 - 16 kHz			Switching Frequency

Hacker Motor GmbH
Hummler Str. 5 D-85416 Niederhummel
Phone: +49-8761-752 129 Fax: +49-8761-754 314
email: info@hacker-motor.com

Appendix F

Wind Alignment MATLAB Code

```
mb = 2.5;  % Mass of balloon (kg)
R = 1;     % Radius of balloon (m)
mp = 0.1;  % Mass of plate (kg)
r = 0.5;     % Moment arm of centroid of drag force (m)
D = 0.05;   % vertical height of plate (m)
L = 2;   % Length of plate  (m)
vw = 5;    % Wind velocity (m/s)
pair = 1.204;    % Density of air  (kg/m^3)
Ap = D*L;        % Projected frontal area
C_d = 2.5;       % Drag coefficient thickness is L2 Thickness of L2/D = 0.5
                 %corresponds to C_d of 2.5
j = 2/5*mb*R^2 + 1/12*mp*D^2 + mp*r^2;   % Inertia
% Rectangular rod, projected area still D*L, thickness is L2:
% Thickness of L2/D = 0.5 corresponds to C_d of 2.5
F_d_r = 0.5*C_d*pair*vw^2*Ap*r;
c = F_d_r/j;
c2 = 1/2*pair*Ap*C_d*r^3/j;
t = [0:0.1:150];
%Numerical solution
options = odeset; %Using default options for ode solver
th0 = [0, 0]; %initial conditions on thdot=0 and th=0
[time,th_vals] = ode113(@wind_alignment_fcn, t, th0,options,c,c2);
figure(1)
plot(time,th_vals(:,1),'r');
title('Wind Stability Response','Fontsize',14)
xlabel('Time (s)','Fontsize',12)
ylabel(texlabel('theta (deg)'),'Fontsize',12)

figure(2)
plot(t,th_vals(:,2))
title('Wind Stability Response: Angular Rate of Change','Fontsize',14)
xlabel('Time (s)','Fontsize',12)
ylabel(texlabel('d*theta/dt(deg/s)'),'Fontsize',12)
```

```
function dth = wind_alignment_fcn(t, th0, c, c2)
% Need to provide function with th and thdot.
% th(1) is theta itself, and
% th(2) is first derivative of theta
th = th0(1);
thdot = th0(2);

thdot = thdot;
thdoubledot = c*cosd(th)*abs(cosd(th)) - c2*thdot*abs(thdot);

dth = [thdot; thdoubledot];
```

Appendix F – 1

Wind Response MATLAB Code

```
clear

T = -20:5:30;                    % Air temperature (C)
F_max = zeros(length(T),1);  V_max = zeros(length(T),1);
g = 9.81;

for i = 1:length(T)
    pair = 1.204;                    % Density of air (kg/m^3)
    v = 8.79302e-8*T(i) + 1.34039e-5; % Kinematic viscosity of air (m^2/s)
    V_wind = [0:0.01:5];       % Relative wind speed range on balloon (m/s)
    C_d = zeros(length(V_wind),1);   % Drag coefficient
    R = 1.065;                        % Radius of balloon (assume spherical
(m)

    Re = V_wind*2*R/v;            % Reynolds number for flow over a sphere
    A = pi*R^2;                % Projected frontal area of spherical balloon

    for j = 1:length(V_wind)
        if Re(j) <= 4e5           % 4 x 10^5 slightly larger than Re_cr
            C_d(j) = 0.5;         % C_d for flow Re < Re_cr
        elseif Re(j) > 4e5 && Re(j) < 1e6
            C_d(j) = 0.1;         % C_d for flow Re > Re_cr
        else
            C_d(j) = 0.2;         % C_d for Re > 1e6
        end

        V_wind_2(j) = V_wind(j)^2;                % Wind speed squared
        F_wind(j) = 0.5*C_d(j)*pair*V_wind_2(j)*A; % Wind force (N)
    end
end

vw = 0.1;       % Desired velocity to analyze motion of balloon
F_w = -1;         % Initializes  force of wind to unrealistic value so it
                  % will be known if no value is found
for i = 1:length(V_wind)
    if V_wind(i) == vw
        F_w = F_wind(i);
        break
    elseif i == length(V_wind) && F_w == -1
        error('Wind speed out of specified range')
    end
end

F_B = pair*4/3*pi*R^3*g;   %% Buoyant force on balloon
mb = 2.5;  % Mass of balloon (kg)
msys = 4;  % System mass (kg)
h = 30;   % Height of balloon (m)

I_o = msys*h^2;   % Inertia about tether-ground

c1 = h*F_w/I_o;
c2 = -(F_B - msys*g)*h/I_o;
c3 = -0.3*pair*pi*R^2*h^3/2/I_o;
c4 = -F_w*h/I_o;    % thrust force should be equal to drag force of wind
t = [0:0.01:120];
```

```
%Numerical solution
options = odeset; %Using default options for ode solver
phi0 = [0, 0]; %initial conditions on thdot=0 and th=0
[time,phi_vals]= ode45(@pendulum_balloon_fcn, t, phi0,options,c1,c2,c3,c4);
plot(time,abs(phi_vals(:,1)),'r');
title('Wind Response','Fontsize',14)
xlabel('Time (s)','Fontsize',12)
ylabel(texlabel('phi  (deg)'),'Fontsize',12)




function dphi = pendulum_balloon_fcn(t, phi0, c1, c2, c3, c4)

% Need to provide function with th and thdot.  th(1) is theta itself, and
% th(2) is first derivative of theta

phi = phi0(1);
phidot = phi0(2);

phidot = phidot;
phidoubledot = c2*cos(phi) + c3*phidot*abs(phidot);
                                    %  Approximate with no damping
                                          %  to obtain max the
dphi = [phidot; phidoubledot];
```

Appendix G

Elevation Rotation Motor Holding Torque MATLAB Code

```
%%% 90 deg Elevation Rotation Motor Holding Torque
%%%
%%%     This program calculates the holding torque necessary from the
%%%     stepper motor providing the 90 degrees of elevation rotation of the
%%%     camera.  An 'L' shaped shaft is attached to the motor output shaft,
%%%     and the camera is attached to the end of the 'L'.  The first
%%%     portion of the L shaft is shaft 1, the second portion is shaft 2
%%%
g = 9.81;                                   % m/s^2
mc = 0.0141;                                % Mass of camera (kg)
ms2 = 0.01;                                 % Mass of shaft 2 (kg)

psi = 0:1.8:90;    % Elevation rotation angle, in increment typical of a
                   % stepper motor (1.8 deg)
L2 = 0:0.005:0.05;                          % Length of shaft 2 (m)

h_torque = g*L2*sind(90)*(0.5*ms2 + mc); % Max torque is when psi = 90

plot(L2, h_torque)
title('Maximum Holding Torque','fontsize', 14)
xlabel('Length of Shaft 2 (m)')
ylabel('Holding Torque (N m)')

h_torque_max = max(h_torque)                % Max Holding torque (N m)
```

Appendix H

Hitec HS-81 Servomotor Datasheet

ANNOUNCED SPECIFICATION OF HS-81 SUB MICRO SERVO

1.TECHNICAL VALUES

CONTROL SYSTEM	:+PULSE WIDTH CONTROL 1500usec NEUTRAL	
OPERATING VOLTAGE RANGE	:4.8V TO 6.0V	
OPERATING TEMPERATURE RANGE	:-20℃ TO +60℃	
TEST VOLTAGE	:AT 4.8V AT 6.0V	
OPERATING SPEED	:0.11sec/60° AT NO LOAD	0.09sec/60° AT NO LOAD
STALL TORQUE	:2.6kg.cm(36.10oz.in)	3kg.cm(41.66oz.in)
OPERATING ANGLE	:40°/ONE SIDE PULSE TRAVELING 400usec	
DIRECTION	:CLOCK WISE/PULSE TRAVELING 1500 TO 1900usec	
IDLE CURRENT	:8.8mA	9.1mA
RUNNING CURRENT	:220mA AT NO LOAD	280mA AT NO LOAD
DEAD BAND WIDTH	:8usec	
CONNECTOR WIRE LENGTH	:160mm (6.29in)	
DIMENSIONS	:29.8x12x29.6mm (1.17x0.47x1.16in)	
WEIGHT	:16.6g(0.58oz)	

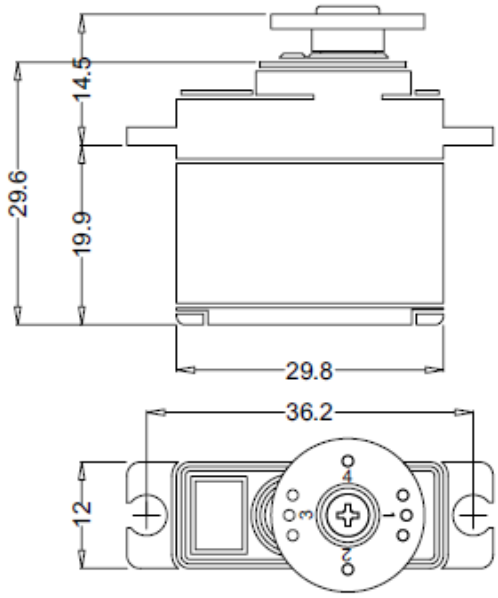

2.FEATURES

3-POLE FERRITE MOTOR
HYBRID I.C
DIRECT POTENTIOMETER DRIVE

Appendix I

Transmissibility MATLAB Code

```
% Transmissibility Curves

w_wn = 0:0.01:3;
z = [0.05;0.10;0.15;0.25;0.50;1];


for i = 1:length(z);
    for j = 1:length(w_wn)
        x(i,j) = (1 + (2*z(i)*w_wn(j))^2)^0.5./sqrt((1 - w_wn(j)^2)^2 + ...
            (2*z(i)*w_wn(j))^2);
    end
end

plot(w_wn,x)
title('Transmissibility','Fontsize',14)
xlabel(texlabel('omega/omega_n'),'Fontsize',14)
ylabel(texlabel(' |X(jw)|/A , F_tr/F_0'),'Fontsize',14)
```

Appendix J

Sorbothane Vibration Isolation Material

Sorbothane® Polymer Sheet Stock

X-Tra Flex Sheet
X-Tra Flex Sheet is molded with hemispherical bumps. The hemispheres permit the material to flex more easily and allow for soft deformation under load. Overall sheet thickness is approximately 0.185-inch. The hemispheres are approximately 0.09 high and 0.12 diameter. X-Tra Flex sheets are easier to apply to curved and irregular surfaces and provide a softer spring rate.

Pressure Sensitive Adhesives
Selected Sizes (max width = 6-inches) are offered with Pressure Sensitive Adhesive (PSA) on one side.

Die Cutting
Sheet stock up to 0.25-inch thick, with or without PSA can be die cut at additional cost. Die cut materials will have a concave edge. Consult factory on costs.

Water Jet Cutting
Sheet stock of any thickness can be water jet cut. Water jet cut materials will have a clean edge. Consult factory on costs.

Gaskets
Sorbothane is a popular material for gaskets because of its **chemical resistance, conformability to irregular surfaces, low creep and reusability**. Its natural tackiness makes it easy to install. Gaskets can be knife-cut, scissor-cut, die cut, molded or water jet cut.

Special Sizes, Colors and Thicknesses
The factory can pour special shapes, colors and thicknesses. Tooling costs can be as low as 500 USD per mold. The tooling charge is normally less than your internal fabrication costs for special work except for the smallest volumes.

Sheet Stock for Vibration Applications
In designing your own vibration mounts from sheet stock keep the following in mind:

- **More is not better**. A large, lightly loaded sheet will have a high spring rate and will not deflect enough to provide good isolation. Over compression will lead to short service life. The proper compression range is 3 to 20 per cent depending on the "Shape Factor." Shape factor is the ratio of contact surface (one side) divided by perimeter area. See page 11 for calculation of shape factors.
- **Geometry matters**. Small circular pieces and rings "bulge" better than squares and rectangles. "Bulgeability" makes for better isolation. Use many small discs rather than a few large rectangles for best vibration isolation performance.
- **Thickness matters**. The thicker the sheet, the lower the natural frequency. You need a sheet at least one-inch thick to get your natural frequency down to 10 Hertz. (10 Hertz is your target natural frequency for a 900 RPM motor.)

- **Do not "bolt through" your Sorbothane sheet**. The bolt will carry the vibration to the base. Use the natural tackiness of Sorbothane, or apply adhesives to glue the Sorbothane to metal plates on both sides, or consider a custom design with molded-in stud mounts.
- **Use vibration-rated connections**. Where bolted connections are used, use high-quality (thread deforming) lock nuts or doubled jam nuts to prevent connections from vibrating loose.

Part Number	Dimensions in inches	Thickness Tolerance in inches	Available Durometer Range	Class & Notes	Unit Price in USA Dollars for Purchase Quantity Ranges		
					5 to 49	50 - 199	200+
0225532	0.19 x 12 x 14	±0.025	40 to 70	Class 1, X-tra flex sheet	26.90	22.10	15.58
					1 to 49	**50 to 99**	**100 to 249**
0208040	0.04 x 4 x 6	±0.007	40 to 70	Class 2	8.29	6.18	5.25
0208045	0.04 x 4 x 6	±0.010	40 to 70	Class 2, with PSA 1-side	10.38	7.79	6.56
0208060	0.06 x 4 x 6	±0.007	40 to 70	Class 2	9.00	6.80	5.71
0208065	0.06 x 4 x 6	±0.010	40 to 70	Class 2, with PSA 1-side	11.13	8.30	7.04
0206080	0.08 x 6 x 6	±0.015	40 to 70	Class 3	8.19	5.85	4.82
0206109	1/10 x 6 x 12	±0.015	40 to 70	Class 3	9.30	6.70	5.15
0206110	1/10 x 6 x 12	±0.020	40 to 70	Class 3, with PSA 1-side	12.69	9.14	7.16
0206111	1/8 x 6 x 12	±0.020	40 to 70	Class 3	9.98	7.25	5.46
0206112	1/8 x 6 x 12	±0.025	40 to 70	Class 3, with PSA 1-side	12.95	9.53	7.43
					1 to 99	**100-499**	**500+**
0212010	1/10 x 12 x 12	±0.015	40 to 70	Class 4	13.40	10.76	8.07
0212012	1/8 x 12 x 12	±0.020	40 to 70	Class 4	15.35	12.26	9.13
0212018	3/16 x 12 x 12	±0.020	30 to 70	Class 4	21.32	17.03	11.94
0212025	1/4 x 12 x 12	±0.025	30 to 70	Class 4	25.81	22.06	14.84
0212037	3/8 x 12 x 12	±0.025	30 to 70	Class 4	40.55	32.24	21.88
0212050	1/2 x 12 x 12	±0.035	30 to 70	Class 4	53.46	43.14	28.73
0212062	5/8 x 12 x 12	±0.035	30 to 70	Class 4	62.80	50.39	34.28
0212075	3/4 x 12 x 12	±0.040	30 to 70	Class 4	79.18	63.86	43.88
0212100	1 x 12 x 12	±0.060	30 to 70	Class 4	106.25	85.90	58.38
0212150	1.50 x 12 x 12	±0.075	30 to 70	Class 4	160.68	129.15	110.91
					1-49	**50-199**	**200+**
0224012	1/8 x 24 x 24	±0.025	40 to 70	Class 5	56.89	45.82	30.85
0224018	3/16 x 24 x 24	±0.030	40 to 70	Class 5	79.12	63.20	42.85
0224025	1/4 x 24 x 24	±0.040	30 to 70	Class 5	104.12	86.97	58.93
0224037	3/8 x 24 x 24	±0.040	30 to 70	Class 5	152.17	122.22	82.58
0224050	1/2 x 24 x 24	±0.045	30 to 70	Class 5	212.95	171.17	116.79
0224062	5/8 x 24 x 24	±0.060	30 to 70	Class 5	263.06	209.41	141.75
0224075	3/4 x 24 x 24	±0.060	30 to 70	Class 5	314.41	255.05	173.00
0224100	1 x 24 x 24	±0.070	30 to 70	Class 5	415.79	341.06	231.00

To order: Specify part number, durometer, color, and quantity. Standard colors are black, gray or royal blue. Special colors quoted upon request. Dimensional variations are available by special order. Durometer tolerance: ±5 units. Factory direct purchases subject to 100 USA dollar minimum per color, per durometer and per class.

Appendix J - 1

Hitec HS-81 Attachment Kit

Hitec Micro Horn & Hardware Set for HS60 / 80 / 81 / 85 / 101 RC Servo (56327)

This is a Hitec micro servo horn & hardware set 56327 which will fit Hitec HS60, Hitec HS80, Hitec HS81, Hitec HS85 and Hitec HS101 rc servos.

Plastic, rubber, and brass construction Hitec servo horn set

- 2 x black T-shaped servo mounts.
- 2 x black rubber dampeners
- 2 x brass eyelets.
- 2 x servo mounting screws (Phillips head)
- 1 x white straight horn.
- 1 x white servo wheel.
- 1 x white cross horn.

Technical Data:

Hitec rc servo horn set 56327

- Fits Hitec servos: HS60, HS80, HS81, HS85, HS101
- Length of straight arm: 29.0mm (1.14")
- Overall length of cross arm: 23.0mm (.91")
- Diameter of wheel: 17.0mm (.67")
- Inside diameter of spline: 6.0mm (.24")

Appendix K

Booster Vision GearCam

| BoosterVision GearCam *(BVGM-1)*

Features: Small Size & Light Weight Low Power Consumption Powered by 9 Volt Battery 2.4 Ghz Wireless Mini Color Camera with Audio from built in microphone.

Size: 20mm (W) 20mm (H) 20mm (D) About 3/4 of an inch…the size of a dime!

Comes with no tuning needed PLL receiver, 12 volt ac/dc supply for receiver and camera 9 volt battery clip, and ac power pack for Mini GearCam. Camera/transmitter weight is only .5oz, 2.5oz with 9 volt battery. Field of view 60 degrees, CMOS 380 TV lines of resolution sensor.

Range 300-700 feet in the air on an aircraft, 300-500 feet on the ground. Over 1 mile with the 14db patch antenna.

Receiver unit has SMA antenna connector with rubber duck antenna. Use optional Hi-Gain receiver antenna avalible for additional range.

Consumer use item, no license needed. FCC certified.

Appendix L

Balloon Data Sheet

7' (2.13m) BALL
OR
Reference Scale: 6' man (1.83m)
SCALE: .5" = 1' (1cm = 24cm)
No. of Panels: 6
Helium Volume: ±180 cu. ft. (±5.00m³)
Net Lift: ±7 lbs. (±3.2kg)
------ = Panel line
——— = Digital Graphics Print Area (±66"X ±30") (±168cm x ±76cm)
Balls can be made with the panels in the horizontal or vertical configurations to fit your graphic needs.
The vertical configuration is recommended because it holds its shape better when exposed to sun and heat.

Appendix M

Microprocessor

MicroProcessor DSPIC30F6015 Features

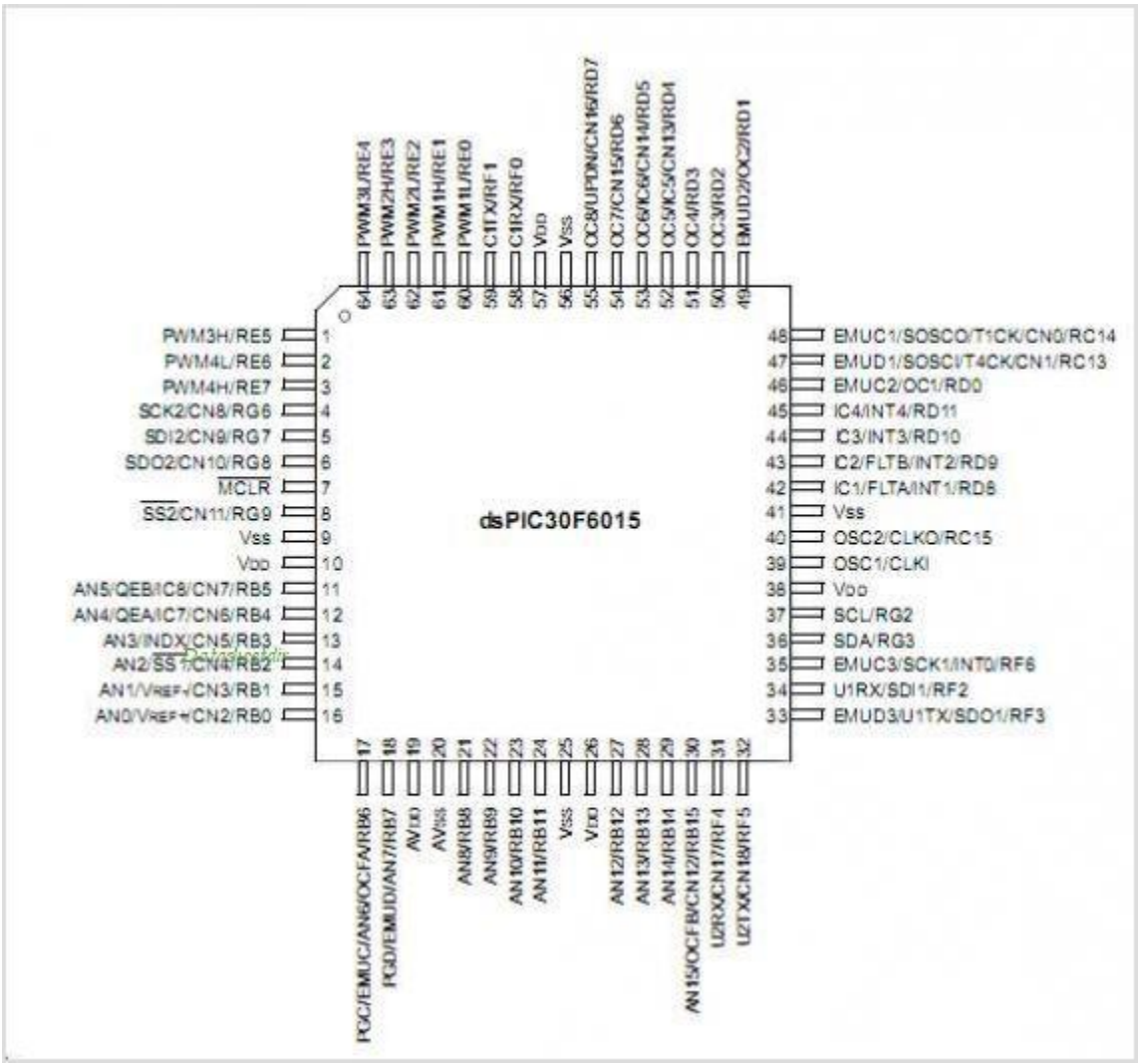

Parameter Name	Value
Architecture	16-bit
CPU Speed (MIPS)	30
Memory Type	Flash
Program Memory (KB)	144
RAM Bytes	8,192
Temperature Range C	-40 to 125
Operating Voltage Range (V)	2.5 to 5.5
I/O Pins	52
Pin Count	64
System Management Features	PBOR, LVD
Internal Oscillator	7.37 MHz, 512 kHz
nanoWatt Features	Fast Wake/Fast Control
Digital Communication Peripherals	2-UART, 2-SPI, 1-I2C
Analog Peripherals	1-A/D 16x10-bit @ 1000(ksps)
Comparators	0
CAN (#, type)	1 CAN
Capture/Compare/PWM Peripherals	8/8
Motor Control PWM Channels	8
Quatrature Encoder Interface (QEI)	1
Timers	5 x 16-bit 2 x 32-bit
Parallel Port	GPIO
Hardware RTCC	No
DMA	0

Features

High-Performance Modified RISC CPU:

- Modified Harvard architecture
- C compiler optimized instruction set architecture
- 84 base instructions with flexible addressing modes
- 24-bit wide instructions, 16-bit wide data path
- 16 x 16-bit working register array
- Up to 30 MIPs operation: - DC to 40 MHz external clock input - 4 MHz-10 MHz

oscillator input with PLL active (4x, 8x, 16x)

- Peripheral and External interrupt sources
- 8 user selectable priority levels for each interrupt
- 4 processor exceptions and software traps
- Primary and Alternate interrupt Vector Tables DSP Engine Features:
- Modulo and Bit-Reversed Addressing modes
- Two, 40-bit wide accumulators with optional saturation logic
- 17-bit x 17-bit single cycle hardware fractional/ integer multiplier
- Single cycle Multiply-Accumulate (MAC) operation

- 40-stage Barrel Shifter
- Dual data fetch Peripheral Features:
- High current sink/source I/O pins: 25 mA/25 mA
- Optionally pair up 16-bit timers into 32-bit timer modules
- 3-wire SPI™ modules (supports 4 Frame modes)
- I2C™ module supports Multi-Master/Slave mode and 7-bit/10-bit addressing
- Addressable UART modules with FIFO buffers Motor Control PWM Module

Features:

- Complementary or Independent Output modes
- Edge and Center Aligned modes
- Multiple duty cycle generators
- Dedicated time base with 4 modes
- Programmable output polarity
- Dead time control for Complementary mode
- Manual output control
- Trigger for synchronized A/D conversions Quadrature Encoder Interface Module

Features:

- Phase A, Phase B and Index Pulse input
- 16-bit up/down position counter
- Count direction status
- Position Measurement (x2 and x4) mode
- Programmable digital noise filters on inputs
- Alternate 16-bit Timer/Counter mode
- Interrupt on position counter rollover/underflow Analog Features:
- 10-bit 1 Msps Analog-to-Digital Converter (A/D)
- A/D Conversion available during Sleep and Idle
- 4 Sample/Hold Channels
- Multiple Conversion Sequencing Options Special Microcontroller Features:
- Enhanced Flash program memory: - 10,000 erase/write cycle (min.) for industrial temperature range, 100K (typical)
- Data EEPROM memory: - 100,000 erase/write cycle (min.) for industrial temperature range, 1M (typical)
- Self-reprogrammable under software control
- Power-on Reset (POR), Power-up Timer (PWRT) and Oscillator Start-up Timer (OST)
- Flexible Watchdog Timer (WDT) with on-chip low power RC oscillator for reliable operation
- Fail-Safe clock monitor operation
- Detects clock failure and switches to on-chip low power RC oscillator
- Programmable code protection
- In-Circuit Serial Programming™ (ICSP™)
- Programmable Brown-out Detection and Reset generation
- Selectable Power Management modes - Sleep, Idle and Alternate Clock modes

CMOS Technology:

- Low power, high speed Flash technology
- Wide operating voltage range (2.5V to 5.5V)
- Industrial and Extended temperature ranges
- Low power consumption

Appendix N

Microprocessor Power Demands

Microprocessor: dsPIC30F6010A/6015

24.0 ELECTRICAL CHARACTERISTICS

This section provides an overview of dsPIC30F electrical characteristics. Additional information will be provided in future revisions of this document as it becomes available. For detailed information about the dsPIC30F architecture and core, refer to the "*dsPIC30F Family Reference Manual*" (DS70046).

Absolute maximum ratings for the dsPIC30F family are listed below. Exposure to these maximum rating conditions for extended periods may affect device reliability. Functional operation of the device at these or any other conditions above the parameters indicated in the operation listings of this specification is not implied.

Absolute Maximum Ratings(†)

Ambient temperature under bias.....-40°C to +125°C
Storage temperature ..... -65°C to +150°
Voltage on any pin with respect to V_{SS} (except V_{DD} and MCLR) **(Note 1)** ..... -0.3V to (V_{DD} + 0.3V)
Voltage on V_{DD} with respect to V_{SS} ..... -0.3V to +5.5V
Voltage on MCLR with respect to V_{SS}..... 0V to +13.25V
Maximum current out of V_{SS} pin .....300 mA
Maximum current into V_{DD} pin **(Note 2)**.....250 mA
Input clamp current, I_{IK} (V_I < 0 or V_I > V_{DD}) .....±20 mA
Output clamp current, I_{OK} (V_O < 0 or V_O > V_{DD}) .....±20 mA
Maximum output current sunk by any I/O pin.....25 mA
Maximum output current sourced by any I/O pin .....25 mA
Maximum current sunk by all ports .....200 mA
Maximum current sourced by all ports **(Note 2)**.....200 mA

Note 1: Voltage spikes below V_{SS} at the MCLR/V_{PP} pin, inducing currents greater than 80 mA, may cause latch-up. Thus, a series resistor of 50-100Ω should be used when applying a "low" level to the MCLR/V_{PP} pin, rather than pulling this pin directly to V_{SS}.

2: Maximum allowable current is a function of device maximum power dissipation. See Table 24-6.

†NOTICE: Stresses above those listed under "Absolute Maximum Ratings" may cause permanent damage to the device. This is a stress rating only and functional operation of the device at those or any other conditions above those indicated in the operation listings of this specification is not implied. Exposure to maximum rating conditions for extended periods may affect device reliability.

Appendix O

Schmart Board

Products - Part# 202-0011-01

Schmartboard.com

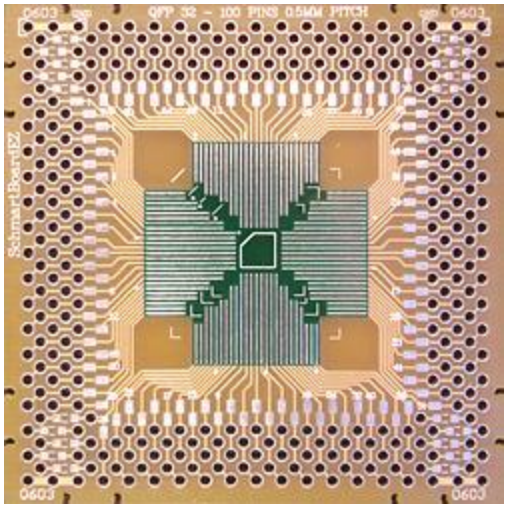

202-0011-01

QFP, 32 - 100 Pins 0.5mm Pitch, 2" X 2" Grid EZ Version

Support up to 100 pins QFP, TQFP, PQFP package IC with 0.5mm pitch, 20 pcs. of 0603 package, and some thru hole passive components. 6 ground holes are connected a copper plane on the bottom side.

This product utilizes the "EZ" technology to assure fast, easy, and flawless hand soldering

Appendix P

Voltage Regulators

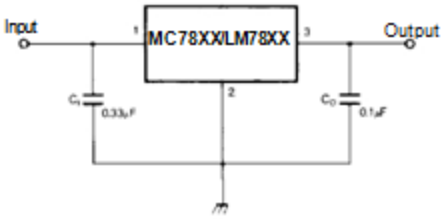

Figure 8. Fixed Output Regulator

LM7805CT and MC7806 Voltage Regulator Data Sheets

Electrical Characteristics (MC7805/LM7805)

(Refer to test circuit ,0°C < T_J < 125°C, I_O = 500mA, V_I = 10V, C_I= 0.33∝F, C_O= 0.1∝F, unless otherwise specified)

Parameter	Symbol	Conditions		MC7805/LM7805			Unit
				Min.	Iyp.	Max.	
Output Voltage	V_O	T_J =+25 °C		4.8	5.0	5.2	V
		5.0mA ≤Io ≤1.0A, P_O ≤15W V_I = 7V to 20V		4.75	5.0	5.25	
Line Regulation (Note1)	Regline	T_J=+25 °C	V_O = 7V to 25V	-	4.0	100	mV
			V_I = 8V to 12V	-	1.6	50	
Load Regulation (Note1)	Regload	T_J=+25 °C	I_O = 5.0mA to1.5A	-	9	100	mV
			I_O =250mA to 750mA	-	4	50	
Quiescent Current	I_Q	T_J =+25 °C		-	5.0	8.0	mA
Quiescent Current Change	ΔI_Q	I_O = 5mA to 1.0A		-	0.03	0.5	mA
		V_I= 7V to 25V		-	0.3	1.3	
Output Voltage Drift	$\Delta V_O/\Delta T$	I_O= 5mA		-	-0.8	-	mV/°C
Output Noise Voltage	V_N	f = 10Hz to 100KHz, T_A=+25 °C		-	42	-	∝V/Vo
Ripple Rejection	RR	f = 120Hz V_O = 8V to 18V		62	73	-	dB
Dropout Voltage	V_{Drop}	I_O = 1A, T_J =+25 °C		-	2	-	V
Output Resistance	r_O	f = 1KHz		-	15	-	mΩ
Short Circuit Current	I_{SC}	V_I = 35V, T_A =+25 °C		-	230	-	mA
Peak Current	I_{PK}	T_J =+25 °C		-	2.2	-	A

Electrical Characteristics (MC7806)

(Refer to test circuit ,0°C < T_J < 125°C, I_O = 500mA, V_I =11V, C_I= 0.33∝F, C_O= 0.1∝F, unless otherwise specified)

Parameter	Symbol	Conditions		MC7806			Unit
				Min.	Typ.	Max.	
Output Voltage	V_O	T_J =+25 °C		5.75	6.0	6.25	V
		5.0mA ≤I_O ≤1.0A, P_O ≤15W V_I = 8.0V to 21V		5.7	6.0	6.3	
Line Regulation (Note1)	Regline	T_J =+25 °C	V_I = 8V to 25V	-	5	120	mV
			V_I = 9V to 13V	-	1.5	60	
Load Regulation (Note1)	Regload	T_J =+25 °C	I_O =5mA to 1.5A	-	9	120	mV
			I_O =250mA to 750A	-	3	60	
Quiescent Current	I_Q	T_J =+25 °C		-	5.0	8.0	mA
Quiescent Current Change	ΔI_Q	I_O = 5mA to 1A		-	-	0.5	mA
		V_I = 8V to 25V		-	-	1.3	
Output Voltage Drift	$\Delta V_O/\Delta T$	I_O = 5 mA		-	-0.8	-	mV/°C
Output Noise Voltage	V_N	f = 10Hz to 100KHz, T_A =+25 °C		-	45	-	∝V/Vo
Ripple Rejection	RR	f = 120Hz V_I = 9V to 19V		59	75	-	dB
Dropout Voltage	V_{Drop}	I_O = 1A, T_J =+25 °C		-	2	-	
	VOutput Resistance			r_O	f = 1KHz	-	19
	- mΩ						
Short Circuit Current	I_{SC}	V_I= 35V, T_A=+25 °C		-	250	-	mA
Peak Current	I_{PK}	T_J =+25 °C		-	2.2	-	A

Appendix Q

Auxiliary to USB Connector

EasyCAP

- Model: DC60

- Supports NTSC, PAL, Video format
- Supports high quality video resolution
- Capture & edit high quality video & audio without sound card
- Include Professional and easy to learn & used video editor software: Ulead Video Studio 8.0 SE DVD
- Plug & play
- Applying to internet conference / net meeting
- Complies With Universal Serial Bus Specification Rev. 2.0
- USB bus power

Appendix R

Remote Control System

BASIC PARAMETER:

- MODEL NAME: 6 CHANNELS TRANSMITTERS
- MODEL NO: FS-CT6X
- CHANNELS: 6 CHANNELS
- MODE TYPE: AIRPLANE, HELICOPTER, GLIDER
- STICK MODE: LEFT HAND OR RIGHT HAND
- MODULATION: FREQUENCY MODULATION
- MODULE FREQUENCY: 35MHZ,40MHz,72MHz,2.4GHz
- ANTENNA LENGTH: 115CM/26MM
- CODE TYPE: PPM/GFSK
- POWER : 12 VDC
- RF POWER: LESS THAN 0.8W
- WEIGHT: 575 GRAMS
- SIZE: 189*72*218MM

Features

1. 6 Channel 2.4GHz R/C Transmitter Complete Set w/ Receiver. Features complete Forward/Backward, Left/Right, Up/Down & Pitch Control (RUDDER, AILERON, ELEVATOR, Pitch AND THROTTLE)
2. New longer 3K battery mounting plate connects to main frame. It makes the center of gravity closed to rotor blade, and can adjust the center of gravity according to the weight of battery, it reduces the correction when the heli rolling.
3. Rotor head for precision and smooth movements.
4. Great stable and sensitive mixing lever design! Can display the great stability and precision for 3D flight.
5. Using Ball and Hiller two systems mixing control. Through simple structure of Ball control system, power-saving of Hiller system and CCPM control, can simultaneously control 3 servo for AILE, EVLE, PIT 3 actions. This control system is great for 3D flying control and extending life cycle of servos.
6. Software for Raido Download Here: Click Here

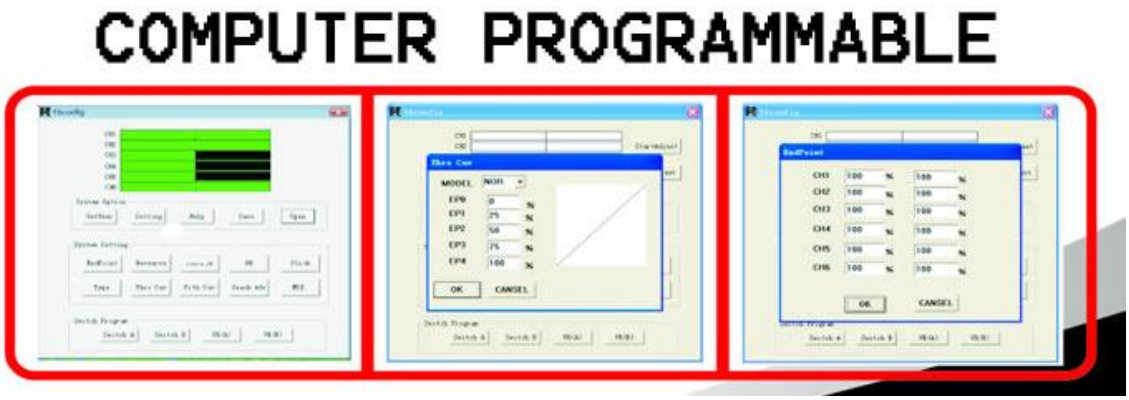

Appendix S

Transmitter

MS Long-Range Handheld Transmitter

The Linx OTX-***-HH-LR8-MS Long-Range Handheld Transmitter is ideal for general-purpose remote control and command applications that require longer transmission distances. This unit has been pre-certified for FCC Part 15, Industry Canada, and European CE (433.92MHz only) compliance, reducing costs and time to market. Available in 315, 418 (standard), or 433.92MHz, this small remote has a transmission range of up to 1,000 feet when combined with the LR or LT Series receiver. The transmitter unit can be configured with 1 to 8 buttons and the keypad and labeling can be modified to meet specific OEM customer requirements. Ease of use and security are dramatically enhanced by the on-board MS Series encoder, which allows instant creation of up to 16,777,216 (2^{24}) unique addresses without cumbersome DIP switches or cut traces. When paired with a MS Series decoder, transmitter identity can be determined and button permissions established. The unit uses a single 3V CR2032 lithium button cell.

Quantity	Standard
<200	$32.80
200-999	$29.50
1,000-4,999	$28.75
5,000+	Call

Part #	OTX-***-HH-LR8-MS
*** = 315, 418 (standard), 433MHz	

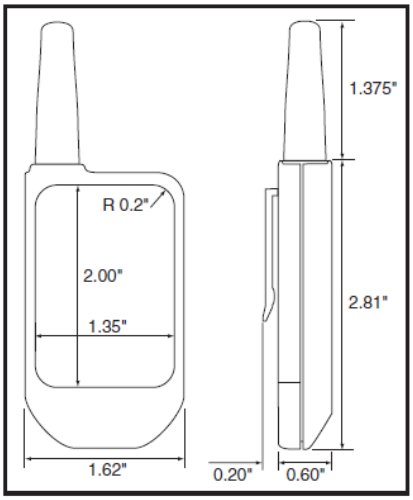

ELECTRICAL SPECIFICATIONS

Parameter	Designation	Min.	Typical	Max.	Units	Notes
POWER SUPPLY						
Operating Voltage	V_{CC}	2.1	3.0	3.6	VDC	–
Supply Current	I_{CC}	–	3.4	–	mA	–
Power-Down Current	I_{PDN}	–	5.0	–	nA	1
TRANSMITTER SECTION						
Transmit Frequency Range:	F_C					
OTX-315-HH-LR8-MS		–	315	–	MHz	–
OTX-418-HH-LR8-MS		–	418	–	MHz	–
OTX-433-HH-LR8-MS		–	433.92	–	MHz	–
Center Frequency Accuracy	–	-50	–	+50	kHz	–
ENVIRONMENTAL						
Operating Temperature Range	–	-40	–	+85	°C	1

Appendix T

Receiver

LR Series - *Long-Range, Low-Cost RF Data Module*

The LR Series is ideal for the wireless transfer of serial data, control, or command information in the favorable 260-470MHz band. The receiver's advanced synthesized superhet architecture achieves an outstanding typical sensitivity of -112dBm, which provides a 5-10 times improvement in range over previous solutions. The transmitter's synthesized architecture minimizes the effects of antenna loading, providing a more stable, consistent performance. When paired, a reliable wireless link is formed, capable of transferring data at rates of up to 10,000bps over distances of up to 3,000 feet. Applications operating at short distances or lower data rates will also benefit from increased link reliability and superior noise immunity. Housed in tiny reflow-compatible SMD packages, the LR Series modules are footprint compatible with the popular LC Series (the transmitter pin-out is slightly different), allowing existing users an instant path to improved range and lower cost. No external components are required (except an antenna), allowing for easy integration, even by engineers without previous RF experience.

- **Long-range**
- **Low cost**
- **PLL synthesized architecture**
- **Direct serial interface**
- **Data rates to 10,000bps**
- **No external RF components required (except antenna)**
- **Low power consumption**
- **Wide temperature range (-40 to +70°C)**
- **Compact surface-mount package**
- **Adjustable transmitter output power**
- **RSSI and power-down functions**
- **No production tuning necessary**

Quantity	TX	RX
<200	$5.95	$9.80
200-999	$5.38	$9.63
1,000-4,999	$4.80	$8.65
5,000+	Call	Call

Part #	Description
TXM-***-LR	LR Series Transmitter
RXM-***-LR	LR Series Receiver

*** = 315, 418 (standard), 433MHz

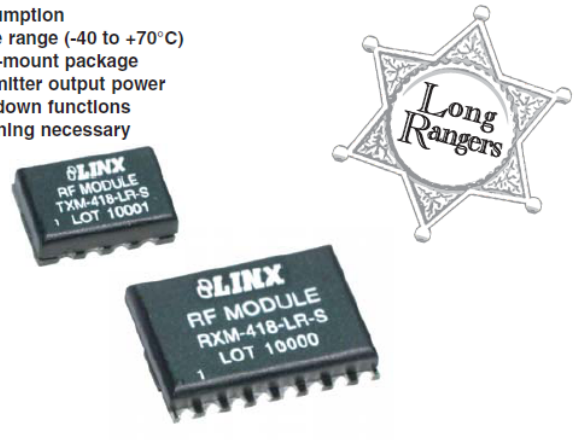

MS Series

MS Series encoders and decoders are ideal for remote control and command, security, keyless entry, and a host of similar applications. The encoder IC allows the status of up to eight buttons or contacts to be transferred with high level of uniqueness via an RF or infrared link. The decoder then reproduces the button states on its outputs. The MS Series has several unique features that make it superior to competitive solutions. These include the ability to easily define user groups and assign permissions to individual output lines. Outputs can be latched or momentary and secure address assignments can be instantly changed without cumbersome DIP switches or cut traces. The large, twenty-four bit address size provides for over 16,000,000 unique addresses, making transmissions highly unique and secure, and minimizing the possibility of multiple devices having conflicting addresses. The decoder can learn up to 40 different encoders and outputs the originating encoder ID for logging or identification. Housed in tiny 20-pin SSOP packages, MS Series parts feature low supply voltage and low current consumption.

Quantity	ENC	DEC
<200	$3.10	$3.10
200-999	$2.95	$2.95
1,000-4,999	$2.73	$2.73
5,000+	Call	Call

Part #	Description
LICAL-ENC-MS001	MS Series Encoder
LICAL-DEC-MS001	MS Series Decoder

Features:

- **Secure 2^{24} possible addresses**
- **8 data lines**
- **Low 2.0-5.5V operating voltage**
- **Low supply current (370µA @ 3V)**
- **Ultra-low 0.1µA standby current**
- **Definable recognition authority**
- **True serial encoding**
- **Excellent noise immunity**
- **Selectable baud rates**
- **No programmer required**
- **Direct serial interface**
- **Small SMD package**
- **Latched or momentary outputs**
- **Encoder ID output by decoder**

Applications Include:

- **Keyless Entry**
- **Door and Gate Openers**
- **Security Systems**
- **Remote Device Control**
- **Car Alarms / Starters**
- **Remote Status Monitoring**
- **Call / Paging Systems**